REVIEWS OF
MODERN PHYSICS

VOLUME 36, NUMBER 4 OCTOBER 1964

Electron Scattering without Atomic or Nuclear Excitation

J. W. MOTZ, HAAKON OLSEN,* H. W. KOCH

National Bureau of Standards, Washington 25, D. C.

CONTENTS

I. INTRODUCTION

This survey is concerned with the process of single electron scattering by an atom without excitation of the atom or the nucleus. If radiative effects are neglected in this process, the energy of the scattered electron in the laboratory system depends only on the energy transferred to the recoiling atom. For low-energy electrons, the atomic recoil is negligible, and the initial and final electron energies in the laboratory system are approximately equal. For high-energy electrons and large scattering angles, the atomic recoil is not negligible, and the final electron energy in the laboratory system is measurably smaller than the initial electron energy.

Extensive calculations pertaining to this scattering process have become available, partly because the process dominates and is less complicated than most of the other processes involved in the interaction of electrons with matter. One of the most important early summaries concerning this process has been given by Mott and Massey (M 49), who presented Born and exact phase-shift calculations, which laid the groundwork for future calculations. Later studies emphasized various aspects of this process such as the effects of the atomic structure in the nonrelativistic energy region (Mo 62) or in the low momentum transfer region (Sc 63), the effects of the nuclear structure in the extreme relativistic energy region or in the high momentum transfer region (H 56), the radiative effects (S 49), and the polarization behavior (Me 55, T 56). Although the work in these different areas has provided a wealth of data, there is a need to tie the results together in order to present a clear consistent picture of the over-all behavior of the process. The purpose of this review is to help satisfy this need by summarizing and integrating the various theoretical results pertaining to the behavior of this process. These results cover a wide range of electron energies extending from the nonrelativistic ($\gtrsim$10 keV) to the extreme relativistic regions and pertain to the kinematics (Sec. III), the radiative effects (Sec. IV), the polarization behavior (Sec. VI), and the cross sections with polarization dependence in differential and integrated form (Sec. VII). No derivations are given and details of the calculations can be found in the references.

The cross section for this process depends on the initial energy and scattering angle of the electron as well as the magnitude of the charge and the structure of the target atom. The atomic or the nuclear charge structures become important approximately in the region where the momentum transfer to the atom (in m_0c units) is less than the inverse of the atomic radius or greater than the inverse of the nuclear radius (in units of the reciprocal Compton wavelength), respectively. At present, a complete and accurate description of the charge structures for all elements is not available, and indeed this process has been used as a method to determine these structures. In the present review, the emphasis is on the behavior of the process rather than on the structure of the atom or the nucleus,

* Permanent address: Institute for Theoretical Physics, Norges Tekniske Högskole, Trondheim, Norway.

and in the absence of exact information about structure or about scattering potentials, various approximations are given in order to permit estimates of the general behavior.

The formulas in this survey are intended specifically for electron scattering; energies, momenta, and lengths are given in units of m_0c^2, m_0c, and $\hbar/m_0c$, respectively, where m_0 is the electron rest mass. These formulas may be applied also to scattering processes in which the incident particle is a positron or a positive or negative muon when the mass is small compared to the mass of the target atom. For the case of the positron, it is necessary simply to replace Z by $-Z$ in the formulas. This procedure has the effect of changing the exact and higher order Born cross-section formulas, while the first Born formulas remain unchanged because of their dependence only on Z^2. For the case of the muon, it is necessary to note that the energies, momenta, and lengths in these formulas are now defined in units of $m_\mu c^2$, $m_\mu c$, and $\hbar/m_\mu c$, respectively, where m_μ is the muon rest mass. Therefore, for the negative muon these formulas may be used with the explicit changes that r_0 is replaced by $(m_0/m_\mu)r_0(=e^2/m_\mu c^2)$ and that m_0/M_0 is replaced by m_μ/M_0. For the positive muon, the formulas are the same as for the negative muon with the additional change that Z is replaced by $-Z$.

II. DEFINITIONS

The following definitions and useful relationships are given for the symbols and constants used in this review. The constants are given with three significant figures although more accurate values are available.

E_1, E_2 = initial and final total energy of the electron in a collision, in m_0c^2 units.

T_1, T_2 = initial and final kinetic energy of the electron in a collision, in m_0c^2 units.

β_1, β_2 = ratio of the initial and final electron velocity in a collision to the velocity of light.

$\mathbf{p}_1$, $\mathbf{p}_2$ = initial and final momentum of the electron in a collision, in m_0c units.

$\mathbf{n}_1$, $\mathbf{n}_2$ = unit vector for the initial and final momentum of the electron in a collision, such that $\mathbf{p}_1=p_1\mathbf{n}_1$ and $\mathbf{p}_2=p_2\mathbf{n}_2$.

$\mathbf{n}$ = unit vector perpendicular to the scattering plane $(\mathbf{p}_1, \mathbf{p}_2)$, such that $\mathbf{n}=(\mathbf{p}_1\times\mathbf{p}_2)/|\mathbf{p}_1\times\mathbf{p}_2|=(\mathbf{n}_1\times\mathbf{n}_2)/|\mathbf{n}_1\times\mathbf{n}_2|$.

$\boldsymbol{\zeta}_1$, $\boldsymbol{\zeta}_2$ = unit polarization vector pertaining to the initial and final electron in a collision. These vectors are defined as the expectation values, $\boldsymbol{\zeta}_1=u_1^\dagger\boldsymbol{\sigma}u_1$ and $\boldsymbol{\zeta}_2=u_2^\dagger\boldsymbol{\sigma}u_2$, where u_1 and u_2 are eigenstates for $\boldsymbol{\zeta}_1\cdot\boldsymbol{\sigma}$ and $\boldsymbol{\zeta}_2\cdot\boldsymbol{\sigma}$, respectively, such that $\boldsymbol{\zeta}_1\cdot\boldsymbol{\sigma}u_1=u_1$ and $\boldsymbol{\zeta}_2\cdot\boldsymbol{\sigma}u_2=u_2$, and where $\boldsymbol{\sigma}$ is the Pauli spin operator. The unit vectors, $\boldsymbol{\zeta}_1$ and $\boldsymbol{\zeta}_2$, may be chosen to have arbitrary directions which can be specified in terms of the coordinate system given by the unit orthogonal vectors $\mathbf{n}$, $\mathbf{n}_1$, $\mathbf{n}_1\times\mathbf{n}$, or $\mathbf{n}$, $\mathbf{n}_2$, $\mathbf{n}_2\times\mathbf{n}$.

$\mathbf{P}_1$, $\mathbf{P}_2$ = polarization vector for the initial and final *electron beam* in a collision. The magnitude of the vector gives the degree of polarization for the beam in the direction of the vector, and is equal to the average expectation value of the spin operator for the beam. This magnitude is less than unity for a partially polarized beam, and is equal to unity and zero, respectively, for the special cases of a completely polarized and an unpolarized beam. The magnitude of $\mathbf{P}_1$ is given by the initial conditions, and its direction is specified by the unit vector $\boldsymbol{\zeta}_1$ in the electron rest system such that $\mathbf{P}_1=P_1\boldsymbol{\zeta}_1$. The magnitude and direction of $\mathbf{P}_2$ are determined by the dynamics of the scattering process. Then $\mathbf{P}_2\cdot\boldsymbol{\zeta}_2$ is the component of $\mathbf{P}_2$ along the chosen axis, $\boldsymbol{\zeta}_2$.

χ_1, χ_2 = angle between the vectors $\mathbf{n}$ and $\mathbf{P}_1$ or $\mathbf{n}$ and $\mathbf{P}_2$, respectively.

θ = angle between the directions of the emitted and the incident electron.

ϕ = azimuthal angle for the scattered electron.

$d\Omega$ = element of solid angle, $\sin\theta\, d\theta\, d\phi$, about the direction of $\mathbf{p}_2$.

$q_0=2p_1\sin\frac{1}{2}\theta$ = momentum transfer to an infinitely heavy atom in a nonradiative elastic collision such that $|\mathbf{p}_1|=|\mathbf{p}_2|$.

$q=|\mathbf{p}_1-\mathbf{p}_2|$ = momentum transfer to an atom in a nonradiative collision, in m_0c units.

$y=|\mathbf{p}_1-\mathbf{p}_2-\mathbf{k}|$ = momentum transfer to an atom in a radiative collision, in m_0c units.

$Q=[(\mathbf{p}_1-\mathbf{p}_2)^2-(E_1-E_2)^2]^{\frac{1}{2}}$= four-dimensional momentum–energy transfer

$=Q_e=q_0/[1+(m_0/M_0)(q_0^2/2E_1)]^{\frac{1}{2}}$ (for elastic scattering at extreme relativistic energies)

$=Q_B=[(\mathbf{p}_1-\mathbf{p}_2)^2-k^2]^{\frac{1}{2}}$ (for scattering with radiation).

θ_M = angle between the directions of the incident particle and the recoiling target atom (See Fig. 1).

Z = atomic number of the target atom.

k = energy of the emitted photon, in m_0c^2 units

$= T_1-T_2$ for an infinitely heavy nucleus.

$\mathbf{r}$ = radius vector from the center of the nucleus, in units of $\lambda\!\!\!^{-}_0$.

S, R, and L = polarization functions for the determination of the polarization vectors, $\mathbf{P}_1$ and $\mathbf{P}_2$. These functions are defined in formula (1A–403) in terms of the F and G or the f and g functions that are specified in the Mott–exact phase-shift formula (1A–109).

$F(q)$, $G_E(q)$ = atomic and nuclear charge form factors, respectively

$$= (4\pi/q)\int_0^\infty \rho(r)(\sin qr)r\,dr.$$

$Ze\,\rho(r)$ = charge density for the atom or nucleus, with normalization such that $\int\rho(r)\,d^3r=1$.

$G_M(q)$ = magnetic nuclear form factor

$$= (4\pi/q)\int_0^\infty \mu(r)(\sin qr)r\,dr.$$

$\mu(r)$ = nuclear magnetic moment distribution, such that $\int\mu(r)\,d^3r$ is equal to the nuclear magnetic moment μ.

$\frac{d\sigma}{d\Omega}$ = elastic electron scattering cross-section differential with respect to the solid angle of the scattered electrons. This form of the cross section is averaged over the initial and summed over the final electron-spin states.

$\frac{d\sigma}{d\Omega}(\boldsymbol{\zeta}_1, \mathbf{n})$ = elastic electron scattering cross-section differential with respect to the solid angle of the scattered electrons. This form of the cross section is summed over the final electron-spin states and designated by its functional dependence on the unit axial vectors $\boldsymbol{\zeta}_1$ and $\mathbf{n}$.

$\frac{d\sigma}{d\Omega}(\mathbf{P}_1, \mathbf{n})$ = same definition as $d\sigma(\boldsymbol{\zeta}_1, \mathbf{n})/d\Omega$ except that $\boldsymbol{\zeta}_1$ is replaced by $\mathbf{P}_1$ in order to apply to a partially polarized incident beam.

$\frac{d\sigma}{d\Omega}(\boldsymbol{\zeta}_2, \mathbf{n})$ = elastic electron scattering cross-section differential with respect to the solid angle of the scattered electrons. This form of the cross section is averaged over the initial electron-spin states and designated by its functional dependence on the unit axial vectors $\boldsymbol{\zeta}_2$ and $\mathbf{n}$.

$\frac{d\sigma}{d\Omega}(\boldsymbol{\zeta}_1, \boldsymbol{\zeta}_2, \mathbf{n})$ = elastic electron scattering cross-section differential with respect to the solid angle of the scattered electrons. This form of the cross section is designated by its functional dependence on the unit axial vectors $\boldsymbol{\zeta}_1$, $\boldsymbol{\zeta}_2$, and $\mathbf{n}$.

$\frac{d\sigma}{d\Omega}(\mathbf{P}_1, \boldsymbol{\zeta}_2, \mathbf{n})$ = same definition as $d\sigma(\boldsymbol{\zeta}_1, \boldsymbol{\zeta}_2, \mathbf{n})/d\Omega$ except that $\boldsymbol{\zeta}_1$ is replaced by $\mathbf{P}_1$ in order to apply to a partially polarized incident beam.

$\frac{d^2\sigma_B}{d\Omega dT_2}$ = bremsstrahlung cross-section differential with respect to the energy and solid angle of the scattered electrons. This form of the cross section is summed over photon polarizations, integrated over all photon angles, and averaged over the initial and summed over the final electron-spin states.

σ = the total elastic scattering cross section, integrated over the electron scattering angles and averaged over the initial and summed over the final electron-spin states.

$\int_{T_1-\Delta E}^{T_1} \frac{d^2\sigma}{d\Omega dT_2} dT_2$ = the integrated cross section that is used to define the radiative correction. This cross section is equal to the sum,

$$\int_{T_1-\Delta E}^{T_1} \frac{d^2\sigma_B}{d\Omega dT_2} dT_2 + \frac{d\sigma'}{d\Omega},$$

in which $(d\sigma'/d\Omega)$ is the elastic electron cross-section differential with respect to the solid angle of the scattered electron with the inclusion of the virtual photon part of the radiative correction.

$$E_1^2 = p_1^2 + 1, \qquad E_2^2 = p_2^2 + 1,$$
$$E_1 = T_1 + 1, \qquad E_2 = T_2 + 1,$$
$$E_1 = 1/(1-\beta_1^2)^{\frac{1}{2}}, \qquad E_2 = 1/(1-\beta_2^2)^{\frac{1}{2}},$$
$$p_1 = [T_1(T_1+2)]^{\frac{1}{2}}, \qquad p_2 = [T_2(T_2+2)]^{\frac{1}{2}},$$
$$p_1 = \beta_1/(1-\beta_1^2)^{\frac{1}{2}}, \qquad p_2 = \beta_2/(1-\beta_2^2)^{\frac{1}{2}},$$
$$\beta_1 = p_1/E_1, \qquad \beta_2 = p_2/E_2.$$

$r_0 = e^2/m_0c^2 = \lambda\!\!\!^{-}_0/137 = 2.82\times10^{-13}$ cm (classical electron radius).

$\lambda\!\!\!^{-}_0 = \hbar/m_0c = 3.86\times10^{-11}$ cm (Compton wavelength).

$a_0 = \hbar^2/m_0e^2 = 137\lambda\!\!\!^{-}_0 = (137)^2 r_0 = 0.530\times10^{-8}$ cm (Bohr radius of hydrogen atom).

$R_{TF} = 0.885 a_0 Z^{-\frac{1}{3}}$ (radius of the Thomas-Fermi atom).

$R_A \approx 0.514 A^{\frac{1}{3}} r_0$ [approximate radius of the nucleus for a spherical nuclear model (H 56)].

$m_0 = 9.11\times10^{-28}$ g (electron rest mass).

$M_0 \approx A\times1.66\times10^{-24}$ g (rest mass of the atomic nucleus).

$m_0/M_0 = 5.5A^{-1}\times10^{-4}$.

$A = Z+N$ (number of neutrons) $\approx 2.6Z$ for high Z, $2Z$ for low Z (mass number of nucleus).

$c = 3.00\times10^{10}$ cm per sec (speed of light in vacuum).

$e = 1.60\times10^{-19}$ C (electron charge).

$e^2 = 1.44\times10^{-13}$ MeV cm.

$\hbar = 6.58\times10^{-22}$ MeV sec $= 1.05\times10^{-27}$ erg sec.

$hc = 12.4$ keV-Å.

$\hbar c = 1.97\times10^{-11}$ MeV cm.

$\alpha = e^2/\hbar c = 1/137$.

$m_0c^2 = 0.511$ MeV.

III. KINEMATICS

The kinematic relationships for electron elastic scattering without radiative effects are derived from a general relativistic treatment of the energy and momentum conservation laws which are given, for example, by Blaton (B 50) and by Baldin *et al.* (B 61). The following kinematic results for this process are given with the system of units defined in Sec. II.

The various parameters for the process in the laboratory system are shown in Fig. 1. These parameters in the center-of-momentum system are identified by the primes on the symbols. Except for special cases, all symbols in the text are defined in Sec. II.

A. Relationships in Laboratory System with Target Atom Initially at Rest

The momentum p_2 of the scattered electron can be written in terms of the scattering angle θ and the energy

E_1 and momentum p_1 of the incident electron as

$$p_2=\frac{p_1}{1+(m_0/M_0)(E_1-p_1\cos\theta)}\times\left[\frac{1+2(m_0/M_0)E_1\cos^2\frac{1}{2}\theta}{1+(m_0/M_0)(E_1+p_1\cos\theta)}\right], \quad (3.01)$$

where $(m_0/M_0)\ll 1$. For the extreme relativistic case, $\beta_1\approx 1$ or $E_1\approx p_1$, and

$$p_2\approx\frac{p_1}{1+2(m_0/M_0)E_1\sin^2\frac{1}{2}\theta}. \quad (3.02)$$

When $E_1\ll(M_0/m_0)$, the recoil energy is negligible and

$$p_2\approx p_1. \quad (3.03)$$

The momentum q transferred to the atom is given by

$$q^2=p_1^2+p_2^2-2p_1p_2\cos\theta, \quad (3.04)$$

where p_2 is given by Eq. (3.01). In terms of the recoil angle θ_M of the atom, q becomes

$$q=\frac{2(M_0/m_0)[E_1+(M_0/m_0)]p_1\cos\theta_M}{[E_1+(M_0/m_0)]^2-p_1^2\cos^2\theta_M}. \quad (3.05)$$

The recoil angle θ_M can be obtained from the following equation:

$$\cot^2\theta_M=[1+(m_0/M_0)E_1]^2\frac{[1+(m_0/M_0)E_1](1-\beta^2\cos^2\theta)-\cos\theta[1+\beta(E_1/p_1)\cos\theta]}{[1+(m_0/M_0)E_1](1-\beta^2\cos^2\theta)+\cos\theta[1+2(m_0/M_0)E_1][1+\beta(E_1/p_1)\cos\theta]}, \quad (3.06)$$

where

$$\beta=\frac{m_0}{M_0}\left[\frac{p_1}{1+(m_0/M_0)E_1}\right]. \quad (3.07)$$

When $E_1\ll(M_0/m_0)$, the recoil energy is negligible and

$$\cot\theta_M=\tan\tfrac{1}{2}\theta. \quad (3.08)$$

B. Conversion Relationships between the Laboratory and the Center-of-Momentum Systems

In the following equations, the primed symbols refer to the center-of-momentum system, and it is assumed that the target atom is initially at rest in the laboratory system.

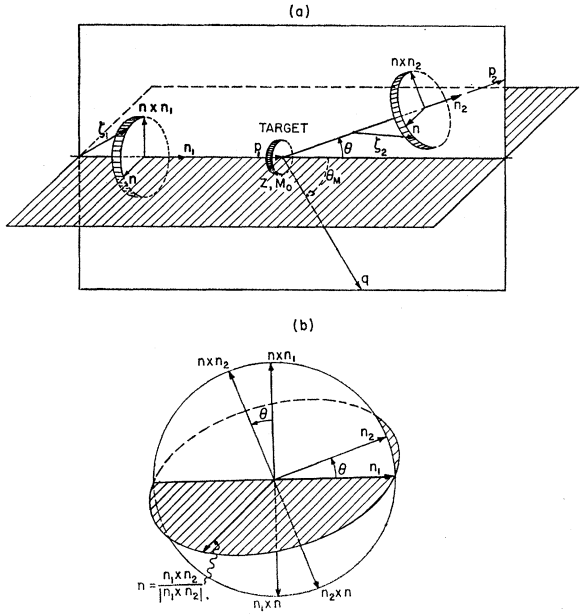

FIG. 1. Diagram for electron elastic scattering by an atom initially at rest in the laboratory system. In part (a), the vectors $\mathbf{p}_1$, $\mathbf{p}_2$, and $\mathbf{q}$ lie in the scattering plane with scattering angles θ for the scattered electron and θ_M for the recoiling atom. The directions of the unit spin vectors, ζ_1 and ζ_2, are specified in the electron rest system by the unit orthogonal vectors (defined in Sec. II) $\mathbf{n}_1$, $\mathbf{n}\times\mathbf{n}_1$, $\mathbf{n}$ and $\mathbf{n}_2$, $\mathbf{n}\times\mathbf{n}_2$, $\mathbf{n}$, for the incident and scattered electron, respectively. In part (b), the relationship of the coordinate systems for the incident and scattered electron is shown in further detail.

The relationship between the scattering angle in the center-of-momentum and the laboratory systems is given as

$$\cos\theta'=\frac{\cos\theta-\beta E_2/p_2}{(\sin\theta)(1-\beta^2)^{\frac{1}{2}}}, \quad (3.09)$$

where β is defined in Eq. (3.07) and p_2 is given in Eq. (3.01). The transformation for the atomic recoil angle θ_M is given as

$$\cos\theta_M'=\frac{(2-\beta^2)\cos^2\theta_M-1}{\beta^2\cos^2\theta_M-1}, \quad (3.10)$$

where β is defined in (3.07).

IV. RADIATIVE EFFECTS

Photon emission is inherent in the process of electron scattering. In fact, *every* electron that is detected after being scattered by a pure Coulomb field has emitted photons with a probability of unity (S 49). Because of this radiative effect in which most of the photon energies are concentrated in the very low or infrared region, an incident beam of monoenergetic electrons scattered at a given angle by a Coulomb field has an energy distribution in the form of an ostensible "elastic" peak plus a low-energy tail. In an arbitrary distinction, this quasi-elastic peak is identified with so-called "soft" or infrared photon emission (J 54, Y 61) and the low-energy tail is identified with "hard" photon emission.

The crux in the process of electron Coulomb scattering lies in the so-called "soft" photon region where $T_2\rightarrow T_1$. In this "soft" region, the inelastic process in which photons are emitted becomes indistinguishable from the idealized elastic process in which photons are not emitted, because all measurements involve a finite energy interval. *This condition has the consequence that the cross section for the elastic process $d\sigma/d\Omega$ is an idealized cross section and requires a radiative correction in order to predict the results of measurements that apply to a finite energy interval.* This radiative correction is calcu-

lated (S 49) from a combination of the matrix elements for real and virtual photon processes which *together* give the necessary result that the cross section integrated over a finite energy interval ΔE in the region of $T_2 \approx T_1$, is finite even though the inelastic cross section $d^2\sigma_B/d\Omega dT_2$ differential in the angle and energy of the scattered electron diverges as $T_2 \rightarrow T_1$. In other words, in the "soft" photon region it is necessary to introduce a composite, integrated cross section

$$\int_{T_1-\Delta E}^{T_1} (d^2\sigma/d\Omega dT_2)\, dT_2$$

which is defined by the equation:

$$\int_{T_1-\Delta E}^{T_1} \frac{d^2\sigma}{d\Omega dT_2}\, dT_2 = \int_{T_1-\Delta E}^{T_1} \frac{d^2\sigma_B}{d\Omega dT_2}\, dT_2 + \frac{d\sigma'}{d\Omega}, \quad (4.01)$$

where $d^2\sigma_B/d\Omega dT_2$ is the bremsstrahlung cross-section differential with respect to the energy and angles of the scattered electron and integrated over all photon angles, and $d\sigma'/d\Omega$ is the elastic cross section with the inclusion of the virtual photon part of the radiative correction. The elastic cross section without the inclusion of the virtual photon part of the radiative correction is designated as $d\sigma/d\Omega$ and is evaluated by the formulas in Secs. VI and VII. Formulas for the inelastic cross section $d^2\sigma_B/d\Omega dT_2$ are given in the following discussion and formulas for the composite cross section defined by Eq. (4.01) are given in the following subsections A and B.

The energy distribution of the scattered electrons in the "hard" photon region where $T_2 < T_1 - \Delta E$ is given by the differential bremsstrahlung cross section $d^2\sigma_B/d\Omega dT_2$. An explicit formula for this cross section was calculated in the first Born approximation for a point nucleus neglecting recoil and target spin effects by Racah (R 34) and later by McCormick, Keiffer, and Parzen (M 56) and is given in the following condensed form by Maximon and Isabelle (M 64):

$$\begin{aligned}\frac{d^2\sigma_B}{d\Omega dT_2} = -\frac{r_0^2}{2\pi}\frac{Z^2}{137}\frac{p_2}{p_1}\frac{4}{kQ^4}\{&(\gamma/\sinh\gamma)\\ &\times[k^2Q^2+\tfrac{1}{2}(Q^2+2)(4E_1E_2-Q^2)]\\ &+[k\ln(E_2+p_2)/2p_2^3][4E_2^2(E_1^2+E_2^2)-2E_1k\\ &+4(E_1E_2+1)-Q^2(E_1E_2+p_2^2)+(16E_2p_1^2\sin^2\theta/Q^4)\\ &\times(2E_1p_2^2-3E_2^2k)]-(k\ln(E_1+p_1)/2p_1^3)\\ &\times[4E_2^2(E_1^2+E_2^2)+2E_2k+4(E_1E_2+1)\\ &-Q^2(E_1E_2+p_2^2)+(16E_1p_2^2\sin^2\theta/Q^4)(2E_2p_1^2-3E_1^2k)]\\ &+(8k^2\sin^2\theta/p_1^2p_2^2Q^4)[2p_1^2p_2^2(E_1^2+E_2^2-E_1E_2)\\ &+3(E_1^2-E_2^2)^2]+(k^2/p_1^2p_2^2)\\ &\times[(p_1^2+p_2^2)(E_1E_2+1)-3(E_1+E_2)^2]\\ &-[(4E_1E_2-Q^2)/2p_1^2p_2^2][p_1^4+p_2^4-k^2(E_1E_2+1)]\},\end{aligned} \quad (4.02)$$

where $Q^2 = Q_B^2 = (\mathbf{p}_1-\mathbf{p}_2)^2-k^2$, $k = T_1-T_2$ (for infinitely heavy nucleus), and $\sinh\frac{1}{2}\gamma = \frac{1}{2}Q$.

Another formula for this cross section, which is calculated in the first Born approximation with the inclusion of arbitrary atomic screening as well as size and magnetic effects of the nucleus, is given in integral form (M 64, G 64) by the following expression[1]:

$$\frac{d^2\sigma_B}{d\Omega dT_2} = \frac{r_0^2}{2\pi}\frac{Z^2}{137}\frac{p_2}{p_1}\int_{y_-^2}^{y_+^2}\frac{d(y^2)}{y^4}\Big[\{G_E(y)-F(y)\}^2R(y) + \frac{J+1}{3J}\left(\frac{ym_0}{2M_0}\right)^2\frac{G_M^2(y)}{Z^2}R_M(y)\Big], \quad (4.03)$$

where the function $R(y)$ is given from the results of Maximon and Isabelle (M 64) as

$$\begin{aligned}R(y) = &[2/(Q^2+k^2)^{\frac{1}{2}}]+(Q^2-y^2)^{-1}(\Delta_1^{-1}-\Delta_2^{-1})\\ &\times[y^4+Q^4-4y^2(E_1^2+E_2^2-1)-16E_1E_2]\\ &-[(4E_2^2-y^2)/\Delta_1^3][Q^2(Q^2-2kE_2)-y^2(Q^2+2kE_1)]\\ &+[(4E_1^2-y^2)/\Delta_2^3][Q^2(Q^2+2kE_1)-y^2(Q^2-2kE_2)]\end{aligned}$$

and the function $R_M(y)$ is given from the results of Ginsberg and Pratt (G 64) as

$$\begin{aligned}R_M(y) = &-[2/(Q^2+k^2)^{\frac{1}{2}}]-(Q^2-y^2)^{-1}(\Delta_1^{-1}-\Delta_2^{-1})\\ &\times[y^4+Q^4-8Q^2+4y^2(E_1^2+E_2^2+1)+16(E_1E_2-1)]\\ &-[(4p_2^2+y^2)/\Delta_1^3][Q^2(Q^2+2kE_2)-y^2(Q^2+2kE_1)]\\ &+[(4p_1^2+y^2)/\Delta_2^3][Q^2(Q^2\quad\ 2kE_1)-y^2(Q^2-2kE_2)].\end{aligned}$$

In the above equations,

$$y_\pm = (Q^2+k^2)^{\frac{1}{2}}\pm k,$$

$$\Delta_1^2 = (E_1y^2-E_2Q^2)^2-(y^2-Q^2)^2+4y^2k^2,$$

$$\Delta_2^2 = (E_2y^2-E_1Q^2)^2-(y^2-Q^2)^2+4y^2k^2.$$

Also as shown by the definitions in Sec. II, $G_E(y)$ and $F(y)$ are the nuclear and atomic charge form factors, respectively, $G_M(y)$ is the nuclear magnetic form factor [formula (1A-104)], and the parameter y is equal to the momentum transferred to the atom in the collision. Because this formula is based on the first Born approximation, it is valid only for low atomic numbers. For the case of a point nucleus where $G_E(y)$ is equal to unity and $G_M(y)$ and $F(y)$ are equal to zero, Eq. (4.03) reduces to the high-energy limit of the Racah formula (4.02). In the region where the momentum transfer y is much less than unity, atomic screening [given by $F(y)$] is important. In the region where y is much greater than unity, both the size [given by

[1] We are grateful to Dr. L. C. Maximon and Dr. R. B. Pratt for providing preprints of their calculations before publication.

$G_E(y)$] and the magnetic effects [given by $G_M(y)$] of the nucleus are important.

For the case where $T_1 \gg 1$ and $q_0 \lesssim 1$, recoil, spin, and size effects of the nucleus can be neglected. Therefore, a formula for the cross section in this region, which includes atomic screening effects can be obtained in the following analytical form from Olsen's results (O 63):

$$\frac{d^2\sigma_B}{d\Omega dT_2} = -\frac{r_0^2}{2\pi}\frac{Z^2}{137}\frac{E_2^2}{k^2}\frac{4}{k}\zeta^2\left\{\frac{\gamma}{\sinh\gamma}\left[(E_1^2+E_2^2)\zeta^{-1}+(2E_1E_2/k)^2\right]\left[1-F(q_0)\right]^2+2\left[\mu-\frac{E_1}{k}\ln\frac{E_1}{k}+\frac{E_2}{k}\ln\frac{E_2}{k}-\frac{E_1^2+E_2^2}{2k^2}\right]\times\left[E_1^2+E_2^2-4E_1E_2\zeta^2w^2\right]+8E_1E_2w^2\zeta^2\times\left[\frac{E_1E_2(E_1+E_2)}{k^3}\ln\frac{E_2}{E_1}+\frac{E_1^2+E_2^2}{2k^2}+1\right]\right\}, \quad (4.04)$$

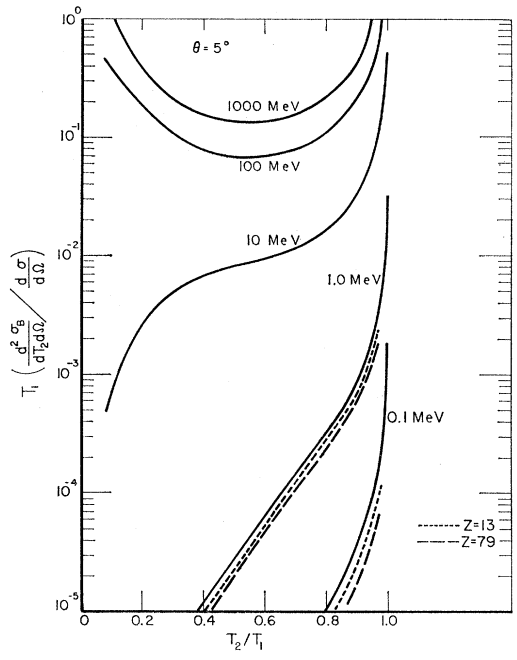

FIG. 2. Dependence of the bremsstrahlung cross section on the electron recoil energy T_2 for an electron scattering angle θ of 5 deg and for initial electron kinetic energies of 0.1, 1.0, 10.0, 100, and 1000 MeV. The results are given in terms of the ratio

$$T_1[(d^2\sigma_B/dT_2d\Omega)/(d\sigma/d\Omega)],$$

where T_1 is the initial electron kinetic energy, $(d^2\sigma_B/dT_2d\Omega)$ is the bremsstrahlung cross section given by the Racah formula (4.02) in Sec. IV, and $d\sigma/d\Omega$ is the elastic scattering cross section given by the Mott–Born formula (1A–101). Both cross sections are evaluated with the first Born approximation for a point nucleus. The dashed lines for 0.1 and 1.0 MeV show screening effects for aluminum and gold, and were obtained from Eq. (4.03) with $G_E(y)$ equal to unity, $F(y)$ given by the Molière form factor in formula (1A–102b) and $R_M(y)$ equal to zero.

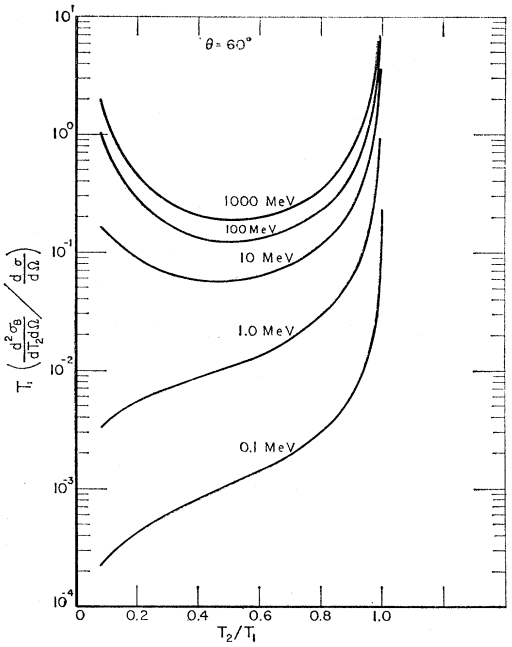

FIG. 3. Same as Fig. 2 except that the electron scattering angle is 60 deg and no screening effects are shown.

where

$$w=(E_1E_2/k)\theta,$$

$$\zeta=(1+w^2)^{-1},$$

$$\sinh\tfrac{1}{2}\gamma=k(4E_1E_2\zeta)^{-\frac{1}{2}},$$

$$\mu=\ln(2E_1E_2/k)+F(k/2E_1E_2\zeta),$$

and $F(q_0)$ is the conventional atomic form factor defined in formula (1A-102). Values for $F(k/2E_1E_2\zeta)$ with Molière screening are given in Table I in Ref. O 59.

The above formulas (4.02)–(4.04) have certain limitations. First, these formulas do not include recoil effects of the nucleus, which may be neglected for $(q_0^2/2E_1)(m_0/M_0)\ll 1$. Second, these formulas are calculated in the first Born approximation and therefore may be expected to be inaccurate for large atomic numbers as indicated for example by Fig. 22 for related measurements in Ref. K 59. Correction factors which may be used with formula (4.02) in the soft-photon region in order to account for the breakdown of the Born approximation are suggested by Eq. (4.10) in Sec. IVA. Because of the restrictions imposed by the Born approximation, the accuracy of formula (4.03) is uncertain for large atomic numbers, even though it includes corrections for the atomic size and for the magnetic and size effects of the nucleus.

Examples of the behavior of the cross-section ratio, $T_1[(d^2\sigma_B/d\Omega dT_2)/(d\sigma/d\Omega)]$, as a function of T_2 for initial electron kinetic energies of 0.1, 1.0, 10, 100, and 1000 MeV are shown in Figs. 2, 3, 4, and 5 for electron scattering angles of 5, 60, 120, and 180 deg, respec-

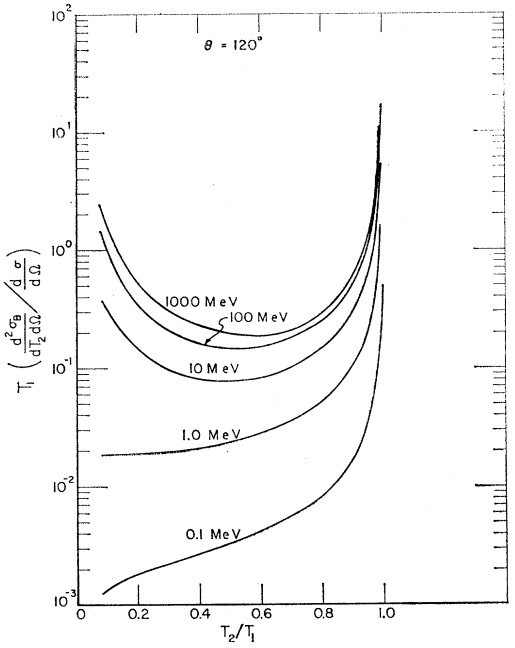

FIG. 4. Same as Fig. 2 except that the electron scattering angle is 120 deg and no screening effects are shown.

tively. These cross sections were evaluated from the Racah formula (4.02) for $d^2\sigma_B/d\Omega dT_2$, and from the Mott–Born formula (1A-101) in Sec. VII for $d\sigma/d\Omega$. For the region in which the momentum transfer is

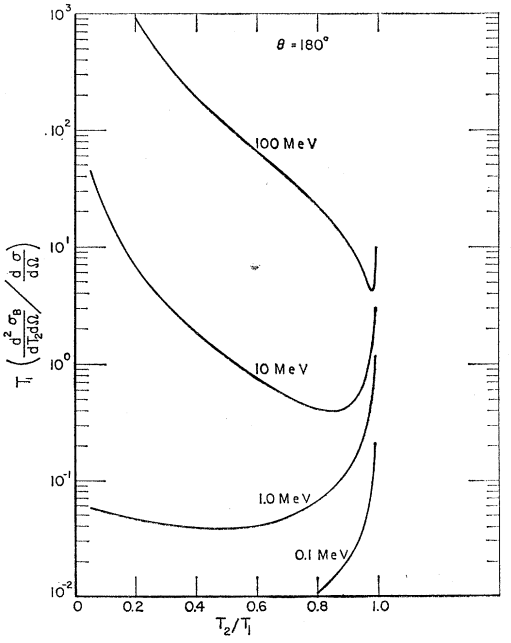

FIG. 5. Same as Fig. 2 except that the electron scattering angle is 180 deg, 1000-MeV results are omitted, and no screening effects are shown.

much larger than unity, these curves must include corrections for the size and magnetic effects of a given nucleus as shown by formula (4.03). The screened cross-section evaluation from formula (4.03) with the Molière form factor for $F(y)$ [given in formula (1A-102b)] is shown by the dashed lines for the 5-deg angle in Fig. 2. Also, Figs. 2–5 show that for $T_1 \gg 1$ and $q_0 \gg 1$, the cross section $d^2\sigma_B/d\Omega dT_2$ increases as T_2 decreases in the low-energy region. This increase, which is more pronounced as T_1 becomes larger, was recognized by Keiffer and Parzen (K 56) who showed that it leads to a low-energy peak in the region where p_2 is of the order of unity.

The radiative effects discussed above for the "soft" and "hard" photon energy regions must be related to the particular experimental situation. For example, the

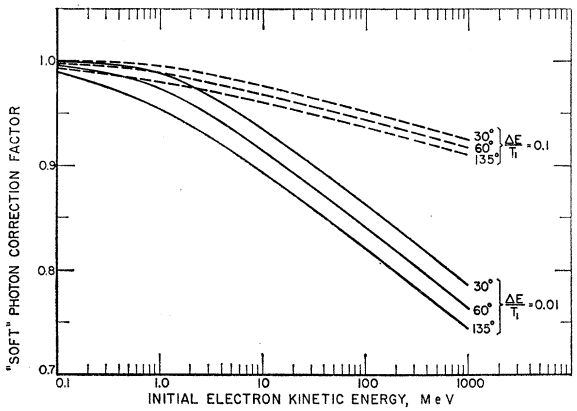

FIG. 6. Dependence of the "soft" photon correction on the initial electron kinetic energy for electron scattering angles of 30, 60, and 135 deg and for values of ΔE equal to $10^{-1}T_1$ and $10^{-2}T_1$. This correction is defined in Eq. (4.05) and is evaluated from Eq. (4.06).

cross section for electron Coulomb scattering at a given angle has different values depending on whether the electron detector accepts (A) electrons confined to a small energy interval at the maximum energy, or (B) all electrons irrespective of their final energies. Case A refers to the "soft" photon correction and case B refers to the "soft plus hard" photon correction, which are discussed respectively in the following subsections A and B. It should be noted that these corrections are obtained with the neglect of atomic screening, nuclear size, and nuclear spin and recoil effects. However, these latter effects probably have a much smaller influence on the radiative correction factor which is a cross-section ratio (see Secs. IVA and IVB) than on the elastic scattering cross section.

A. The "Soft" Photon Correction

The first successful treatment of the "soft" photon region was given by Schwinger (S 49). Schwinger calcu-

lated the "soft" photon correction factor, $1-\delta_R$, which is defined in the following equation by the ratio

$$\int_{T_1-\Delta E}^{T_1} \frac{d^2\sigma}{d\Omega dT_2}\, dT_2 \Big/ \frac{d\sigma}{d\Omega} = 1-\delta_R, \qquad (4.05)$$

where the "soft" photon energy interval is contained between zero and ΔE with $\Delta E \ll T_1$, $d\sigma/d\Omega$ is the idealized elastic cross section, and

$$\int_{T_1-\Delta E}^{T_1} (d^2\sigma/d\Omega dT_2)\, dT_2$$

is defined in Eq. (4.01) and in Sec. II. The radiative correction δ_R which is given by Schwinger (S 49) in terms of an integral, may be written in the following form (O 64):

$$\delta_R = \frac{2}{137\pi}\left[\left(\ln\frac{E_1}{\Delta E} - \frac{13}{12}\right)(2\eta\coth 2\eta - 1) + \frac{2\eta}{3\sinh 2\eta}(\coth^2\eta - \tfrac{7}{4}) - \tfrac{1}{3}(\coth^2\eta - \tfrac{29}{12}) - L + \frac{\eta\tanh\eta}{2E_1(1-\beta_1^2\sin^2\tfrac{1}{2}\theta)}\right], \qquad (4.06)$$

where η is defined by $q_0 = 2\sinh\eta$ and

$$L = -\tfrac{1}{2}\coth 2\eta\left\{\frac{1}{2}\ln\left(\frac{1+b}{1-b}\right)\ln\left[\frac{4a^2(a+b)^2}{(1-b^2)(1-b)^2}\right] + \frac{1}{2}\ln\left(\frac{a+b}{a-b}\right)\ln\left[\frac{(1-b)^4}{4(a^2-b^2)}\right] + \ln\left(\frac{a+b}{2a}\right)\ln\left(\frac{a-b}{2a}\right)\right.$$
$$- \ln\left(\frac{1+b}{2}\right)\ln\left(\frac{1-b}{2}\right) + 2L_2\left(\frac{a+b}{2a}\right) - 2L_2\left(\frac{1+b}{2}\right) + 2L_2\left(\frac{a-b}{1-b}\right) - 2L_2\left(\frac{a+b}{1+b}\right) + 2\eta\ln\left(\frac{\cosh\eta}{2E_1^2}\right) + L_2\left(\frac{1}{1+e^{2\eta}}\right)$$
$$\left. - L_2\left(\frac{1}{1+e^{-2\eta}}\right)\right\} - \ln 2E_1 + \frac{1}{2\beta_1}\left(\frac{1+\beta_1}{1-\beta_1}\right)$$

with

$$a = \frac{1-\beta_1\cos\tfrac{1}{2}\theta}{1+\beta_1\cos\tfrac{1}{2}\theta}, \qquad b = \left(a\frac{1-\cos\tfrac{1}{2}\theta}{1+\cos\tfrac{1}{2}\theta}\right)^{\frac{1}{2}} = \sqrt{a}\tan\tfrac{1}{4}\theta,$$

and $L_2(x)$ = Euler's dilogarithm (Mi 49). Values for $L_2(x)$ are given in Table XIII in Sec. X

In the nonrelativistic region with $\beta_1 \ll 1$,

$$\delta_R \approx (8/3)(\beta_1^2/137\pi)\sin^2\tfrac{1}{2}\theta[\ln(1/2\Delta E) + (19/30)]. \qquad (4.07)$$

The term containing 19/30 comes from the anomalous magnetic moment and vacuum polarization effects, indicating that even in the low-energy region, electron-spin effects are important. In the extreme-relativistic large-angle region with $\beta_1 \approx 1$ and $q_0^2 \gg 1$, δ_R may be expressed by the following equation (O 64)[2]:

$$\delta_R = (4/137\pi)\{[\ln(E_1/\Delta E) - \tfrac{13}{12}](\ln q_0 - \tfrac{1}{2}) + \tfrac{17}{72} + \tfrac{1}{4}[(\pi^2/6) - L_2(\cos^2\tfrac{1}{2}\theta)]\}. \qquad (4.08)$$

Formula (4.08) is estimated to have better than 1% accuracy even for moderate electron energies of the order of 1 MeV. The radiative correction δ_R has been evaluated from Eq. (10) in Ref. S 49 by Elton and Robertson (E 52) for particular values of T_1, θ, and ΔE, and their results are given in Table I.

A more complete summary of the "soft" photon correction factor, $1-\delta_R$, is shown in Fig. 6 for (a) electron kinetic energies ranging from 10^{-1} to 10^3 MeV, (b) electron scattering angles of 30, 60, and 135 deg, and (c) values of ΔE equal to $10^{-2}T_1$ and $10^{-1}T_1$. These curves which were computed from Eq. (4.06) show that the "soft" photon correction becomes more important with increasing values of θ, E_1, and $1/\Delta E$. In the limits where θ and p_1 approach zero, it can be shown that the radiative correction factor, $1-\delta_R$, is equal to unity.

[2] The term $\frac{1}{4}\{\pi^2/6 - L_2(\cos^2\frac{1}{2}\theta)\}$ is equal to Schwinger's integral, $\Phi(\vartheta)$, Eq. (10) in Ref. S 49. It should be noted that the value of $\Phi(\vartheta)$ at $\vartheta=\pi/2$ given by Schwinger and quoted by Jauch and Rohrlich (J 54, p. 339), is $\Phi(\pi/2)=0.292$. The correct value is $\Phi(\pi/)2 = \frac{1}{4}[\pi^2/6 - L_2(\frac{1}{2})] = 0.266$. It should furthermore be noted that the approximation for $\Phi(\vartheta)$ given by Eq. (11) in Ref. S 49 exceeds the correct value by 19% for $\vartheta=\pi/2$, rather than 8.6% as stated by Schwinger.

TABLE I. Evaluation of the radiative correction term δ_R.

	100 δ_R								
0.511 T_1(MeV)...		2.5			4.0			9.5	
θ (deg)	45	90	135	45	90	135	45	90	135
511 ΔE (keV)									
10	4.8	7.4	8.7	6.9	9.9	11.3	12.4	15.9	17.5
25	3.9	6.0	7.1	5.7	8.1	9.3	10.5	13.5	14.8
50	3.2	5.0	5.9	4.7	6.8	7.9	9.0	11.7	12.8
100	2.5	3.9	4.7	3.8	5.5	6.4	7.6	9.9	10.8

Equation (4.08) for the extreme-relativistic, large-angle region, is valid only for $\Delta E \ll T_1$. For the case where ΔE is comparable to T_1, it is necessary to use the following expression (O 64):

$$\delta_R=\frac{4}{137\pi}\Big\{[\ln(E_1/\Delta E)-\tfrac{13}{12}][\ln q_0-\tfrac{1}{2}]+\tfrac{17}{72}+\tfrac{1}{4}[(\pi^2/6)-L_2(\cos^2\tfrac{1}{2}\theta)]+\tfrac{1}{8}\{(\ln x)^2-(2\ln x)/x-4\ln x\ln(1-x)$$
$$+4[(\pi^2/6)-L_2(x)]+x^2-1\}+\tfrac{1}{4}\ln 2E_1[\ln x+\tfrac{5}{2}-x-\tfrac{1}{2}x^2-x^{-1}]+(\ln\sin\tfrac{1}{2}\theta/2\cos^2\tfrac{1}{2}\theta)(\ln x-x+1)$$
$$-(8\cos^2\tfrac{1}{2}\theta)^{-1}[\ln x-x+x^{-1}+\tfrac{1}{2}x^2-\tfrac{1}{2}]\Big\}, \quad (4.09)$$

where $x=1-(\Delta E/E_1)$ and $L_2(x)=$ Euler's dilogarithm (see Table XIII). This formula is valid provided that p_2^2 is large compared to unity, which restricts the formula to the region above the low-energy peak predicted by formula (4.02). Another calculation which applies to the region where ΔE is comparable to T_1 but which is less accurate than formula (4.09) because of additional approximations is given by Schiff (S 52). As pointed out by Schiff (S 52), the value of δ_R for these large ΔE values changes sign and the radiative correction becomes positive rather than negative as in the case of formula (4.06) where $\Delta E \ll T_1$.

A unified treatment of the "soft" photon correction for a class of high-energy scattering experiments is given by Meister and Yennie (M 63). Other general treatments of radiative effects are given by Yennie, Frautschi, and Suura (Y 61) and by Mahanthappa (M 62). For the special case of high-energy electron–proton scattering, radiative corrections are particularly important and are complicated by recoil effects which are not discussed here and which are estimated in some detail by Tsai (T 61) and by Krass (K 62).

The radiative correction δ_R which is given in Eq. (4.06) was calculated by Schwinger in the first Born approximation for the interaction between the electron and the nuclear potential. Suura (S 55) has shown that in the high-energy region, there is a negligible difference in the radiative correction obtained by calculations either to the first order or to all orders of the Born approximation for the nuclear potential. This latter result suggests the following approximate relationship between a first Born and an exact calculation for the bremsstrahlung cross section $d\sigma_B/d\Omega dT_2$ in the soft-photon region:

$$\frac{d^2\sigma_B}{d\Omega dT_2}(\text{EXACT})$$
$$\approx\left(\frac{d\sigma}{d\Omega}(\text{EXACT})\Big/\frac{d\sigma}{d\Omega}(\text{BORN})\right)\frac{d^2\sigma_B}{d\Omega dT_2}(\text{BORN}), \quad (4.10)$$

where $(d^2\sigma_B/d\Omega dT_2)$(BORN) is given by the Racah formula (4.02) and the ratio $[(d\sigma/d\Omega)(\text{EXACT})]/[(d\sigma/d\Omega)(\text{BORN})]$ is evaluated for selected values of Z, E_1, and θ in some of the curves shown in Sec. VIII. Although the simple relationship given by Eq. (4.10) has not been experimentally verified, it may be expected to give fairly accurate results providing it is applied in the region where the recoil-electron energy T_2 is such that $T_1-T_2 \ll T_1$.

The "soft" photon correction, defined in Eq. (4.05) is used for quantitative predictions of electron Coulomb scattering in a specific experimental situation (see Ref. T 60) in which the detector of the scattered electrons is operated as an energy-sensitive spectrometer with a given energy resolution. (This correction is *not* applicable to the case in which the electron detector accepts all electrons irrespective of their final energies.) Such predictions require a careful interpretation of the experimental data obtained with the particular spectrometer. For example, the following results apply to the data obtained either with a pulse-height spectrometer or with a magnetic spectrometer.

With a pulse-height spectrometer, the detection of an electron is indicated by a pulse at the spectrometer output. Then for given values of T_1, θ, and Z, the number of pulses per unit pulse-height interval at the

pulse height h is defined as $N(T_1, h)$ and is given by the following expression:

$$N(T_1, h) = mn\Delta\Omega \int_0^{T_1} \frac{d^2\sigma}{d\Omega dT_2} R(T_2, h)\, dT_2, \quad (4.11)$$

where $\Delta\Omega$ is the solid angle subtended by the entrance aperture of the spectrometer from a point at the center of the target, m is the number of electrons incident on the target, n is the number of target atoms per cm², $d^2\sigma/d\Omega dT_2$ is defined in integral form in Eq. (4.01), and $R(T_2, h)$ is the spectrometer response function which gives the probability that an electron with energy T_2 will be detected at the pulse height h. In order to interpret the measured pulse-height spectrum $N(T_1, h)$ in terms of the "soft" photon correction factor defined by Eq. (4.05), the following simplifying assumptions are made about $R(T_2, h)$: (a) for a given T_2, $R(T_2, h)$ has a rectangular line shape with a width Δh and a midpoint $h_2 = bT_2$ (where b is a constant), such that the spectrometer resolution r is equal to $\Delta h/h_2$; (b) $R(T_2, h)$ is a function such that $R(T_2, h) = 0$ if $h \leq h_2(1-r/2)$ or $h \geq h_2(1+r/2)$; and (c)

$$\int_0^\infty R(T_2, h)\, dh = 1.$$

With the above assumptions, the following relationship is obtained by integrating Eq. (4.11):

$$\frac{1}{mn\Delta\Omega} \int_{h_c}^\infty N(T_1, h)\, dh = \int_{T_1-\Delta E}^{T_1} \frac{d^2\sigma}{d\Omega dT_2} dT_2 + \int_{T'}^{T_1-\Delta E} Y \frac{d^2\sigma_B}{d\Omega dT_2} dT_2, \quad (4.12)$$

where T' is equal to $[(2-r)/(2+r)](T_1-\Delta E)$ and Y, which is equal to

$$\int_{h_c}^\infty R(T_2, h)\, dh,$$

is less than unity in the energy interval for T_2 specified by the integral limits $T_1-\Delta E$ and T'. The integral

$$\int_{h_c}^\infty N(T_1, h)\, dh$$

is the area measured under the line shape with a lower cutoff value of h_c in the pulse-height distribution. The energy interval ΔE is then determined from the experimental quantities h_c, b, and r, such that $\Delta E = T_1 - [2h_c/b(2-r)]$. Because Y is less than unity and the cross section $d^2\sigma_B/d\Omega dT_2$ decreases rapidly as T_2 decreases, the second term on the right-hand side of Eq. (4.12) is negligible compared to the first term. Therefore for this case the integrated cross section defined in Eqs. (4.01) and (4.05) is simply related to the number of counts in the elastic line shape area of the measured pulse-height distribution.

With the magnetic spectrometer operating at a given magnetic field H, electrons are accepted in a momentum interval corresponding to the range $H(\rho_1-\rho_2)$, where ρ_1 and ρ_2 are the effective radii of curvature limits of the spectrometer. The spectrometer focuses electrons with a given momentum in a finite region corresponding to an interval $H\Delta\rho$. For the simplifying assumption that $\Delta\rho \ll (\rho_1-\rho_2)$, the elastic peak occurs at a value of $H = H_1$ such that the momentum limits, p_1 (or $H_1\rho_1$) and p_2 (or $H_1\rho_2$), correspond to the energies T_1 and $T_1-\Delta E$, respectively. It then follows that for given values of T_1, θ, and Z, the number of electrons $N(T_1, H_1)$ per unit momentum interval at the peak field H_1 is given by the expression

$$\int_{T_1-\Delta E}^{T_1} \frac{d^2\sigma}{d\Omega dT_2} dT_2 = \left(\frac{p_1-p_2}{\Delta\Omega mn}\right) N(T_1, H_1), \quad (4.13)$$

where the integrated cross section

$$\int_{T_1-\Delta E}^{T_1} (d^2\sigma/d\Omega dT_2)\, dT_2$$

is defined in Eqs. (4.01) and (4.05). For the general case in which $\Delta\rho$ is comparable to $(\rho_1-\rho_2)$, the analysis becomes more complicated and must be carried through by a procedure similar to the pulse-height analysis given above.

As a final word of caution, the "soft" photon correction shown by the curves in Fig. 6, gives no information about the energy and angular distribution of the electrons in the "hard" photon region where $0 \leq T_2 \leq T_1-\Delta E$. This means that at a given scattering angle, the ratio

$$\int_{T_1-\Delta E}^{T_1} \frac{d^2\sigma}{d\Omega dT_2} dT_2 \Big/ \int_0^{T_1-\Delta E} \frac{d^2\sigma_B}{d\Omega dT_2} dT_2$$

of the area under the elastic peak ("soft" photon region) to the area under the low-energy tail ("hard" photon region shown by the curves in Figs. 2–5) *cannot be determined from the value of the "soft" photon correction.* The kinematics changes drastically in the two regions and it is necessary to consider each region separately as shown in the following discussion of the "soft plus hard" photon correction.

B. The "Soft plus Hard" Photon Correction

The "soft plus hard" photon correction factor is required for the calculation of the total number of electrons measured at a given angle with an energy insensitive detector that accepts all electrons irrespective of their final energy.[3] This correction factor differs from the "soft" photon correction factor in Eq. (4.05) by the addition of an extra term containing the appropriate bremsstrahlung cross section. Specifically, the

[3] The additional influence of inelastic processes other than bremsstrahlung is not considered in this case.

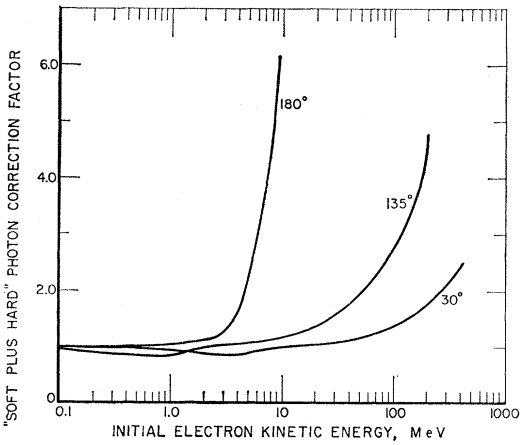

FIG. 7. Dependence of the "soft plus hard" photon correction on the initial electron kinetic energy for electron scattering angles of 30, 135, and 180 deg. This correction is evaluated from Eq. (4.14) where the first term (soft) is given by Eq. (4.05) and the second term (hard) is given by the Racah formula (4.02) for $d^2\sigma_B/d\Omega dT_2$ and by the Mott–Born formula (1A–101) for $d\sigma/d\Omega$. For the energies larger than 10 MeV, these curves were evaluated from Eq. (4.16).

"soft plus hard" photon correction factor is defined as the ratio in the following equation:

$$\int_0^{T_1}\frac{d^2\sigma}{d\Omega dT_2}\,dT_2\Big/\frac{d\sigma}{d\Omega}=\int_{T_1-\Delta E}^{T_1}\frac{d^2\sigma}{d\Omega dT_2}\,dT_2\Big/\frac{d\sigma}{d\Omega}+\int_0^{T_1-\Delta E}\frac{d^2\sigma_B}{d\Omega dT_2}\,dT_2\Big/\frac{d\sigma}{d\Omega},\quad(4.14)$$

where the first term on the right-hand side is the "soft" photon correction given in Eq. (4.05), the second term is the "hard" photon correction, and the cross-section symbols are defined in Sec. II.

In the nonrelativistic region with $\beta_1\ll 1$, Schwinger (S 49) gives the following approximate expression for the "soft plus hard" photon correction factor:

$$\int_0^{T_1}\frac{d^2\sigma}{d\Omega dT_2}\,dT_2\Big/\frac{d\sigma}{d\Omega}=1-\tfrac{8}{3}(\beta_1^2/137\pi)\sin^2\tfrac{1}{2}\theta\times[\ln(8T_1)^{-1}+\tfrac{19}{30}+(\pi-\theta)\tan\tfrac{1}{2}\theta+(\cos\theta/\cos^2\tfrac{1}{2}\theta)\times\ln(\csc\tfrac{1}{2}\theta)].\quad(4.15)$$

In the extreme relativistic region for large scattering angles, Keiffer and Parzen (K 56) evaluated numerically the integrated cross section,

$$\int_0^{T_1-\Delta E}(d^2\sigma_B/d\Omega dT_2)\,dT_2,$$

shown by the "hard" photon contribution in Eq. (4.14). An analytical formula for the "soft plus hard" photon correction factor for this case is given as (O 64):

$$\int_0^{T_1}\frac{d^2\sigma}{d\Omega dT_2}\,dT_2\Big/\frac{d\sigma}{d\Omega}=1+(E_1/137\pi)\times[\sin\theta/(1+\cos\theta)^3]\{\pi-\theta-\sin\theta\cos\theta+2\cos\theta\times[2\Lambda_2(\tan\tfrac{1}{2}\theta)-\pi\ln(\tan\tfrac{1}{2}\theta)]\},\quad(4.16)$$

where $\Lambda_2(x)=(1/2i)\{L_2(ix)-L_2(-ix)\}=$ Im $L_2(ix)$ and $L_2(z)=$ Euler's dilogarithm (Mi 49). For this case, the low-energy peak given by the "hard" photon term in Eq. (4.14) is dominant over the "soft" photon term and the "soft plus hard" photon correction factor becomes larger than unity.

In order to evaluate this correction for the general case given in Eq. (4.14), it is necessary to use calculations that are consistent for the "soft" and "hard" terms to the extent that the sum is independent of the choice of ΔE. Now the Schwinger calculations for the "soft" correction [Eqs. (4.05) and (4.06)] are Z-independent. Therefore, if one uses the Schwinger calculations for the first term in (4.14), then the second term in (4.14) (the "hard" correction) must be chosen to be independent of Z. This will be the case if the second term in (4.14) is evaluated from the unscreened first Born calculations of Racah [Eq. (4.02)] and of Mott [formula (1A–101)]. With the first Born unscreened calculations specified above, the behavior of the "soft plus hard" photon correction defined by Eq. (4.14) is shown in Fig. 7. The curves for 30° and 135° in the energy region above 10 MeV are evaluated from Eq. (4.15). The curves in Fig. 7 show the dependence of the correction on the initial electron kinetic energy in the region from 0.1 to 1000 MeV for electron scattering angles of 30, 135, and 180 deg. It is interesting to note that this correction becomes much larger than unity as the electron energy increases, particularly for the larger angles. However, because these results are obtained with first Born calculations for an unscreened point nucleus, Z-dependent effects are not revealed and the accuracy of this correction factor is uncertain.

For the total idealized elastic cross section σ, the "soft plus hard" photon correction is obtained by integrating the cross sections in Eq. (4.14) over the electron scattering angles and is given by the following expression:

$$\frac{1}{\sigma}\int d\Omega\int_0^{T_1}\frac{d^2\sigma}{d\Omega dT_2}\,dT_2=\frac{1}{\sigma}\int d\Omega\int_{T_1-\Delta E}^{T_1}\frac{d^2\sigma}{d\Omega dT_2}\,dT_2+\frac{1}{\sigma}\int d\Omega\int_0^{T_1-\Delta E}\frac{d^2\sigma_B}{d\Omega dT_2}\,dT_2.\quad(4.17)$$

The important contributions to the first ("soft" correction) and second ("hard" correction) terms on the right-hand side of Eq. (4.17) come from the region of small q_0 values (or large impact parameters) where

TABLE II. Classification of cross-section formulas for electron scattering with radiation.

Cross section	Formula	Principal authors	Approximations
$d^2\sigma_B/d\Omega dT_2$	(4.02)	Racah	a. First Born approximation b. Unscreened point nucleus c. No recoil or nuclear-spin effects
	(4.03)	Maximon–Isabelle, Ginsberg–Pratt	a. First Born approximation b. Screened finite nucleus with nuclear-spin effects c. No recoil
	(4.04)	Olsen	a. First Born approximation b. Screened point nucleus c. $T_1 \gg 1$ and $q_0 \leq 1$
	(4.10)		a. Exact in Z b. Unscreened point nucleus c. $T_1 - T_2 \ll T_1$ d. No recoil or nuclear-spin effects
$\int_{T_1-\Delta E}^{T_1} \frac{d^2\sigma}{d\Omega dT_2} dT_2$	(4.05) and (4.06)	Schwinger	a. First Born approximation b. Unscreened point nucleus c. $\Delta E \ll T_1$ d. No recoil or nuclear-spin effects
	(4.05 and (4.07)	Schwinger	a. First Born approximation b. Unscreened point nucleus c. $\beta_1 \ll 1$ and $\Delta E \ll T_1$
	(4.05) and (4.08)	Schwinger	a. First Born approximation b. Unscreened point nucleus c. $\beta_1 \approx 1$, $\Delta E \ll T_1$, and $q_0^2 \gg 1$ d. No recoil or nuclear spin effects
	(4.05) and (4.09)	Olsen–Mork	a. First Born approximation b. Unscreened point nucleus c. $\Delta E \approx T_1$ and $p_2^2 \gg 1$ d. No recoil or nuclear-spin effects
$\int_0^{T_1} \frac{d^2\sigma}{d\Omega dT_2} dT_2$	(4.15)	Schwinger	a. First Born approximation b. Unscreened point nucleus c. $\beta_1 \ll 1$
	(4.16)	Keiffer and Parzen	a. First Born approximation b. Unscreened point nucleus c. $q_0 \gg 1$ d. No recoil or nuclear-spin effects

the radiative corrections become negligible. For a pure Coulomb field, the total cross section σ diverges as q_0 approaches zero and the total "soft plus hard" correction given by the ratio in Eq. (4.17) is equal to unity. For a screened Coulomb field, the total correction given by Eq. (4.17) is equal to $(1-\Delta)$, where in the high-energy limit, Δ is of the order (O 64) of $(1/137\pi)\times(Z^{\frac{1}{3}}/111)^2 \ln (Z^{\frac{1}{3}}/111)$ with an energy dependence that is approximately proportional to β_1^2. These results indicate that radiative effects have a negligible influence on the total cross section.

A summary of the cross-section formulas in Sec. IV for electron scattering without atomic or nuclear excitation but with photon emission is shown in Table II. This table lists the formulas according to the form of the cross section, the authors, and the main approximations.

V. TYPES OF SCATTERING CROSS-SECTION CALCULATIONS

In Secs. VI–VIII, the theoretical treatments of electron scattering without excitation are based on the idealized process involving only the exchange of virtual photons and neglect the radiative effects discussed in Sec. IV. In addition, these calculations are limited by the following two important considerations: (a) the Dirac wave equation cannot be solved in a closed form in general, as indicated for example by the discussion in Ref. B 54, and (b) the scattering potential must be estimated from various models of the charge structure of the atom and the nucleus. As a result, various approximations and procedures involving the wave function and the potential have been used, and a plethora of approximate calculations has become available. Each calculation yields a cross-section formula which is valid only for a particular set of conditions. These calculations can be broadly classified as "exact" or as "Born," depending on the wave-function approximations.

The so-called "exact" calculations involve a partial-wave expansion valid for all atomic numbers. Specifically, the "phase-shift" calculations (see Chap. IV in Ref. M 49) give the cross-section formula in the form of an infinite (and in many cases, slowly convergent) series, each term of which depends on the potential through the phase shift. Also there are closed-form relativistic calculations [see Ref. M 47, formula (6.6) and Ref. O 57, formula (9.2)] which are limited

to values of $q_0 \lesssim 1$. These "exact" formulas give the most accurate estimates of the cross section, but have the disadvantage that in most cases they must be evaluated numerically. In addition, the problem of including atomic screening and nuclear charge-density effects is much more complicated for "exact" than for first-order Born calculations.

The "Born approximation" calculations are carried out with free-particle wave functions perturbed to *first* or *higher* orders in Z. The validity of the first Born approximation requires that the momentum transfer involved in the interaction is small compared to the electron momenta before and after the collision, or that $\sin \frac{1}{2}\theta(2\pi Z/137) \ll 1$. (See for example the discussion on p. 121 of Ref. B 57.) Higher order Born calculations are carried out to the nth order in the interaction with the nucleus. The higher order Born calculations have a greater region of validity and are more accurate than the first Born calculations. In addition, the higher order formulas approach the "exact" formulas as n increases and in some cases can be evaluated more easily.

The scattering potential for this process is determined by the charge and magnetic structures of the atom and the nucleus. The problem of including the correct potential in the "exact" calculations is very complicated, and few "exact" calculations are available which represent the atom as anything but a point charge. Such exceptions are given in the energy region below 1 keV for the atomic screening of certain elements as indicated in the references with formula (1A–110), and in the extreme relativistic region for various nuclear models as shown for example by Yennie, Ravenhall, and Wilson (Y 54). Most calculations that account for the charge and magnetic structure of the nucleus or the atom are based on the first Born approximation and use a central potential such that the charge and the magnetic moment distributions are spherically symmetric. Under these conditions, the first Born cross-section formula for a point charge and point magnetic moment can be corrected for the finite structure by multiplying the contribution due to the point charge by the factor $[G_E(q) - F(q)]^2$, and the contribution due to the point magnetic moment by the factor $[G_M(q)/\mu]^2$. As defined in Sec. II, the nuclear- and atomic-charge form factors $G_E(q)$ and $F(q)$, respectively, are given by the quantity

$$(4\pi/q)\int_0^\infty \rho(r)\,(\sin qr)r\,dr,$$

with $Ze\,\rho(r)$ equal to the charge density for the nucleus or the atom, respectively. Also, the magnetic form factor $G_M(q)$ is given by the quantity

$$(4\pi/q)\int_0^\infty \mu(r)\,(\sin qr)r\,dr,$$

with $\mu(r)$ equal to the magnetic moment distribution for the nucleus such that $\int\mu(r)\,d^3r$ is equal to μ, the magnetic moment of the nucleus.

The nuclear form factors, $G_E(q)$ and $G_M(q)$, are important for large values of the momentum transfer $q \gg 1$. For small q values, magnetic scattering effects are negligible and the nucleus may be considered to be a point charge with $G_E(q)$ equal to unity. Extensive data relating to the nuclear form factor and the nuclear-charge distribution for various nuclear models are given in the detailed summaries by Hofstadter and his collaborators (see Refs. H 56, H 57, and H 60).

The atomic form factor $F(q)$ is important mainly for small values of the momentum transfer $q \ll 1$. For large q values, the impact parameter is close to the nucleus and $F(q)$ is approximately equal to zero. The form factor is calculated on the basis of the following different atomic models described by the charge distribution $\rho(r)$ of the atomic electrons: (a) The most accurate calculations use the Hartree–Fock independent-particle model in which each electron is assumed to be in the field of the nucleus plus an average field due to the other electrons. The wave function for this model is calculated by Hartree's self-consistent field method which was first discussed in Refs. H 28 and F 30. The atomic form factors based on the self-consistent field method must be evaluated numerically, and some results are given for example by Ibers (I 62) for most of the elements and for q_0 values extending from zero to 0.058. (b) The Thomas–Fermi statistical model of the atom gives a smooth charge distribution that does not show the atomic shell structure. (See, for example, the discussion in Ref. N 55.) Although the form factor for this model can be approximated by an analytical expression [see formula (1A–102)] and is relatively simple to evaluate, it is less accurate than the Hartree form factor discussed in (a) over certain regions of the momentum transfer q_0: the potential given by the statistical model is particularly inaccurate at large distances (small q_0 values or small scattering angles) and at small distances (large q_0 values or large scattering angles) from the nucleus. (Differences in these two models are also discussed in Ref. L 54.) (c) The exponential atomic model is described by the exponential potential $V(r) = -(Ze^2/r)\exp(-\Lambda r)$, where $\Lambda = (\mu/0.885)Z^{\frac{1}{3}}/137$ and μ depends on Z and is of the order of unity [see formula (1A–102)]. This model gives the simplest screening approximation, but can be expected to give only a qualitative account of the screening unless empirical methods are used to improve the accuracy. (For example, see Ref. B 60.)

With the various types of calculations and approximations outlined above, the problem is to select the cross-section formula that applies to a given set of conditions. A brief summary of the most accurate formulas with recommendations for various conditions is given in Sec. VIII.

TABLE III. Values of the polarization functions[a] S, R, and L for $Z=79$.

θ (deg)	Function[a]	Electron kinetic energy, keV 50	100	200	400	600	1000
10	S	-2.40×10^{-4}	4.11×10^{-4}	1.29×10^{-3}	1.43×10^{-3}	1.26×10^{-3}	9.69×10^{-4}
	R	−0.156	−0.143	−0.122	−0.0941	−0.0767	−0.0562
	L	0.988	0.990	0.993	0.996	0.997	0.998
	D	1.016	1.019	1.027	1.044	1.054	1.063
30	S	0.0165	0.0179	0.0107	0.00437	0.00217	0.00073
	R	−0.447	−0.391	−0.322	−0.244	−0.198	−0.145
	L	0.895	0.920	0.947	0.970	0.980	0.989
	D	1.00	1.05	1.15	1.24	1.28	1.32
60	S	−0.00784	−0.0531	−0.0726	−0.0696	−0.0610	−0.0472
	R	−0.701	−0.631	−0.538	−0.419	−0.344	−0.253
	L	0.713	0.774	0.840	0.905	0.937	0.966
	D	1.14	1.34	1.54	1.69	1.75	1.80
90	S	−0.236	−0.264	−0.262	−0.229	−0.197	−0.151
	R	−0.900	−0.848	−0.759	−0.621	−0.522	−0.393
	L	0.366	0.459	0.595	0.750	0.830	0.907
	D	1.43	1.63	1.77	1.84	1.85	1.85
110	S	−0.350	−0.379	−0.386	−0.355	−0.315	−0.250
	R	−0.936	−0.920	−0.875	−0.767	−0.669	−0.523
	L	−0.0304	0.0970	0.292	0.534	0.673	0.815
	D	1.64	1.74	1.75	1.67	1.61	1.55
130	S	−0.356	−0.403	−0.446	−0.459	−0.438	−0.376
	R	−0.815	−0.851	−0.885	−0.872	−0.818	−0.692
	L	−0.457	−0.336	−0.134	0.167	0.372	0.617
	D	1.84	1.80	1.63	1.37	1.22	1.09
150	S	−0.257	−0.309	−0.377	−0.455	−0.491	−0.499
	R	−0.548	−0.608	−0.697	−0.804	−0.853	−0.854
	L	−0.796	−0.731	−0.610	−0.382	−0.176	0.151
	D	2.01	1.83	1.48	1.06	0.834	0.624
170	S	−0.092	−0.114	−0.152	−0.210	−0.260	−0.344
	R	−0.194	−0.220	−0.269	−0.357	−0.435	−0.567
	L	−0.977	−0.969	−0.951	−0.910	−0.862	−0.749
	D	2.11	1.84	1.39	0.862	0.593	0.341

[a] These functions are defined in formula (1A–403) for the case of an unscreened, point nucleus. The quantity D is the ratio of the Mott–exact cross section [formula (1A–109a)] to the Rutherford cross section [formula (1A–100)]. Values of these functions for various elements, angles, and energies are being prepared by Dr. J. Coyne at the National Bureau of Standards.

The results for the cross-section formulas that have been obtained on the basis of the above approximations are given in Sec. VII. It is important to note that these results apply to a target nucleus initially at rest. Electron polarization effects are included in Secs. VI and VII. Effects due to the polarization of the target nucleus have not been included (see, for example, Ref. Sc 59). In addition, all of the formulas require radiative corrections which must be evaluated according to the procedure discussed in Sec. IV.

VI. POLARIZATION EFFECTS

Mott has shown that polarization effects for the elastic scattering of an unpolarized electron beam can be predicted *only* by calculations of higher order than the first Born approximation (M 49, p. 82). The spin-dependent cross section can be obtained from the Mott phase-shift calculations as shown by Mendlowitz and Case (Me 55) and by Tolhoek (T 56). This cross section can be written in the following form which correlates the initial and final spin and momentum vectors of the electron:

$$d\sigma(\boldsymbol{\zeta}_1,\boldsymbol{\zeta}_2,\mathbf{n})/d\Omega=\tfrac{1}{2}[d\sigma/d\Omega]_{109}[1+(\mathbf{n}\cdot\boldsymbol{\zeta}_1)(\mathbf{n}\cdot\boldsymbol{\zeta}_2)+S\mathbf{n}\cdot(\boldsymbol{\zeta}_1+\boldsymbol{\zeta}_2)+(L\cos\theta-R\sin\theta)(\mathbf{n}\times\boldsymbol{\zeta}_1)\cdot(\mathbf{n}\times\boldsymbol{\zeta}_2)+(R\cos\theta+L\sin\theta)\mathbf{n}\cdot(\boldsymbol{\zeta}_1\times\boldsymbol{\zeta}_2)], \quad (6.01)$$

where $\mathbf{n}$, $\boldsymbol{\zeta}_1$, and $\boldsymbol{\zeta}_2$ are unit vectors defined in Sec. II.

This formula is given in further detail in formula (1A–403), where it is shown that $[d\sigma/d\Omega]_{109}$, S, L, and R can be expressed in terms of the basic pair of functions F and G, or f and g. These functions are defined in formula (1A–109a) for an unscreened point nucleus and in formula (1A–109b) for a point or finite nucleus with screening. Sherman (S 56) has evaluated F and G for an unscreened point nucleus. Values for $[d\sigma/d\Omega]_{109}$, S, L, and R which are defined in formula (1A–403) are shown in Table III for different energies, atomic numbers, and angles. As pointed out by Gürsey (G 57), it is useful to note the identity $S^2+L^2+R^2=1$. Other

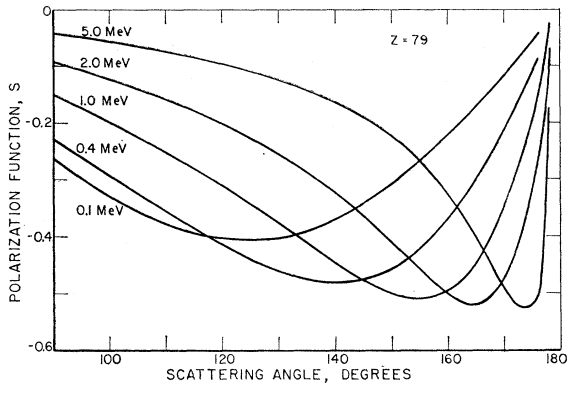

FIG. 8. Dependence of the polarization function S on the electron scattering angle for a gold target and for various electron kinetic energies designated on the curves. The function S is defined and evaluated from the equation given in formula (1A–403).

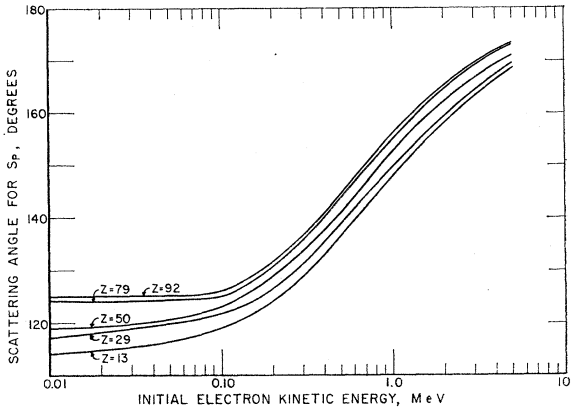

FIG. 10. Dependence of the electron scattering angle corresponding to the peak polarization S_p (see Figs. 8 and 9) on the electron kinetic energy, for different atomic numbers.

results which show the graphical behavior of S, L, and R are given in Figs. 8, 9, 10, 11, and 12.

The function S which is defined in formula (1A–401) by Sherman (S 56) on the basis of the early work of Mott (p. 78 in Ref. M 49), and the functions L and R are key parameters in the determination of the polarization sensitivity of the cross section. In particular for the case of elastic scattering of unpolarized electrons, the degree of polarization of the scattered electron beam is equal to S and is in the direction perpendicular to the scattering plane as shown in Sec. VIA. Values of S for an unscreened point nucleus are given by Sherman (S 56) for various angles, energies, and atomic numbers. More detailed data for S, which were numerically calculated from the definition given in formula (1A–403), are shown by the curves in Figs. 8, 9, and 10. These data show that as the electron energy increases, the peak value of S occurs at larger scattering angles and asymptotically approaches a maximum value. Although the curves in Fig. 8 extend up to 5 MeV, Gluckstern and Lin[4] have found that for energies up to 45 MeV with Z equal to 79 the peak value of S approaches -0.7, which is consistent with the high-energy asymptotic value indicated in Fig. 9. Also, Fig. 9 shows that the peak value for S at a given energy increases with Z, and the results of additional calculations reveal that this peak value approaches unity in the high-energy limit as Z approaches 137.

The values of S given in Table III and Figs. 8 and 9 do not include atomic screening or nuclear size corrections. [Other corrections due to inelastic scattering effects have been found to be negligible by Felsner and Rose (F 61).] Corrections due to atomic screening may be expected to appreciably change the values of S

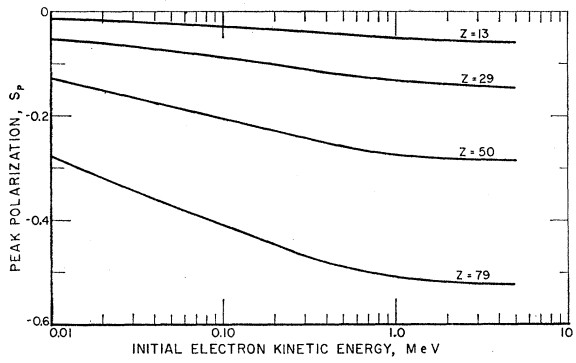

FIG. 9. Variation of the peak polarization S_p with electron kinetic energy for different atomic numbers. The values of S_p for gold are given in Fig. 8 by the peak value of S for a given electron energy, and are calculated for the other atomic numbers from the defining equation given in formula (1A–403).

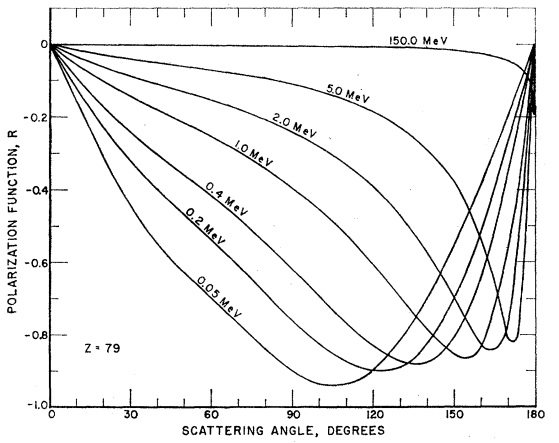

FIG. 11. Dependence of the polarization function R on the electron scattering angle for a gold target and for the various electron kinetic energies designated on the curves. The function, R, is defined and evaluated from the equation given in formula (1A–403).

[4] R. L. Gluckstern and S. R. Lin (in private communication).

in the region where $q_0<1$ as indicated for example by the calculations of Massey (Ma 41), Bartlett and Welton (B 41), Mohr (M 43), Mohr and Tassie (M 54), Tassie (T 57), and Lin (L 64), and by the experimental data some of which is summarized by Frauenfelder and Rossi (see Fig. 11 in Ref. F 63) and by Mikaelyan *et al.* (Mi 63). At present, few calculations are available which indicate the effect on S of corrections due to the finite nuclear size. These nuclear size effects may be appreciable for impact parameters comparable to the nuclear radius. Some results pertaining to nuclear size effects are given by Kerimov and Arutyunyan (K 60) and Kresnin and Tishchenko (Kr 60).

The polarization function S is related to the Mott azimuthal asymmetry parameter, δ, [M 49, Eq. (31) in Chap. IV] for doubly scattered electrons by the following equation:

$$S(\theta_1)\,S(\theta_2)=\delta(\theta_1,\theta_2). \tag{6.02}$$

For $\theta_1=\theta_2=90°$, Mott finds that in the second Born approximation

$$\delta\approx\left(\frac{Z}{137}\right)^2\frac{\beta_1^2(1-\beta_1^2)}{(2-\beta_1^2)^2}\,. \tag{6.03}$$

Some theoretical values for δ which include screening corrections are given in Refs. B 41, M 43, and M 54. Some experimental values for δ are given in Refs. P 58 and Ne 59.

The spin-dependent cross section, $d\sigma(\boldsymbol{\zeta}_1,\boldsymbol{\zeta}_2,\mathbf{n})/d\Omega$, given by Eq. (6.01) is the starting point for predicting polarization effects. Other useful forms of the cross section, which are defined in Sec. II, can be derived from this basic cross section by averaging over the initial or summing over the final spin states as shown by the following equations:

$$d\sigma(\boldsymbol{\zeta}_2,\mathbf{n})/d\Omega$$
$$=\tfrac{1}{2}\{[d\sigma(\boldsymbol{\zeta}_1,\boldsymbol{\zeta}_2,\mathbf{n})/d\Omega]+[d\sigma(-\boldsymbol{\zeta}_1,\boldsymbol{\zeta}_2,\mathbf{n})/d\Omega]\}, \tag{6.04}$$

$$d\sigma(\boldsymbol{\zeta}_1,\mathbf{n})/d\Omega$$
$$=[d\sigma(\boldsymbol{\zeta}_1,\boldsymbol{\zeta}_2,\mathbf{n})/d\Omega]+[d\sigma(\boldsymbol{\zeta}_1,-\boldsymbol{\zeta}_2,\mathbf{n})/d\Omega], \tag{6.05}$$

$$d\sigma/d\Omega$$
$$=\tfrac{1}{2}\{[d\sigma(\boldsymbol{\zeta}_1,\mathbf{n})/d\Omega+[d\sigma(-\boldsymbol{\zeta}_1,\mathbf{n})/d\Omega]\}$$
$$=[d\sigma(\boldsymbol{\zeta}_2,\mathbf{n})/d\Omega]+[d\sigma(-\boldsymbol{\zeta}_2,\mathbf{n})/d\Omega]. \tag{6.06}$$

In these equations, the functional dependence of the cross sections is explicitly shown only for the three axial vectors $\boldsymbol{\zeta}_1$, $\boldsymbol{\zeta}_2$, and $\mathbf{n}$.

Electron polarization measurements for this process involve a partially polarized electron beam which is described by the polarization vectors $\mathbf{P}_1$ for the incident beam and $\mathbf{P}_2$ for the scattered beam. The magnitude of either vector is zero, less than unity, or unity, respectively, for an unpolarized, a partially polarized, or a completely polarized beam. This magnitude can be determined in terms of the spin-dependent cross sections represented by Eqs. (6.01), (6.04), and (6.05). The direction of either vector is specified in terms of the unit vectors, $\mathbf{n}$, and $\mathbf{n}_1$ or $\mathbf{n}_2$.

First consider the polarization vector $\mathbf{P}_1$ for the incident electron beam, such that $\mathbf{P}_1=P_1\boldsymbol{\zeta}_1$. This partially polarized beam can evidently be represented by the incoherent superposition of an unpolarized and a completely polarized component with relative intensities $(1-P_1)$ and P_1, respectively. Therefore, if multiple scattering effects are negligible, the intensity of the beam scattered in a given direction is given by the following expressions:

$$I(\mathbf{n})=C\{(1-P_1)(d\sigma/d\Omega)+P_1[d\sigma(\boldsymbol{\zeta}_1,\mathbf{n})/d\Omega]\}$$
$$=C[d\sigma(\mathbf{P}_1,\mathbf{n})/d\Omega] \tag{6.07}$$

or

$$I(-\mathbf{n})=C\{(1-P_1)(d\sigma/d\Omega)+P_1[d\sigma(\boldsymbol{\zeta}_1,-\mathbf{n})/d\Omega]\}$$
$$=C[d\sigma(\mathbf{P}_1,-\mathbf{n})/d\Omega],$$

where C is the product of (a) the number of incident electrons per second, (b) the number of target atoms per cm^2, and (c) the solid angle subtended from the center of the target by the detector of the scattered electrons. It has been shown for example by Kolbenstvedt and Olsen (K 61) that any spin-sensitive cross section for fermions is linear in $\boldsymbol{\zeta}_1$, and contains a spin-independent and a spin-dependent term of the form $A+\mathbf{V}\cdot\boldsymbol{\zeta}_1$, as illustrated by the expression in the curly brackets in Eq. (6.07). Therefore it follows that a partially polarized incident beam characterized by $\mathbf{P}_1$

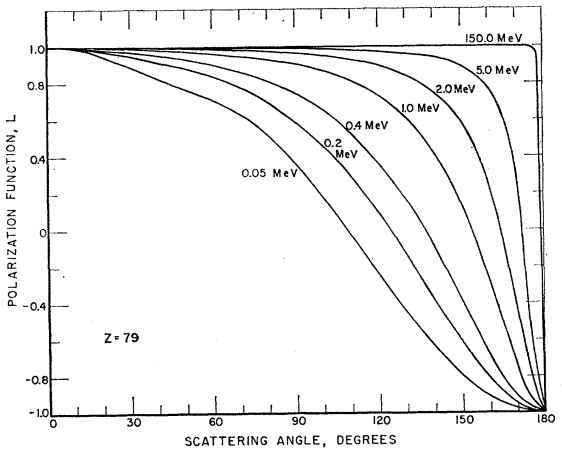

FIG. 12. Same caption as Fig. 11 except that R is replaced by L.

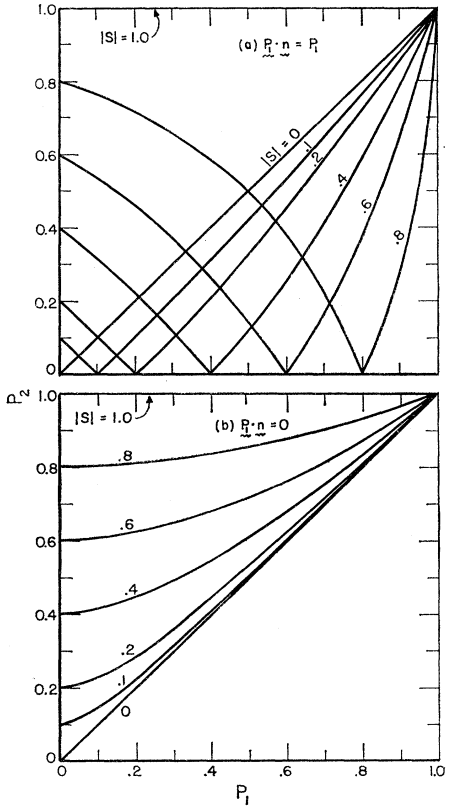

FIG. 13. Relationship between the polarization magnitudes P^1 and P_2, for different values of the polarization function S [defined in formula (1A–403)]. Parts (a) and (b) show the special cases where the direction of the polarization vector P_1 is perpendicular and parallel, respectively, to the incident electron momentum.

may be treated in the same way as a completely polarized incident beam characterized by ζ_1, provided that ζ_1 is replaced by $\mathbf{P}_1=P_1\zeta_1$ in the spin-sensitive cross sections $d\sigma(\zeta_1,\mathbf{n})/d\Omega$ or $d\sigma(\zeta_1,\zeta_2,\mathbf{n})/d\Omega$. Also it follows from Eq. (6.07) that

$$P_1=\frac{r-1}{r+1}\frac{2(d\sigma/d\Omega)}{[d\sigma(\zeta_1,\mathbf{n})/d\Omega]-[d\sigma(\zeta_1,-\mathbf{n})/d\Omega]}, \quad (6.08)$$

where r is equal to the ratio $I(\mathbf{n})/I(-\mathbf{n})$.

Second, consider the polarization vector $\mathbf{P}_2$ for the scattered electron beam. The magnitude and direction of this vector is given by the following equation for the general case where $0\leq P_1\leq 1$ such that the incident beam is partially polarized ($0<P_1<1$), completely polarized ($P_1=\zeta_1=1$), or unpolarized ($P_1=0$):

$$\mathbf{P}_2\cdot\zeta_2=\frac{[d\sigma(\mathbf{P}_1,\zeta_2,\mathbf{n})/d\Omega]-[d\sigma(\mathbf{P}_1,-\zeta_2,\mathbf{n})/d\Omega]}{[d\sigma(\mathbf{P}_1,\zeta_2,\mathbf{n})/d\Omega]+[d\sigma(\mathbf{P}_1,-\zeta_2,\mathbf{n})/d\Omega]}, \quad (6.09)$$

where $d\sigma(\mathbf{P}_1,\zeta_2,\mathbf{n})/d\Omega$ is given by Eq. (6.01) with ζ_1 replaced by $\mathbf{P}_1$, as indicated in Eq. (6.07).

These results are sufficient to predict the complete polarization behavior for this process, as shown in the following Secs. VI A and VI B. This behavior involving partially polarized beams has been described by other equivalent methods of calculation based on the density-matrix method, as shown for example by Mendlowitz and Case (Me 55), Tolhoek (T 56), Fano (F 57), Bernardini, Brovetto, and Ferroni (B 58), and McMaster (M 61).

A. Polarization of the Scattered Electron Beam

The polarization of the scattered electron beam for any incident beam characterized by the polarization vector $\mathbf{P}_1$ is readily obtained from Eq. (6.09). For the general case where $0\leq P_1\leq 1$,

$$\mathbf{P}_2=\frac{(S+\mathbf{n}\cdot\mathbf{P}_1)\mathbf{n}+(R\sin\theta-L\cos\theta)\mathbf{n}\times(\mathbf{n}\times\mathbf{P}_1)+(R\cos\theta+L\sin\theta)(\mathbf{n}\times\mathbf{P}_1)}{1+S(\mathbf{n}\cdot\mathbf{P}_1)}. \quad (6.10)$$

This expression is derived for the case where the cross section $d\sigma(\mathbf{P}_1,\zeta_2,\mathbf{n})/d\Omega$, is given by Eq. (6.01) with ζ_1 replaced by $\mathbf{P}_1$ and with S, R, and L defined in formula (1A–403). From Eq. (6.10) it can be shown that the magnitude of $\mathbf{P}_2$ can be expressed simply in terms of S and $\mathbf{P}_1$ as follows:

$$P_2^2=1-[(1-P_1^2)(1-S^2)]/(1+\mathbf{n}\cdot\mathbf{P}_1S)^2. \quad (6.11)$$

Eq. (6.11) demonstrates the well-known fact that for a completely polarized beam, the magnitude of the polarization remains constant in the scattering process. The relationships in Eq. (6.11) are exhibited in Figs. 13(a) and (b) for the special cases where the direction of the polarization vector $\mathbf{P}_1$ is perpendicular ($\mathbf{n}_1\cdot\mathbf{P}_1=0$) and parallel ($\mathbf{n}_1\cdot\mathbf{P}_1=P_1$), respectively, to the incident beam direction. Also from Eq. (6.10) it can be shown that the angle χ_2 between the vectors $\mathbf{n}$ and $\mathbf{P}_2$ is given by the following simple equation:

$$\tan\chi_2=\frac{|\mathbf{P}_1\times\mathbf{n}|(1-S^2)^{\frac{1}{2}}}{S+\mathbf{n}\cdot\mathbf{P}_1}=\frac{P_1\sin\chi_1(1-S^2)^{\frac{1}{2}}}{S+P_1\cos\chi_1}, \quad (6.12)$$

where χ_1 is the angle between $\mathbf{n}$ and $\mathbf{P}_1$.

It is useful for polarization measurements to express $\mathbf{P}_2$ in the form of three orthogonal components with directions given by the unit vectors $\mathbf{n}$, $\mathbf{n}_1$, and $\mathbf{n}_1\times\mathbf{n}$ or $\mathbf{n}$, $\mathbf{n}_2$, and $\mathbf{n}_2\times\mathbf{n}$, as shown by the coordinate systems in Fig. 1(b). The following two alternative expressions are given for the cases that (1) the unit vectors for the components of $\mathbf{P}_2$ and $\mathbf{P}_1$ are given by $\mathbf{n}$, $\mathbf{n}_1$, and $\mathbf{n}_1\times\mathbf{n}$, and (2) the unit vectors for the components of

$\mathbf{P}_2$ are given by $\mathbf{n}$, $\mathbf{n}_2$, and $\mathbf{n}_2\times\mathbf{n}$, and the unit vectors for the components of $\mathbf{P}_1$ are given by $\mathbf{n}$, $\mathbf{n}_1$, and $\mathbf{n}_1\times\mathbf{n}$:

$$\mathbf{P}_2=[\mathbf{n}(S+\mathbf{P}_1\cdot\mathbf{n})+\mathbf{n}_1\{(L\cos\theta-R\sin\theta)\mathbf{P}_1\cdot\mathbf{n}_1 +(R\cos\theta+L\sin\theta)\mathbf{P}_1\cdot[\mathbf{n}_1\times\mathbf{n}]\}+[\mathbf{n}_1\times\mathbf{n}] \times\{(L\cos\theta-R\sin\theta)\mathbf{P}_1\cdot[\mathbf{n}_1\times\mathbf{n}] -(R\cos\theta+L\sin\theta)\mathbf{P}_1\cdot\mathbf{n}_1\}]/[1+S(\mathbf{n}\cdot\mathbf{P}_1)] \quad (6.13)$$

and

$$\mathbf{P}_2=\{\mathbf{n}(S+\mathbf{P}_1\cdot\mathbf{n})+\mathbf{n}_2(L\mathbf{P}_1\cdot\mathbf{n}_1+R\mathbf{P}_1\cdot[\mathbf{n}_1\times\mathbf{n}]) +[\mathbf{n}_2\times\mathbf{n}](L\mathbf{P}_1\cdot[\mathbf{n}_1\times\mathbf{n}]-R\mathbf{P}_1\cdot\mathbf{n}_1)\}/[1+S(\mathbf{n}\cdot\mathbf{P}_1)]. \quad (6.14)$$

The following special cases are readily derived from the general case given by Eq. (6.14):

1. Initial beam is completely polarized in the transverse direction such that $\mathbf{P}_1\cdot\mathbf{n}=1$:

$$\mathbf{P}_2=\mathbf{n}. \quad (6.15)$$

2. Initial beam is completely polarized in the longitudinal direction such that $\mathbf{P}_1\cdot\mathbf{n}_1=1$,

$$\mathbf{P}_2=\mathbf{n}S+\mathbf{n}_2L-\mathbf{n}_2\times\mathbf{n}R. \quad (6.16)$$

3. Initial beam is unpolarized such that $\mathbf{P}_1=0$:

$$\mathbf{P}_2=\mathbf{n}S. \quad (6.17)$$

Finally consider the case of double scattering by this process. The general expression for the polarization vector $\mathbf{P}_3$ of a beam that has been doubly scattered is derived from the general expression given by Eq. (6.14). This derivation is carried out simply by substituting $\mathbf{P}_2$ for $\mathbf{P}_1$ in Eq. (6.14) with $\mathbf{P}_2$ given by Eq. (6.14). Then if we introduce the subscript I for the first scattering such that $\mathbf{n}=\mathbf{n}_\mathrm{I}=(\mathbf{n}_1\times\mathbf{n}_2)/(|\mathbf{n}_1\times\mathbf{n}_2|)$, $S=S_\mathrm{I}$, $L=L_\mathrm{I}$, and $R=R_\mathrm{I}$, and the subscript II for the second scattering such that $\mathbf{n}=\mathbf{n}_\mathrm{II}=(\mathbf{n}_2\times\mathbf{n}_3)/(|\mathbf{n}_2\times\mathbf{n}_3|)$, $S=S_\mathrm{II}$, $L=L_\mathrm{II}$, and $R=R_\mathrm{II}$, we obtain the following general result for the polarization of a doubly scattered beam:

$$\mathbf{P}_3=\frac{\mathbf{n}_\mathrm{II}(S_\mathrm{II}+A)+\mathbf{n}_3(L_\mathrm{II}B+R_\mathrm{II}C)+\mathbf{n}_3\times\mathbf{n}_\mathrm{II}(L_\mathrm{II}C-R_\mathrm{II}B)}{1+S_\mathrm{II}A}, \quad (6.18)$$

where

$$A=\mathbf{P}_2\cdot\mathbf{n}_\mathrm{II}=[\mathbf{n}_\mathrm{I}\cdot\mathbf{n}_\mathrm{II}a+\mathbf{n}_2\cdot[\mathbf{n}_\mathrm{I}\times\mathbf{n}_\mathrm{II}]c]/d,$$

$$B=\mathbf{P}_2\cdot\mathbf{n}_2=b/d,$$

$$C=\mathbf{P}_2\cdot[\mathbf{n}_2\times\mathbf{n}_\mathrm{II}]=[-\mathbf{n}_2\cdot[\mathbf{n}_\mathrm{I}\times\mathbf{n}_\mathrm{II}]a+\mathbf{n}_\mathrm{I}\cdot\mathbf{n}_\mathrm{II}c]/d,$$

with

$$a=S_\mathrm{I}+\mathbf{P}_1\cdot\mathbf{n}_\mathrm{I},$$

$$b=L_\mathrm{I}\mathbf{P}_1\cdot\mathbf{n}_1+R_\mathrm{I}\mathbf{P}_1\cdot[\mathbf{n}_1\times\mathbf{n}_\mathrm{I}],$$

$$c=L_\mathrm{I}\mathbf{P}_1\cdot[\mathbf{n}_1\times\mathbf{n}_\mathrm{I}]-R_\mathrm{I}\mathbf{P}_1\cdot\mathbf{n}_1,$$

$$d=1+S_\mathrm{I}\mathbf{P}_1\cdot\mathbf{n}_\mathrm{I}.$$

For the special case in which it is desired to produce the maximum degree of polarization from an incident unpolarized beam, $P_1=0$, the geometry for this double scattering process is arranged so that there is only one scattering angle and one scattering plane to give the conditions that $S=S_\mathrm{I}=S_\mathrm{II}$, $R=R_\mathrm{I}=R_\mathrm{II}$, and $\mathbf{n}=\mathbf{n}_\mathrm{I}=\mathbf{n}_\mathrm{II}$. This maximum polarization, $\mathbf{P}_3$, obtained from Eq. (6.18) is transverse to the scattering plane and is given as

$$\mathbf{P}_3=\mathbf{n}2S/(1+S^2). \quad (6.19)$$

B. Polarization Analysis of the Incident Electron Beam

The polarization $\mathbf{P}_1$ of an incident electron beam can be analyzed by this process according to Eq. (6.08). It is necessary to measure the azimuthal asymmetry of the scattered electron intensity for a given scattering angle, as specified by the intensity ratio, $r=I(\mathbf{n})/I(-\mathbf{n})$, for a given scattering plane. Then with $d\sigma(\zeta_1,\mathbf{n}/d\Omega)$ and $d\sigma(\zeta_1,-\mathbf{n})/d\Omega$ determined from Eqs. (6.05) and (6.01), the following relationship is obtained from Eq. (6.08):

$$\mathbf{P}_1\cdot\mathbf{n}=(r-1)/[(r+1)S]. \quad (6.20)$$

The result given by Eq. (6.20) shows that for the case of single scattering, the measured asymmetry ratio r determines only that particular component of the polarization vector $\mathbf{P}_1$ which is parallel to the unit vector $\mathbf{n}$. The vector $\mathbf{P}_1$ is completely determined only if all three orthogonal components are known such that in this coordinate system

$$\mathbf{P}_1=\mathbf{n}(\mathbf{P}_1\cdot\mathbf{n})+\mathbf{n}_1(\mathbf{P}_1\cdot\mathbf{n}_1)+[\mathbf{n}_1\times\mathbf{n}](\mathbf{P}_1\cdot[\mathbf{n}_1\times\mathbf{n}]),$$

or

$$P_1=[(\mathbf{P}_1\cdot\mathbf{n})^2+(\mathbf{P}_1\cdot\mathbf{n}_1)^2+(\mathbf{P}_1\cdot[\mathbf{n}_1\times\mathbf{n}])^2]^{\frac{1}{2}}. \quad (6.21)$$

The two transverse components, $\mathbf{P}_1\cdot\mathbf{n}$ and $\mathbf{P}_1\cdot[\mathbf{n}_1\times\mathbf{n}]$, can be determined by measuring the asymmetry ratio r for two cases in which the scattering planes are orthogonal to each other. The longitudinal component $\mathbf{P}_1\cdot\mathbf{n}_1$ may be determined by measuring the asymmetry ratio for a beam that has been doubly scattered. With the subscript I for the first scattering such that $\mathbf{n}=\mathbf{n}_\mathrm{I}$, $S=S_\mathrm{I}$, $R=R_\mathrm{I}$, and $L=L_\mathrm{I}$, and the subscript II for the second scattering such that $\mathbf{n}=\mathbf{n}_\mathrm{II}$, $S=S_\mathrm{II}$, $R=R_\mathrm{II}$, $L=L_\mathrm{II}$, and $r=r_\mathrm{II}=I(\mathbf{n}_\mathrm{II})/I(-\mathbf{n}_\mathrm{II})$, it fol-

TABLE IV. Classification of cross-section formulas for elastic electron scattering.

Type of calculation[a]		$d\sigma/d\Omega$	$d\sigma(\zeta_1, \mathbf{n})/d\Omega$	$d\sigma(\zeta_2, \mathbf{n})/d\Omega$	$d\sigma(\zeta_1, \zeta_2, \mathbf{n})/d\Omega$	σ
Classical	UPN	Rutherford ($\beta_1 \ll 1$) (1A–100)				
First Born	UPN	Mott–Born (1A–101)			First Born (1A–400)	
	SPN	Mott–Born (1A–102)				Mott–Born (1A–500)
	UFN	Mott–Born (1A–103)				
	UFN	Rosenbluth (1A–104)				
Higher order Born	UPN	McKinley–Feshbach (1A–105)	Second Born (1A–200)	Second Born (1A–300)	Second Born (1A–401)	
	UPN	Johnson–Weber–Mullin (1A–106)	Johnson–Weber–Mullin (1A–201)	Johnson–Weber–Mullin (1A–301)	Johnson–Weber–Mullin (1A–402)	
	SPN	Dalitz (1A–107)				
	SFN	Gorshkov (1A–108)	Gorshkov (1A–202)			
Exact	UPN	Mott–exact (1A–109a)	Mott–exact (1A–203)	Mott–exact (1A–302)	Mott–exact (1A–403)	
	SFN	Mott–exact (1A–109b)				
	SPN	Mott–exact ($\beta_1 \ll 1$) (1A–110)				Mott–exact ($\beta_1 \ll 1$) (1A–501)
	SPN	Molière–exact (1A–111)				

[a] UPN=unscreened point nucleus; UFN=unscreened finite nucleus; SPN=screened point nucleus; SFN=screened finite nucleus.

lows from Eq. (6.20) that

$$\mathbf{P}_2 \cdot \mathbf{n}_{II} = (r_{II}-1)[(r_{II}+1)\, S_{II}]. \qquad (6.22)$$

Then with the substitution for $\mathbf{P}_2$ given by Eq. (6.14), the general expression for the longitudinal component, $\mathbf{P}_1 \cdot \mathbf{n}_1$, becomes

$$\mathbf{P}_1 \cdot \mathbf{n}_1 = (L_I/R_I)\mathbf{P}_1 \cdot [\mathbf{n}_1 \times \mathbf{n}_I] - \frac{(S_I M - S_{II}\mathbf{n}_I \cdot \mathbf{n}_{II})\mathbf{P}_1 \cdot \mathbf{n}_I}{g S_{II}} - \frac{M - S_I S_{II} \mathbf{n}_I \cdot \mathbf{n}_{II}}{g S_{II}}, \qquad (6.23)$$

where $M=(r_{II}-1)/(r_{II}+1)$, $g=\mathbf{n}_2 \cdot [\mathbf{n}_I \times \mathbf{n}_{II}] R_I$. This result shows that the longitudinal component $\mathbf{P}_1 \cdot \mathbf{n}_1$ of the polarization vector $\mathbf{P}_1$ can be determined from the measured asymmetry ratio r_{II} of a doubly scattered beam, providing the transverse components $\mathbf{P}_1 \cdot \mathbf{n}_I$ and $\mathbf{P}_1 \cdot [\mathbf{n}_1 \times \mathbf{n}_I]$ are known.

VII. CROSS-SECTION FORMULAS INCLUDING POLARIZATION DEPENDENCE

The cross-section formulas for the idealized process of elastic electron scattering are classified into five main groups as shown in Table IV. The first four groups apply to the cross section which is differential with respect to the electron scattering angles and which is divided into four subgroups depending on whether polarized or unpolarized electrons are scattered into a detection system that is insensitive or sensitive to the spin states of the scattered electrons. The fifth group applies to the cross section integrated over electron scattering angles and summed over electron spin states. The formulas for a particular cross-section form (differential or integrated) are classified according to the type of calculation discussed in Sec. V.

Each cross-section formula is identified by three symbols. First is a one-digit number (unity in this case) that refers to the particular process. Second is a letter which identifies the classification chart (Table IV in this review) for the formulas. Third is a three-digit number: the first digit to the left ranges from one to five to distinguish the following five forms of the cross section (defined in Sec. II), (1) $d\sigma/d\Omega$, (2) $d\sigma(\zeta_1, \mathbf{n})/d\Omega$ (3) $d\sigma(\zeta_2, \mathbf{n})/d\Omega$, (4) $d\sigma(\zeta_1, \zeta_2, \mathbf{n})/d\Omega$, and (5) σ, and the remaining two digits list the different formulas according to the particular set of approximations for which the formula is valid. All of these formulas refer to the laboratory system with the target atom initially at rest and do not include the radiative correction discussed in Sec. IV. Also, each formula has a numerical and a qualitative title which indicates the important approximations and the names of the principal authors.

The cross-section formulas for $d\sigma/d\Omega$, which contains the parameters E_1, θ, and Z, are grouped from (1A–100) to (1A–111) as shown by the separate de-

TABLE V. Cross-section formulas for $d\sigma/d\Omega$.

Type of calculation	Formula	Principal authors	Conditions
Classical	(1A–100)	Rutherford	Point charge with $\beta_1 \ll 1$.
First Born approximation	(1A–101)	Mott	Point nucleus, without screening.
	(1A–102)	Mott	Point nucleus, $q_0 \ll 1$, with (a) exponential, (b) Thomas–Fermi and Molière, and (c) Hartree-type screening.
	(1A–103)	Mott	Finite nucleus, without screening, $\beta_1 \ll 1$.
	(1A–104)	Rosenbluth, Walecka–Pratt	Finite nucleus with magnetic moment, $\beta_1 \approx 1$.
Second or higher order Born approximation	(1A–105)	McKinley–Feshbach	Point nucleus, without screening.
	(1A–106)	Dalitz	Point nucleus, exponential screening.
	(1A–107)	Johnson–Weber–Mullin	Point nucleus, without screening.
	(1A–108)	Gorshkov	Finite nucleus, Thomas–Fermi screening.
Exact	(1A–109)	Mott	Point nucleus (a) without screening, (b) with arbitrary screening.
	(1A–110)	Mott	Point nucleus with arbitrary screening, $\beta_1 \ll 1$.
	(1A–111)	Molière	Point nucleus with arbitrary screening, $(q_0/2E_1) \ll 1$.

tailed chart in Table V. The cross-section formulas for $d\sigma(\boldsymbol{\zeta}_1, \mathbf{n})/d\Omega$, which involves the parameters E_1, θ, Z, $\boldsymbol{\zeta}_1$, and $\mathbf{n}$, are grouped from (1A–200) to (1A–203). The cross-section formulas for $d\sigma(\boldsymbol{\zeta}_2, \mathbf{n})/d\Omega$, which involves the parameters, E_1, θ, Z, $\boldsymbol{\zeta}_2$, and $\mathbf{n}$, are grouped from (1A–300) to (1A–302). The cross-section formulas for $d\sigma(\boldsymbol{\zeta}_1, \boldsymbol{\zeta}_2, \mathbf{n})/d\Omega$, which involves the parameters, E_1, θ, Z, $\boldsymbol{\zeta}_1$, $\boldsymbol{\zeta}_2$, and $\mathbf{n}$, are grouped from (1A–400) to (1A–403). Finally, the cross-section formulas for σ, which involves the parameters E_1 and Z and which can be derived only for a screened Coulomb field, are grouped from (1A–500) to (1A–501).

Formula (1A–100)

[The Rutherford formula: point nucleus with no screening for nonrelativistic electrons.]

$$d\sigma/d\Omega = 4Z^2r_0^2E_1^2/q_0^4.$$

(1) Conditions of Validity

a. Nonrelativistic: $\beta_1 \ll 1$ or $\alpha Z/\beta_1 \gg 1$.
b. No screening: $\alpha Z^{1/3} \ll q_0$.
c. Point-charge nucleus: $R_A \ll 2\pi/p_1$.
d. Infinitely heavy nucleus: $2E_1(m_0/M_0) \ll 1$.

(2) References

R 11, formula (5); J 55, formula (15–8).

Formula (1A–101)

[The Mott–Born formula: point nucleus with no screening.]

$$d\sigma/d\Omega = (4Z^2r_0^2E_1^2/q_0^4)[1 - q_0^2/4E_1^2].$$

(1) Conditions of Validity

a. First Born approximation: $\alpha Z/\beta_1 \ll 1$.
b. No screening: $\alpha Z^{1/3} \ll q_0$.
c. Point-charge nucleus: $R_A \ll 2\pi/p_1$.
d. Infinitely heavy nucleus: $2E_1 m_0/M_0 \ll 1$.
e. Nucleus with negligible spin effects: $(q_0/Z)^2(m_0/M_0)^2 \ll 1$.

(2) References

M 49, formula (42) p. 80.

(3) Notes

This formula applies to relativistic electrons. A comparison with the nonrelativistic formula (1A–100) shows that electron-spin effects are given by the term $[1 - q_0^2/4E_1^2]$.

Formula (1A–102)

[The Mott–Born formula with screening for small momentum transfer: point nucleus with (a) exponential, (b) Thomas–Fermi and Molière, and (c) Hartree-type screening.]

$$\frac{d\sigma}{d\Omega}=\frac{4Z^2r_0^2E_1^2}{q_0^4}[1-F(q_0)]^2=\frac{f(q_0)^2}{1-\beta_1^2},$$

where $F(q_0)$ is the so-called atomic form factor divided by the atomic number. Formulas for $F(q_0)$ are given below for the different screening approximations. From Born approximation calculations (M 49, p. 116), the scattering amplitude $f(q_0)$ for a central potential $V(r)$ is given as

$$f(q_0)=-2\int\frac{\sin q_0r}{q_0r}V(r)r^2\,dr.$$

(a) Exponential screening:

$$\frac{1-F(q_0)}{q_0^2}=\frac{1}{\Lambda^2+q_0^2},$$

where

$$\Lambda=(\mu/0.885)(Z^{\frac{1}{3}}/137)\text{ in units of }\lambda\!\!\!^{-}_0{}^{-1},$$

with Λ defined by the exponential potential $V(r)=-(Ze^2/r)\exp(-\Lambda r)$, and

$$\mu\approx 0.72\text{ (B 60)}$$

$$\approx 1.12\text{ or }1.8\text{ (N 59)}$$

$$\approx 2.18\text{ for beryllium (N 59)}.$$

[For light elements, see formula (1A–501) and Ref. M 41. The value of μ must be determined empirically for specific cases, as shown by the above examples.]

(b) Thomas–Fermi and Molière screening: For the Thomas–Fermi potential, the atomic form factor has been evaluated for a limited range of q_0 and Z values by Ibers in Table 3.3.1B, p. 210 in Ref. I 62. Other tabulations are given in Ref. B 31. The Thomas–Fermi atomic model is expected to break down for small atomic numbers and for very small or very large q_0 values. Molière has given the following analytical approximation for the Thomas–Fermi potential:

$$V(r)=-\frac{Ze^2}{r}\sum_{i=1}^{3}a_i\exp\left(-b_i\frac{r}{R_{\mathrm{TF}}}\right),$$

where $a_1=0.10$, $a_2=0.55$, $a_3=0.35$, $b_1=6.0$, $b_2=1.20$, $b_3=0.30$. The atomic form factor derived from the Molière potential (B 57) is given by the following expression:

$$\frac{1-F(q_0)}{q_0^2}=\sum_{i=1}^{3}\frac{a_i}{\Lambda_i^2+q_0^2},$$

where $\Lambda_i=(Z^{\frac{1}{3}}/121)b_i$ in units of $\lambda\!\!\!^{-}_0{}^{-1}$. This Molière approximation has a sharper drop in the electron distribution at the edge of the atom and is expected to give more accurate results than the Thomas–Fermi model.

(c) Hartree-type screening:

$$\frac{1-F(q_0)}{q_0^2}=\frac{q_0^2f(q_0)}{4Z^2r_0^2}.$$

Tables of $F(q_0)$ and of the atomic scattering amplitude, $f(q_0)$, for Hartree-type screening have been prepared by Ibers [see Tables 3.3.1A and 3.3.3A(1) in Ref. I 62] for most of the elements and for small q_0 values where the Hartree-type calculations give the best screening approximation. A summary of the atomic scattering amplitudes $f(q_0)$ obtained with Hartree-type screening is shown in Table VI. This table is condensed from Iber's Table 3.3.3A(1) and covers a range of q_0 values from zero to approximately 0.06 and a range of Z values from 1 to 80.

(1) Conditions of Validity

a. First Born approximation: $\alpha Z/\beta_1 \ll 1$.
b. Negligible electron-spin effects: $q_0/2E_1 \ll 1$.
c. Point-charge nucleus: $R_A \ll 2\pi/p_1$.
d. Infinitely heavy nucleus: $2E_1(m_0/M_0) \ll 1$.
e. Nucleus with negligible spin effects: $(q_0/Z)^2(m_0/M_0)^2 \ll 1$.

(2) References

a. Exponential screening: Ma 52, formula (24); N 59, formula (13).

b. Thomas–Fermi and Molière screening: M 49, formula (8) of Chap. VII, formula (13) of Chap. IX; B 30, formula (18); M 47, formulas (6.1), (6.6), and (7.1) (Molière).

c. Hartree-type screening: M 49, formula (11) of Chap. IX; M 55, formulas (1.2), (2.2), and (2.3); M 49, formula (9) of Chap. IX (exact screening for hydrogen and helium).

(3) Notes

a. These formulas are not valid for very slow electrons (<1 keV) which have wavelengths and q_0 values comparable to the atomic radius such that diffraction effects are important.

b. These formulas are not valid for large q_0 values for which the Born approximation breaks down and electron-spin effects become important.

c. For multiple scattering calculations, the Molière "screening angle" θ_0 [discussed by Bethe (B 53)] is given by the following expression:

$$\theta_0 = [1.13 + 3.76(Z/137\beta_1)^2]/(P_1 R_{TF})^2.$$

Reference N 59 indicates that a more accurate screening angle is obtained from the Dalitz calculations [see formula (1A–107)].

d. These formulas are further developed and analyzed at small scattering angles for applications to electron microscopy by Lenz (L 54) and by Burge and Smith (B 62).

e. Some experimental results for the elastic cross section in the region of small q_0 are given in Ref. B 60.

f. Some numerical estimates of the first Born cross section for Thomas–Fermi and Hartree-type screening is given by Tietz (T 59).

g. An excellent review of the cross-section formulas that are applicable to small-angle scattering is given by Scott (Sc 63).

h. A comparison of experimental cross sections with theoretical cross sections obtained from formula (1A–102b) and from exact phase-shift calculations including Hartree screening is given in Ref. Mo 63 for a gold target and for q_0 values in the region of 0.2. This comparison indicates the limitations of formula (1A–102b) for electron energies less than 100 keV.

i. Analytical expressions which approximate the Thomas–Fermi and Hartree–Fock screening potentials of various atoms are given by Bonham and Strand (B 63) and by Byatt (By 56).

Formula (1A–103)

[The Mott–Born formula for large momentum transfer: finite nucleus with recoil and with no atomic screening.]

$$\frac{d\sigma}{d\Omega} = \frac{4Z^2 r_0^2 E_1^2}{q_0^4} \frac{[1 - q_0^2/4E_1^2]}{[1 + (m_0/M_0)(q_0^2/2E_1)]} G_E^2(Q),$$

where $G_E(Q)$ is defined as the nuclear form factor such that

$$G_E(Q) = \int_\tau \rho(\mathbf{r}) \exp(i\mathbf{Q}\cdot\mathbf{r})\, d^3\mathbf{r} = 1 \text{ for point-charge nucleus or for } Q = 0,$$

τ = nuclear volume,

$Ze\,\rho(\mathbf{r})$ = nuclear charge density distribution, with normalization such that

$$\int_\tau \rho(\mathbf{r})\, d^3\mathbf{r} = 1.$$

The evaluation of $G_E(Q)$ for a given nucleus depends on the nuclear charge distribution $\rho(\mathbf{r})$. At present there is no single analytical expression of a nuclear model that applies to all nuclei, and it is necessary to try to fit the

experimental data for a given nucleus with a particular model. This procedure is highly specialized and is discussed in great detail by Hofstadter (H 56) and (H 57), and by Herman and Hofstadter (H 60), who give extensive tables of different nuclear models and the corresponding nuclear form factors.

The most accurate estimates of the cross section can be made by referring to the available data (H 60) for each nucleus. Very rough estimates of the cross section can be obtained by assuming that the nucleus is a uniformly charged sphere with radius R_A such that

$$R_A \approx 0.514 A^{\frac{1}{3}} r_0, \tag{H 56}$$

$$\rho_c = (Z/A) \times 0.080 \text{ proton charges per F}^3, \tag{H 56}$$

where 1 F $= 1 \times 10^{-13}$ cm. Then for spherical symmetry

$$G_E(Q) = \frac{4\pi\rho_c}{Q} \int_0^\infty \sin(Qr) r \, dr.$$

This assumption of a spherical nucleus introduces inaccuracies in the cross sections calculated by the above formula that are probably comparable to the inaccuracies introduced by the Born approximation. Tables of the form factor $G_E(Q)$ for such a uniformly charged nucleus are also presented in Ref. H 60. Values of $G_E^2(Q)$ for typical charge distributions are given in Fig. 3 of Ref. H 56.

(1) Conditions of Validity

a. First Born approximation: $\alpha Z/\beta_1 \ll 1$.

b. No atomic screening: $\alpha Z^{1/3} \ll q_0$.

c. Nucleus with negligible spin effects: $(q_0/Z)^2(m_0/M_0)^2 \ll 1$.

(2) References

H 60, formula (2).

(3) Notes

This formula is most accurate for light elements and intermediate angles. For medium and heavy nuclei, the Born approximation is inadequate, particularly in certain regions of momentum transfer where diffraction effects occur (see H 60). Nuclear size effects become more important with increasing values of T_1 and q_0. Examples of this behavior for gold and carbon are given in Figs. 1, 2, and 4 in Ref. H 60.

Formula (1A–104)

[The Rosenbluth and Walecka–Pratt formulas: finite nucleus with magnetic moment for extreme-relativistic electrons.]

(a) The Rosenbluth formula: finite proton or neutron with recoil for extreme-relativistic electrons.

$$\frac{d\sigma}{d\Omega} = \frac{4r_0^2 E_1^2}{q_0^4} \frac{\cos^2(\theta/2)}{[1+(m_0/M_0)(q_0^2/2E_1)]} \{F_1^2 + \left(\frac{Q}{2}\frac{m_0}{M_0}\right)^2 [2(F_1+KF_2)^2 \tan^2(\theta/2) + K^2F_2^2]\}$$

or, as given by Sachs and his collaborators (E 60, S 62)

$$\frac{d\sigma}{d\Omega} = \frac{4r_0^2 E_1^2}{q_0^4} \frac{\cos^2(\theta/2)}{[1+(m_0/M_0)(q_0^2/2E_1)]} \left\{ \frac{G_E^2 + (Q/2)^2(m_0/M_0)^2 G_M^2}{1+(Q/2)^2(m_0/M_0)^2} + 2(Q/2)^2(m_0/M_0)^2 G_M^2 \tan^2(\theta/2) \right\},$$

where $G_E = F_1 - [(Q/2)(m_0/M_0)]^2 KF_2 =$ charge form factor; $G_M = F_1 + KF_2 =$ magnetic form factor; $F_1 =$ form factor for the Dirac structure of the proton or neutron; $F_2 =$ form factor for the Pauli structure of the proton or neutron [Note: The form factors F_1 and F_2 are functions of Q^2, and experimental values are given in Refs. H 60 (Figs. 7 and 8) and Bu 61 for a proton, and Ref. H 60 (Figs. 19 and 20) for a neutron. For a point proton, $F_1 = F_2 = 1$, and for a point neutron $F_1 = 0$, $F_2 = 1$. A recent summary concerning these form factors is given in Ref. H 63]; $M_0 =$ Rest energy of proton (938.211 MeV) or neutron (939.505 MeV); $K =$ the anomalous (Pauli) magnetic moment of the proton with $K = 1.79270$, or of the neutron with $K = -1.913148$.

(b) The Walecka–Pratt formula: finite nucleus with magnetic moment neglecting recoil for extreme-relativistic electrons.

$$\frac{d\sigma}{d\Omega}=\frac{4Z^2r_0^2E_1^2}{q_0^4}\cos^2(\theta/2)\left\{G_E^2+\frac{J+1}{3J}\frac{G_M^2}{Z^2}\left(\frac{Q}{2}\frac{m_0}{M_0}\right)^2[1+2\tan^2(\theta/2)]\right\},$$

where the spin and magnetic moment of the nucleus are given by J and K, respectively, and $G_M=K$ for $Q\approx 0$.

(1) Conditions of Validity

a. First Born approximation: $\alpha Z/\beta_1\ll 1$.
b. No atomic screening: $\alpha Z^{1/3}\ll q_0$.
c. Extreme-relativistic energies: $\beta_1\approx 1$.

(2) References

a. Rosenbluth formula: R 50, formula (1); Y 57, formula (2.14); H 60, formula (29), (33), (37), and (38).
b. Walecka–Pratt formula: W 62 and G 64, formulas (9) and (10).

(3) Notes

a. The Rosenbluth formula is derived in the one-photon exchange approximation and includes relativistic effects introduced both by the incident electron and the target proton or neutron. The inclusion of the proton's spin in the calculations has the effect of increasing the cross section as the scattering angle (or momentum transfer) increases, in distinction to the case of a particle with zero spin (see Figs. 5, 6, and 7 in H 57).

Early interpretations of the form factors, F_1 and F_2, in terms of the charge and magnetic form factors, G_E and G_M, are given by Ernst, Sachs, and Wali (E 60) and by Sachs (S 62). The advantages of using the formula containing G_E and G_M are pointed out by Hand *et al.* in Ref. H 63.

b. Examples of the dependence of the cross section predicted by the Rosenbluth formula on Q for different values of E_1 are shown in Figs. 7, 8, 19, 20, 27–31 in Ref. H 60.

c. Radiative effects are important for electron–proton scattering and estimates of the radiative correction for this case have been given by Tsai (T 61) and by Meister and Yennie (M 63).

d. Magnetic scattering effects were first estimated by Jauch (J 40) for the case of a point nucleus with a magnetic moment and arbitrary Z compared to the case of a finite nucleus given by the Walecka–Pratt formula.

e. An example of experimental investigations of magnetic scattering pertaining to the Walecka–Pratt formula for arbitrary Z is given by the results of Goldemberg and Torizuka (G 63).

Formula (1A–105)

[The McKinley–Feshbach formula: point nucleus with no screening.]

$$\frac{d\sigma}{d\Omega}=\frac{4Z^2r_0^2E_1^2}{q_0^4}\left[1-\left(\frac{q_0}{2E_1}\right)^2+\frac{\pi\alpha Zq_0}{2E_1}\left(1-\frac{q_0}{2p_1}\right)\right]$$

(1) Conditions of Validity

a. Second Born approximation: $(\alpha Z/\beta_1)^2\ll 1$.
b. No screening: $\alpha Z^{1/3}\ll q_0$.
c. Point-charge nucleus: $R_A\ll 2\pi/p_1$.
d. Infinitely heavy nucleus: $2E_1(m_0/M_0)\ll 1$.
e. Nucleus with negligible spin effects: $(q_0/Z)^2(m_0/M_0)^2\ll 1$.

(2) References

M 48, formula (7).

(3) Notes

a. This formula differs from the Mott–Born formula (1A–101) in that it permits a wider range of Z values. A comparison of the cross sections predicted by the two formulas is shown by the curves in Figs. 19–22.
b. See Note d in the Dalitz formula (1A–107).

Formula (1A–106)

[The Johnson–Weber–Mullin formula: point nucleus with no screening.]

$$d\sigma/d\Omega=(4Z^2r_0^2E_1^2/q_0^4)I_3,$$

where

$$I_3=1-\beta_1^2x^2+\pi\alpha Z\beta_1x(1-x)+(\alpha Z)^2x\{L_2(1-x^2)-4L_2(1-x)+2x\ln^2x+\pi^2(1-x)/2+\pi^2x/6+\beta_1^2x\times[L_2(1-x^2)+(x^2\ln^2x)/(1-x^2)+\pi^2(1-x)/4(1+x)-\pi^2/6]\};$$

$L_2(x)=$ Euler's dilogarithm (Mi 49), Sec. X, $x=\sin\frac{1}{2}\theta$.

(1) Conditions of Validity

a. Higher order Born approximation: $(\alpha Z/\beta_1)^3 \ll 1$.
b. No screening: $\alpha Z^{1/3} \ll q_0$.
c. Point-charge nucleus: $R_A \ll 2\pi/p_1$.
d. Infinitely heavy nucleus: $2E_1(m_0/M_0) \ll 1$.
e. Nucleus with negligible spin effects: $(q_0/Z)^2(m_0/M_0)^2 \ll 1$.

(2) References

J 61, formulas (20a) and (26).

(3) Notes

a. A comparison of the cross sections obtained with this formula and with the Mott–exact formula (1A–109a) for different values of E_1, Z, and θ, is shown in Fig. 1 of Ref. J 61.

b. Mitter and Urban (M 53) derived this cross section in the third Born approximation. Their formula is given in integral form and does not give the same results as the Johnson–Weber–Mullin formula, which are confirmed by the work of Rosen (R 63).

c. It may be expected that future higher order calculations will provide cross-section formulas that have a greater range of validity and are more accurate than formula (1A–106). For example, a recent calculation by Rosen (R 63) gives a cross-section formula correct to fifth order in $\alpha Z/\beta_1$ (fourth-order Born approximation). The third-order Born terms in Rosen's calculations can be shown to be identical to those given by the Johnson, Weber, and Mullin formula (1A–106). Rosen's fourth-order Born terms involve the same functions as appear in the third-order terms, namely, Euler's dilogarithm $L_2(X)$ discussed in Sec. X. However, Born terms higher than the fourth order would involve complicated untabulated functions, and the usefulness of these functions depends on both the effort required to evaluate the cross section and the accuracy desired. These criteria must be used as the basis of comparison with the Mott–exact phase-shift calculations given in formula (1A–109), which can be evaluated by numerical methods with a computer. Such a comparison is particularly important when the calculations include corrections for atomic screening and for the finite nuclear size.

Formula (1A–107)

[The Dalitz formula: point nucleus with exponential screening.]

$$\frac{d\sigma}{d\Omega}=\frac{4Z^2r_0^2E_1^2}{q_0^4}\left\{\left(1-\frac{q_0^2}{4E_1^2}\right)\left(\frac{q_0^2}{q_0^2+\Lambda^2}\right)+\alpha Z\frac{q_0^2}{q_0^2+\Lambda^2}\left(\frac{q_0}{E_1}\right)\left[\tan^{-1}\left(\frac{q_0}{2\Lambda}\right)-\sin(\theta/2)\tan^{-1}\left(\frac{2p_1}{\Lambda}\right)\right.\right.$$
$$\left.\left.+(\Lambda^2+4E_1^2-q_0^2/2)\tan^{-1}\left(\frac{\Lambda q_0}{2V}\right)V^{-1}\right]\right\},$$

where

$$V=[p_1^2q_0^2+\Lambda^2(\Lambda^2+4p_1^2)]^{\frac{1}{2}},$$

and

$\Lambda=(\mu/0.885)(Z^{\frac{1}{3}}/137)$ in units of $\lambda\!\!\!^{-}_0{}^{-1}$ with Λ defined by the exponential potential

$$V(r)=-(Ze^2/r)\exp(-\Lambda r)$$

and

$\mu\approx 0.72$ (B 60)

≈ 1.12, 1.8 (N 59)

≈ 2.18 for beryllium (N 59) [See formula (1A–500) and Ref. M 41 for other light elements.]

(1) Conditions of Validity

a. Second Born approximation: $(\alpha Z/\beta_1)^2 \ll 1$.
b. Exponential screening potential: See values of screening parameter Λ given with formula (1A–107).
c. Point-charge nucleus: $R_A \ll 2\pi/p_1$.
d. Infinitely heavy nucleus: $2E_1(m_0/M_0) \ll 1$.
e. Nucleus with negligible spin effects: $(q_0/Z)^2(m_0/M_0)^2 \ll 1$.

(2) References

D 51, formula (2.5) p. 514; N 59, formula (40).

(3) Notes

a This formula reduces to formula (1A–105) in the limiting case of $\Lambda \sim 0$ (no screening).

b. Multiple scattering calculations are based on a screening angle discussed by Bethe (B 53). The screening angle θ_0 which

is derived from the Dalitz formula is given by the following expression (N 59):

$$\theta_0^2=(\mu/p_1R_{TF})^2[1+(4Z/137)(\mu/p_1R_{TF})\{[(1-\beta_1^2)/\beta_1]\times\ln(\mu/p_1R_{TF})+(0.231/\beta_1)+1.448\beta_1\}].$$

c. The accuracy of the cross sections predicted by the Dalitz formula is subject to the limitations of the second Born approximation and the simple exponential screening approximation. A comparison of the Dalitz cross section with the cross section predicted from formula (1A–109b) with Hartree-type screening is given in Table XII.

d. An excellent discussion of many of the higher order Born approximation calculations for the scattering cross section is given by Dalitz (D 51).

Formula (1A–108)

[The Gorshkov formula: (a) point nucleus with Molière screening and (b) finite nucleus with no screening.]

(a) Formula for point nucleus with Molière screening valid for small momentum transfer:

$$\frac{d\sigma}{d\Omega}=\frac{4Z^2r_0^2E_1^2}{q_0^4}\left\{\left(1-\frac{q_0^2}{4E_1^2}\right)A_1^2+\alpha ZA_1\frac{q_0}{E_1}\left[-\sin\left(\frac{\theta}{2}\right)\sum_{i=1}^{3}a_i\tan^{-1}\left(\frac{2p_1}{\Lambda_i}\right)+\sum_{i=1}^{3}\sum_{j=1}^{3}a_ia_j\left[\tan^{-1}\left(\frac{q_0}{\Lambda_i+\Lambda_j}\right)+\sin\left(\frac{\theta}{2}\right)(\Lambda_i^2+4E_1^2-q_0^2/2)W_1/V_1\right]\right]\right\},$$

where

$$A_1=1-F(q_0)=\sum_{i=1}^{3}a_i\frac{q_0^2}{q_0^2+\Lambda_i^2},$$

$$V_1=\{(q_0^2+\Lambda_i^2+\Lambda_j^2)^2-4\Lambda_i^2\Lambda_j^2\cos^2(\tfrac{1}{2}\theta)\}^{\frac{1}{2}},$$

and

$$W_1=\tan^{-1}\left\{\frac{2p_1V_1(\Lambda_i+\Lambda_j)}{q_0^2(4p_1^2-\Lambda_i\Lambda_j)+(\Lambda_i+\Lambda_j)^2(4p_1^2+\Lambda_i\Lambda_j)}\right\}.$$

With Molière screening, $\Lambda_i=(Z^{\frac{1}{3}}/121)b_i$ in units of λ_0^{-1}, $a_1=0.10$, $a_2=0.55$, $a_3=0.35$, $b_1=6.0$, $b_2=1.2$, $b_3=0.30$.

(b) Formula for finite nucleus with no screening valid for large momentum transfer:

$$\frac{d\sigma}{d\Omega}=\frac{4Z^2r_0^2E_1^2}{q_0^4}\left(\left(1-\frac{q_0^2}{4E_1^2}\right)A_2^2+\alpha ZA_2\frac{q_0}{E_1}\left\{-\sin(\tfrac{1}{2}\theta)\int_0^\infty d\lambda\frac{\chi(\lambda)}{q_0^2+\lambda^2}(\lambda^2+8E_1^2-q_0^2)\tan^{-1}\left(\frac{\lambda}{2p_1}\right)+2\int_0^\infty d\lambda\chi(\lambda)\tan^{-1}\left(\frac{\lambda}{q_0}\right)+\int_0^\infty d\lambda_1\int_0^\infty d\lambda_2\chi(\lambda_1)\chi(\lambda_2)\left[-\tan^{-1}\left(\frac{\lambda_1+\lambda_2}{q_0}\right)+\sin(\tfrac{1}{2}\theta)\left(\lambda_1^2+4E_1^2-\frac{q_0^2}{2}\right)W_2/V_2\right]\right\}\right),$$

where

$$A_2=\int_0^\infty d\lambda\frac{\lambda^2\chi(\lambda)}{q_0^2+\lambda^2},$$

$$V_2=\{(q_0^2+\lambda_1^2+\lambda_2^2)-4\lambda_1^2\lambda_2^2\cos^2(\tfrac{1}{2}\theta)\}^{\frac{1}{2}},$$

$$W_2=\tan^{-1}\left\{\frac{2p_1V_2(\lambda_1+\lambda_2)}{q_0^2(4p_1^2-\lambda_1\lambda_2)+(\lambda_1+\lambda_2)^2(4p_1^2+\lambda_1\lambda_2)}\right\}.$$

The nuclear charge density $\rho(r)$ is related to the function $\chi(\lambda)$ by the equation

$$r\rho(r)=\frac{1}{4\pi}\int_0^\infty d\lambda\chi(\lambda)\lambda^2\exp(-\lambda r).$$

The normalization,

$$\int \rho(r)\, d^3r = 1,$$

gives

$$\int_0^\infty d\lambda \chi(\lambda) = 1.$$

(1) Conditions of Validity

a. Higher order Born approximation: $(\alpha Z/\beta_1)^2 \ll 1$.

b. Infinitely heavy nucleus: $2E_1(m_0/M_0) \ll 1$.

c. Thomas–Fermi screening and nucleus with negligible spin effects: $(q_0/Z)^2(m_0/M_0)^2 \ll 1$.

(2) References

Formulas (1A–108a) and (1A–108b) were derived from Gorshkov's work given in Refs. G 61 and G 62.

(3) Notes

a. In the region $(Z^{1/3}/121) \ll q_0 \ll R_A^{-1}$, formulas (1A–108a) and (1A–108b) become identical to the McKinley–Feshbach formula (1A–105). Therefore, formulas (1A–108a) and (1A–108b) together give the cross section for all values of q_0 in the second-order Born approximation.

b. If only one exponential potential is inserted in formula (1A–108a), i.e. $a_1=1$, $a_2=a_3=0$, or $V=-(Ze^2/r)\exp(-\Lambda r)$, then the formula reduces to the Dalitz formula (1A–107) with $\Lambda_1=\Lambda$.

c. Other formulas for the cross section which are derived with second or higher order Born approximations for a finite nucleus are given by Lewis (L 56) in integral form for different models of the nuclear charge distribution, and by Schiff (Sc 55). Such calculations are also discussed by Nagel (N 60).

Formula (1A–109)

[The Mott-exact "phase-shift" formula: (a) point nucleus with no screening and (b) point or finite nucleus with arbitrary screening.]

$$d\sigma/d\Omega = (r_0/\alpha p_1)^2(|F'|^2 \csc^2\tfrac{1}{2}\theta + |G|^2 \sec^2\tfrac{1}{2}\theta)$$

or

$$d\sigma/d\Omega = |f|^2 + |g|^2,$$

where $f=r_0/\alpha p_1(G-F')$, $g=r_0/\alpha p_1(F' \cot\frac{1}{2}\theta + G\tan\frac{1}{2}\theta)$, $F'=i\alpha ZF/p_1$.

(a) Point nucleus with no screening:

$$\frac{d\sigma}{d\Omega} = \frac{4Z^2r_0^2E_1^2}{q_0^4}\left\{\frac{q_0^2}{E_1^2p_1^2}|F|^2 + \frac{|G|^2}{(\alpha Z)^2}\frac{q_0^4}{E_1^2(4p_1^2-q_0^2)}\right\} = \frac{4Z^2r_0^2E_1^2}{q_0^4}\{B\},$$

where B is the cross-section ratio of the Mott–exact formula (1A–109a) to the Rutherford formula (1A–100). This ratio is evaluated in Refs. D 56 and S 56 as a function of the parameters E_1, Z, and θ, as shown by Table VII which is taken from the work of Doggett and Spencer in Ref. D 56.

Also in the above equation: $F=F_0+F_1$, and $G=G_0+G_1$,

$$F_0 = \frac{i\Gamma(1-i\alpha Z/\beta_1)}{2\Gamma(1+i\alpha Z/\beta_1)} \exp[i\alpha Z/\beta_1 \ln\sin^2\tfrac{1}{2}\theta],$$

$$F_1 = \tfrac{1}{2}i\sum_{l=0}^{\infty}[lD_l + (l+1)D_{l+1}](-1)^l P_l(\cos\theta),$$

$$G_0 = -i\alpha Z/\beta_1[\cot^2\tfrac{1}{2}\theta]F_0,$$

$$G_1 = \tfrac{1}{2}i\sum_{l=0}^{\infty}[l^2D_l - (l+1)^2D_{l+1}](-1)^l P_l(\cos\theta),$$

$$D_l = \frac{\exp(-i\pi l)}{(l+i\alpha Z/\beta_1)}\frac{\Gamma(l-i\alpha Z/\beta_1)}{\Gamma(l+i\alpha Z/\beta_1)} - \frac{\exp(-i\pi\rho_l)}{\rho_l+i\alpha Z/\beta_1}\frac{\Gamma(\rho_l-i\alpha Z/\beta_1)}{\Gamma(\rho_l+i\alpha Z/\beta_1)},$$

$\rho_l = [l^2-(\alpha Z)^2]^{\frac{1}{2}}$, l = any integer,

$\Gamma(\mu)$ = gamma function of argument μ,

P_l = Legendre polynomial of order l.

Note: For small angles, the following approximate expression for the above formula is obtained from the work of Bartlett and Watson (B 39):

$$\frac{d\sigma}{d\Omega}\approx\frac{4Z^2r_0^2E_1^2}{q_0^4}\left[1+\frac{\pi}{\sqrt{2}}\frac{Z\beta_1}{137}\cos\gamma(1-\cos\theta)^{\frac{1}{2}}\right],$$

where

$$\exp(i\alpha)=\frac{\Gamma(\frac{1}{2}-i\alpha Z/\beta_1)\,\Gamma(1+i\alpha Z/\beta_1)}{\Gamma(\frac{1}{2}+i\alpha Z/\beta_1)\,\Gamma(1-i\alpha Z/\beta_1)}.$$

This approximation is introduced to evaluate the Mott-exact formula at small angles because an excessive number of phase-shift terms are required. Although this formula is not valid at small angles because it does not include screening effects, it is useful for studies of the screening correction. The ratio of this formula to the Rutherford formula (1A-100) approaches unity as the electron scattering angle approaches zero.

(b) Point or finite nucleus with arbitrary screening:

$$d\sigma/d\Omega=|f|^2+|g|^2,$$

where

$$f=\frac{137r_0}{2ip_1}\sum[(l+1)\{\exp(2i\eta_l)-1\}+l\{\exp(2i\eta_{-l-1})-1\}]P_l(\cos\theta),$$

$$g=\frac{137r_0}{2ip_1}\sum\{\exp(2i\eta_{-l-1})-\exp(2i\eta_l)\}P_l^1(\cos\theta).$$

The phase shift η_l is defined by the expression, $\sin(p_1r-\frac{1}{2}l\pi+\eta_l)$, which vanishes at the origin and is obtained from the asymptotic solution of the following differential equation

$$d^2G_l/dr^2+\{p_1^2+[l(l+1)/r^2]-U_l\}G_l=0.$$

Similarly η_{-l-1} is the phase shift given in the above asymptotic solution, with l replaced by $-(l+1)$. The effect of the nuclear and/or the atomic charge structure is contained in the effective Dirac potential U_l which is given as

$$U_l=2E_1V-V^2-\frac{(l+1)}{r}\frac{D'}{D}+\frac{3}{4}\frac{D'^2}{D^2}-\frac{1}{2}\frac{D''}{D},$$

where $D=E_1-V+1$, $D'=dD/dr$, $D''=d^2D/dr^2$, $l=$ any integer, and $V=$ spherically symmetric potential arising from the charge structure of the nucleus and/or the atom.

(1) Conditions of Validity

a. Point-charge nucleus: $R_A\ll 2\pi/p_1$.
b. Infinitely heavy nucleus: $2E_1(m_0/M_0)\ll 1$.
c. Nucleus with negligible spin effects: $(q_0/Z)^2(m_0/M_0)^2\ll 1$.
d. No screening for formula (1A-109a): $\alpha Z^{1/3}\ll q_0$.

(2) References

a. No screening: M 49, formula (41), p. 80; S 56, formula (1).
b. Arbitrary screening: M 54, formulas (1) and (2); M 49, p. 74-76.

(3) Notes

a. These formulas must be evaluated for a particular case by numerical methods. For an unscreened point nucleus, some cross-section values obtained from formula (1A-109a) are given in Tables III and VI, which are obtained from the results of Sherman (S 56) and of Doggett and Spencer (D 56). For a point nucleus with particular screening potentials in formula (1A-109b), cross-section data for various values of T_1, Z, and θ are given in Refs. B 41 (Table IV), M 43 (Fig. 1), M 54 (Fig. 21), L 63, L 64, and Table XII in Sec. VIII. Calculations pertaining to formula (1A-109b) by Lin, Sherman, and Percus (L 63, L 64) show good agreement with experimental results (Mo 63). Other results for the f and g functions in formula (1A-109b) are given in tabulated form for atomic numbers from one to ten by Bhalla (B 64).

b. It is important to note that formula (1A-109b) can include the charge-structure effect of the nucleus and the atom, providing this structure is assumed to be spherically symmetric.

c. An approximate expression for the Mott-exact formula in terms of a single power series with given coefficients is obtained in Ref. C 55.

d. Estimates of the nuclear size correction based on the Mott-exact formula (1A-109b) are given in Refs. E 50, P 50, Y 54, and F 54.

e. An approximate expression of the cross section for small-angle scattering by a pure Coulomb field and by a finite nucleus is given by Drell and Pratt (D 62).

f. Various experimental results have been compared with the predictions of the Mott–exact formula. These comparisons have shown agreement as well some inconsistencies and discrepancies. A partial summary of these results is given in Table VIII.

g. Calculations based on formula (1A–109) are given in Refs. F 58 and R 58 for muon scattering from a finite nucleus and in Ref. D 56 for positron scattering from a point nucleus.

Formula (1A–110)

[The nonrelativistic Mott–exact "phase-shift" formula: point nucleus with arbitrary screening for nonrelativistic electrons.]

$$\frac{d\sigma}{d\Omega}=\left(\frac{137r_0}{2p_1}\right)^2 \left| \sum_{l=0}^{\infty}(2l+1)[\exp(2i\eta_l)-1]P_l(\cos\theta) \right|^2,$$

where $P_l(\cos\theta)$ is the lth Legendre coefficient (Ref. W 27, p. 302); η_l is the phase shift which depends on p_1 and the scattering potential $V(r)$.

In general, η_l is not explicitly defined by a single, closed, analytical formula, and it must be evaluated for a given element [or potential $V(r)$] by numerical integration. Except for a pure Coulomb potential, the contribution of all terms except the first ($l=0$) is negligible as β_1 approaches zero, and because P_0 is equal to unity, the angular distribution becomes isotropic. As β_1 increases, higher l values are introduced and the angular distribution becomes more complicated.

(a) Exact expression for the phase shift: The phase shift η_l is defined exactly in the expression

$$G\sim \sin(p_1r-\tfrac{1}{2}l\pi+\eta_l),$$

where G is the asymptotic solution of the differential equation:

$$(\partial^2G/\partial r^2)+\{p_1^2-2V(r)-[l(l+1)/r^2\}G=0,$$

where $V(r)$ is the atomic scattering potential.

(b) Approximate expression for small phase shift (<0.1 radian): For the atomic potential, $V(r)\ll l(l+1)/2r^2$ with $p_1r\sim\{l(l+1)\}^{\frac{1}{2}}$,

$$\eta_l\approx -\pi\int_0^{\infty}V(r)[J_{l+\frac{1}{2}}(p_1r)]^2r\,dr,$$

where J is a Bessel function (Ref. W 27, p. 355).

(c) Approximate expression for large phase shift:

$$\eta_l\approx\int_{r_1}^{\infty}\left\{p_1^2-2V(r)-\frac{(l+\frac{1}{2})^2}{r^2}\right\}^{\frac{1}{2}}dr-\int_{r_2}^{\infty}\left\{p_1^2-\frac{(l+\frac{1}{2})^2}{r^2}\right\}^{\frac{1}{2}}dr,$$

where $V(r)$ is the atomic potential and where r_1 and r_2 are the zeros of the respective integrands. This formula may be used with good accuracy for phases as low as 0.2 rad. A discussion of this formula is given in Ref. L 37.

(1) *Conditions of Validity*

a. Nonrelativistic electrons: $\beta_1\ll 1$.

b. Point-charge nucleus: $R_A\ll 2\pi/p_1$.

c. Infinitely heavy nucleus: $2E_1(m_0/M_0)\ll 1$.

(2) *References*

M 49: Chap. II, formulas (17), (19), and (27); Chap. VII, formulas (12) and (30).

(3) *Notes*

a. Because the dominant terms in the series are such that $\eta_l\approx\frac{1}{2}\pi$, the cross section for a given T_1 (with $\beta_1\ll 1$) has the approximate form $d\sigma/d\Omega\sim\{P_l(\cos\theta)\}^2$. This behavior shows maximum and minimum values (diffraction effects) in the angular distribution of the electrons.

b. For a given Z and for $\theta=0$, the value of $d\sigma/d\Omega$ is independent of T_1.

c. For a given Z and T_1, $d\sigma/d\Omega$ decreases as θ becomes larger. The rate of decrease in $d\sigma/d\Omega$ becomes larger as T_1 becomes larger.

d. The value of $d\sigma/d\Omega$ approaches a constant value as $\theta \to 0$. This condition occurs because the phase shifts η_l become smaller as θ decreases (larger impact parameter) and although a larger number of l values are required, there is a maximum number l_{max} beyond which the contribution of the remaining terms become negligible.

e. Various estimates of this cross section for specific values of T_1, θ, and Z with different screening approximations and in some cases with the inclusion of exchange and polarization effects, are discussed in Chap. X of Ref. M 49 and Chap. III of Ref. M 52. Recent improved calculations are given by Karle and Bonham (K 64).

f. For $\theta = 0$, $d\sigma/d\Omega$ has a finite value because of screening effects.

g. For electron Coulomb scattering from the hydrogen atom, $d\sigma/d\Omega$ is evaluated in the energy region from 3 to 14 eV in Ref. T 61. Other pertinent results for scattering by hydrogen are given for example in Refs. Gi 61, R 60, and are summarized in the comprehensive review by Burke and Smith (Bu 62).

Formula (1A–111)

[The Molière–exact formula with screening for small momentum transfer: point nucleus with arbitrary screening.]

$$\frac{d\sigma}{d\Omega} = (137r_0)^2 E_1^2 \left| \int_0^\infty \rho \, d\rho \; J_0(\rho q_0) \left\{ \exp\left[-\frac{2i}{\beta_1} \int_0^\infty V(r) \, dz \right] - 1 \right\} \right|^2,$$

where ρ and z are the components of r perpendicular and parallel, respectively, to the incident electron momentum such that r is equal to $(\rho^2+z^2)^{\frac{1}{2}}$, $J_0(\rho q_0)$ is the zero-order Bessel function, and $V(r)$ is the scattering potential.

(1) Conditions of Validity

Small momentum transfer and negligible electron-spin effects: $(q_0/2E_1) \ll 1$.

(2) References

M 47, formula (4.6′); O 57, formula (9.2).

(3) Notes

This formula which is derived from the Klein–Gordon equation for a spinless particle, reduces to the Rutherford formula for the case of no screening.

Formula (1A–200)

[The "second born" formula: point nucleus with no screening.]

$$d\sigma(\boldsymbol{\zeta}_1, \mathbf{n})/d\Omega = [d\sigma/d\Omega]_{105}[1 + S\mathbf{n}\cdot\boldsymbol{\zeta}_1],$$

where $[d\sigma/d\Omega]_{105} = (4Z^2 r_0^2 E_1^2/q_0^4) I_2 =$ formula (1A–105) with I_2 and $I_2 S$ defined in formula (1A–401).

(1) Conditions of Validity

Same conditions as given in formula (1A–401).

(2) References

Equation (6.05) and formula (1A–401).

(3) Notes

See Note (c) in formula (1A–106).

Formula (1A–201)

[The Johnson–Weber–Mullin formula: point nucleus with no screening.]

$$d\sigma(\boldsymbol{\zeta}_1, \mathbf{n})/d\Omega = [d\sigma/d\Omega]_{106}[1+S\mathbf{n}\cdot\boldsymbol{\zeta}_1],$$

where $[d\sigma/d\Omega]_{106} = (4Z^2r_0^2E_1^2/q_0^4)I_3 =$ formula (1A–106) with I_3 and I_3S defined in formula (1A–402).

(1) Conditions of Validity

Same conditions as given in formula (1A–402).

(2) References

Equation (6.05) and formula (1A–402).

(3) Notes

Same notes as given in formula (1A–402).

Formula (1A–202)

[The Gorshkov formula: (a) point nucleus with Molière screening and (b) finite nucleus with no screening.]

(a) Formula for point nucleus with Molière screening valid for small momentum transfer:

$$d\sigma(\boldsymbol{\zeta}_1, \mathbf{n})/d\Omega = [d\sigma/d\Omega]_{108a}[1+S\mathbf{n}\cdot\boldsymbol{\zeta}_1],$$

where

$$[d\sigma/d\Omega]_{108a} = (4Z^2r_0^2E_1^2/q_0^4)I_a = \text{ formula (1A–108a)},$$

with

$$I_a = \left(1-\frac{q_0^2}{4E_1^2}\right)A_1^2 + \alpha Z A_1 \frac{q_0}{E_1}\left\{-\sin(\tfrac{1}{2}\theta)\sum_{i=1}^{3} a_i \tan^{-1}\left(\frac{2p_1}{\Lambda_i}\right) + \sum_{i=1}^{3}\sum_{j=1}^{3} a_i a_j \left[\tan^{-1}\left(\frac{q_0}{\Lambda_i+\Lambda_j}\right) + \sin\tfrac{1}{2}\theta(\Lambda_i^2+4E_1^2-\tfrac{1}{2}q_0^2)W_1/V_1\right]\right\}$$

and

$$SI_a = -\alpha Z \tan(\tfrac{1}{2}\theta)\sin^2(\tfrac{1}{2}\theta)A_1\frac{1}{E_1}\left\{\sum_{i=1}^{3} a_i \ln\frac{\Lambda_i^2}{\Lambda_i^2+4p_1^2} + \tfrac{1}{2}\sum_{i=1}^{3}\sum_{j=1}^{3} a_i a_j (q_0^2+2\Lambda_i^2)L_1/V_1\right\},$$

where

$$A_1 = \sum_{i=1}^{3} a_i \frac{q_0^2}{q_0^2+\Lambda_i^2},$$

$$V_1 = \{(q_0^2+\Lambda_i^2+\Lambda_j^2)^2 - 4\Lambda_i^2\Lambda_j^2\cos^2(\tfrac{1}{2}\theta)\}^{\frac{1}{2}},$$

$$W_1 = \tan^{-1}\left\{\frac{2p_1V_1(\Lambda_i+\Lambda_j)}{q_0^2(4p_1^2-\Lambda_i\Lambda_j)+(\Lambda_i+\Lambda_j)^2(4p_1^2+\Lambda_i\Lambda_j)}\right\},$$

$$L_1 = \ln\frac{\Lambda_i^2\Lambda_j^2(\Lambda_i+\Lambda_j)^2+p_1^2(q_0^2+(\Lambda_i+\Lambda_j)^2+V_1)^2}{\Lambda_i^2\Lambda_j^2(\Lambda_i+\Lambda_j)^2+p_1^2(q_0^2+(\Lambda_i+\Lambda_j)^2-V_1)^2}.$$

With Molière screening, $\Lambda_i = (Z^{\frac{1}{3}}/121)b_i$ in units of λ_0^{-1}; $a_1=0.10$, $a_2=0.55$, $a_3=0.35$, $b_1=6.0$, $b_2=1.2$, $b_3=0.30$.

(b) Formula for finite nucleus with no screening valid for large momentum transfer:

$$d\sigma(\boldsymbol{\zeta}_1, \mathbf{n})/d\Omega = [d\sigma/d\Omega]_{108b}[1+S\mathbf{n}\cdot\boldsymbol{\zeta}_1],$$

where

$$[d\sigma/d\Omega]_{108b} = (4Z^2r_0^2E_1^2/q_0^4)I_b = \text{formula (1A–108b)}$$

with

$$I_b = \left(1-\frac{q_0^2}{4E_1^2}\right)A_2^2 + \alpha Z A_2 \frac{q_0}{E_1}\left\{-\sin(\tfrac{1}{2}\theta)\int_0^\infty d\lambda \frac{\chi(\lambda)}{q_0^2+\lambda^2}(\lambda^2+8E_1^2-q_0^2)\tan^{-1}\left(\frac{\lambda}{2p_1}\right)+2\int_0^\infty d\lambda\chi(\lambda)\tan^{-1}\left(\frac{\lambda}{q_0}\right)\right.$$
$$\left.+\int_0^\infty d\lambda_1\int_0^\infty d\lambda_2\chi(\lambda_1)\chi(\lambda_2)\left[-\tan^{-1}\left(\frac{\lambda_1+\lambda_2}{q_0}\right)+\sin\tfrac{1}{2}\theta(\lambda_1^2+4E_1^2-q_0^2/2)W_2/V_2\right]\right\}$$

and

$$SI_b = -\alpha Z\tan\tfrac{1}{2}\theta\sin^2(\tfrac{1}{2}\theta)A_2(1/E_1)\left\{2\ln(\sin\tfrac{1}{2}\theta)-2\int_0^\infty d\lambda\chi(\lambda)\ln\frac{q_0^2+\lambda^2}{\lambda 2p_1}\right.$$
$$\left.+\tfrac{1}{2}\int_0^\infty d\lambda_1\int_0^\infty d\lambda_2\chi(\lambda_1)\chi(\lambda_2)(q_0^2+2\lambda^2)L_2/V_2\right\},$$

where

$$A_2 = \int\frac{\lambda^2\chi(\lambda)\,d\lambda}{q_0^2+\lambda^2},$$

$$V_2 = \{(q_0^2+\lambda_1^2+\lambda_2^2)-4\lambda_1^2\lambda_2^2\cos^2(\tfrac{1}{2}\theta)\}^{\frac{1}{2}},$$

$$W_2 = \tan^{-1}\left\{\frac{2p_1V_2(\lambda_1+\lambda_2)}{q_0^2(4p_1^2-\lambda_1\lambda_2)+(\lambda_1+\lambda_2)^2(4p_1^2+\lambda_1\lambda_2)}\right\},$$

$$L_2 = \ln\frac{\lambda_1^2\lambda_2^2(\lambda_1+\lambda_2)^2+p_1^2[q_0^2+(\lambda_1+\lambda_2)^2+V_2]^2}{\lambda_1^2\lambda_2^2(\lambda_1+\lambda_2)^2+p_1^2[q_0^2+(\lambda_1+\lambda_2)^2-V_2]^2}.$$

The nuclear charge density, $\rho(r)$, is related to the function $\chi(\lambda)$, by the equation

$$r\rho(r) = \frac{1}{4\pi}\int d\lambda\chi(\lambda)\lambda^2\exp(-\lambda r).$$

(1) Conditions of Validity

a. Higher order Born approximation $(\alpha Z/\beta_1)^2 \ll 1$.

b. Infinitely heavy nucleus: $2E_1(m_0/M_0) \ll 1$.

c. Thomas–Fermi screening and nucleus with negligible spin effects: $(q_0/Z)^2(m_0/M_0)^2 \ll 1$.

(2) References

Formulas (a) and (b) were derived from Gorshkov's work given in Refs. G 61 and G 62.

(3) Notes

Formulas (1A–202a) and (1A–202b) together give the cross section for all values of q_0 in the second Born approximation.

Formula (1A–203)

[The Mott–exact "phase-shift" formula: (a) point nucleus with no screening and (b) point or finite nucleus with arbitrary screening.]

$$d\sigma(\boldsymbol{\zeta}_1, \mathbf{n})/d\Omega = [d\sigma/d\Omega]_{109}[1+S\mathbf{n}\cdot\boldsymbol{\zeta}_1],$$

where $\mathbf{n}$ and $\boldsymbol{\zeta}_1$ are unit vectors defined in Sec. II.

$$[d\sigma/d\Omega]_{109} = (137r_0/p_1)^2(|F'|^2\csc^2\tfrac{1}{2}\theta + |G|^2\sec^2\tfrac{1}{2}\theta) = |f|^2+|g|^2 = \text{formula (1A–109)},$$

$$F' = i\alpha ZF/p_1,$$

$$S = (-2i\csc\theta)(F'G^*-GF'^*)/(|F'|^2\csc^2\tfrac{1}{2}\theta+|G|^2\sec^2\tfrac{1}{2}\theta) = i(fg^*-gf^*)/(|f|^2+|g|^2).$$

(a) Point nucleus with no screening: For this case, the basic pair of functions F and G which are used in the above equations, are defined in formula (1A–109a).

For an unscreened, point nucleus, values of $[d\sigma/d\Omega]_{109}$ and S for various energies, atomic numbers, and angles are given in Tables III and VII and Figs. 8 and 9.

(b) Point or finite nucleus with arbitrary screening: For this case, the basic pair of functions f and g, which are used in the above equations, are defined in formula (1A–109b).

For a point nucleus with Hartree screening, values of $[d\sigma/d\Omega]_{109}$ are given in Table XII. Results for a finite nucleus are noted in formula (1A–109).

(1) Conditions of Validity

a. Infinitely heavy nucleus: $2E_1(m_0/M_0)\ll 1$.

b. Nucleus with negligible spin effects: $(q_0/Z)^2(m_0/M_0{}^2\ll 1$.

c. For point-charge nucleus: $R_A\ll 2\pi/p_1$.

d. For no screening: $\alpha Z^{1/3}\ll q_0$.

(2) References

Equation (6.05) in Sec. VI and formula (1A–403).

(3) Notes

Recent results pertaining to cases (a) and (b) are given in formula (1A–109).

Formula (1A–300)

[The "second Born" formula: point nucleus with no screening.]

$$d\sigma(\boldsymbol{\zeta}_2,\mathbf{n})/d\Omega=\tfrac{1}{2}[d\sigma/d\Omega]_{105}[1+S\mathbf{n}\cdot\boldsymbol{\zeta}_2],$$

where

$$[d\sigma/d\Omega]_{105}=(4Z^2r_0{}^2E_1{}^2/q_0{}^4)I_2=\text{ formula (1A–105)}$$

with I_2 and I_2S defined in formula (1A–401).

(1) Conditions of Validity

Same conditions as given in formula (1A–401)

(2) References

Equation (6.04) in Sec. VI and formula (1A–401).

(3) Notes

See Note (c) in formula (1A–106).

Formula (1A–301)

[The Johnson–Weber–Mullin formula: point nucleus with no screening.]

$$d\sigma(\boldsymbol{\zeta}_2,\mathbf{n})/d\Omega=\tfrac{1}{2}[d\sigma/d\Omega]_{106}[1+S\mathbf{n}\cdot\boldsymbol{\zeta}_2],$$

where

$$[d\sigma/d\Omega]_{106}=(4Z^2r_0{}^2E_1{}^2/q_0{}^4)I_3=\text{ formula (1A–106)}$$

with I_3 and I_3S defined in formula (1A–402).

(1) Conditions of Validity

Same conditions as given in formula (1A–402).

(2) References

Equation (6.04) in Sec. VI and formula (1A–402).

(3) Notes

Same notes as given in formula (1A–402).

Formula (1A–302)

[The Mott–exact "phase-shift" formula: (a) point nucleus with no screening and (b) point or finite nucleus with arbitrary screening.]

$$d\sigma(\zeta_2, \mathbf{n})/d\Omega = \tfrac{1}{2}[d\sigma/d\Omega]_{109}[1+S\mathbf{n}\cdot\zeta_2],$$

where $\mathbf{n}$ and ζ_2 are unit vectors defined in Sec. II,

$$[d\sigma/d\Omega]_{109} = (r_0/\alpha p_1)^2(|F'|^2\csc^2\tfrac{1}{2}\theta + |G|^2\sec^2\tfrac{1}{2}\theta) = |f|^2 + |g|^2 = \text{formula (1A–109)},$$

$$F' = i\alpha ZF/p_1,$$

$$S = (-2i\csc\theta)(F'G^* - GF'^*)/(|F'|^2\csc^2\tfrac{1}{2}\theta + |G|^2\sec^2\tfrac{1}{2}\theta) = i(fg^* - gf^*)/(|f|^2 + |g|^2).$$

(a) Point nucleus with no screening: For this case, the basic pair of functions F and G, which are used in the above equations, are defined in formula (1A–109a).

For an unscreened point nucleus, values of $[d\sigma/d\Omega]_{109}$ and S for various energies, atomic numbers, and angles are given in Tables III and VII, and Figs. 8 and 9.

(b) Point or finite nucleus with arbitrary screening: For this case, the basic pair of functions f and g, which are used in the above equations, are defined in formula (1A–109b).

For a point nucleus with Hartree screening, values of $[d\sigma/d\Omega]_{109}$ are given in Table XII. Results for a finite nucleus are noted in formula (1A–109).

(1) Conditions of Validity

a. Infinitely heavy nucleus: $2E_1(m_0/M_0) \ll 1$.

b. Nucleus with negligible spin effects: $(q_0/Z)^2(m_0/M_0)^2 \ll 1$.

c. For point-charge nucleus: $R_A \ll 2\pi/p_1$.

d. For no screening: $\alpha Z^{1/3} \ll q_0$.

(2) References

Equation (6.04) in Sec. VI and formula (1A–403).

(3) Notes

Recent results pertaining to cases (a) and (b) are given in formula (1A–109).

Formula (1A–400)

[The "first Born" formula: point nucleus with no screening.]

$$d\sigma(\zeta_1, \zeta_2, \mathbf{n})/d\Omega = \tfrac{1}{2}[d\sigma/d\Omega]_{101}[1 + (\mathbf{n}\cdot\zeta_1)(\mathbf{n}\cdot\zeta_2) + S\mathbf{n}\cdot(\zeta_1+\zeta_2) + (L\cos\theta - R\sin\theta)(\mathbf{n}\times\zeta_1)\cdot(\mathbf{n}\times\zeta_2) + (R\cos\theta + L\sin\theta)\mathbf{n}\cdot(\zeta_1\times\zeta_2)],$$

where

$$[d\sigma/d\Omega]_{101}=(4Z^2r_0^2E_1^2/q_0^4)I_1=\text{ formula (1A-101)},$$

$$I_1=1-\beta_1^2x^2,$$

$$I_1S=0,$$

$$I_1L=1-2x^2+\beta_1^2x^2,$$

$$I_1R=-2x(1-x^2)^{\frac{1}{2}}/E_1,$$

with $R^2+I^2=1$, and $x=\sin\frac{1}{2}\theta$. $\mathbf{n}$, $\boldsymbol{\zeta}_1$, and $\boldsymbol{\zeta}_2$ are unit vectors defined in Sec. II.

(1) Conditions of Validity

a. First Born approximation: $\alpha Z/\beta_1\ll 1$.
b. No screening: $\alpha Z^{1/3}\ll q_0$.
c. Point-charge nucleus: $R_A\ll 2\pi/p_1$.
d. Infinitely heavy nucleus: $2E_1\, m_0/M_0\ll 1$.
e. Nucleus with negligible spin effects: $(q_0/Z)^2(m_0/M_0)^2\ll 1$.

(2) References

This formula was obtained from first Born calculations as given for example by Toptygin (To 59).

Formula (1A–401)

[The "second Born" formula: point nucleus with no screening.]

$$d\sigma(\boldsymbol{\zeta}_1,\boldsymbol{\zeta}_2,\mathbf{n})/d\Omega=\tfrac{1}{2}[d\sigma/d\Omega]_{105}[1+(\mathbf{n}\cdot\boldsymbol{\zeta}_1)(\mathbf{n}\cdot\boldsymbol{\zeta}_2)+S\mathbf{n}\cdot(\boldsymbol{\zeta}_1+\boldsymbol{\zeta}_2)+(L\cos\theta-R\sin\theta)(\mathbf{n}\times\boldsymbol{\zeta}_1)\cdot(\mathbf{n}\times\boldsymbol{\zeta}_2)$$
$$+(R\cos\theta+L\sin\theta)\mathbf{n}\cdot(\boldsymbol{\zeta}_1\times\boldsymbol{\zeta}_2),$$

where

$$[d\sigma/d\Omega]_{105}=(4Z^2r_0^2E_1^2/q_0^4)I_2=\text{ formula (1A-105)},$$

$$I_2=1-\beta_1^2x^2+\pi\alpha Z\beta_1x(1-x),$$

$$I_2S=(2\alpha Zx^3\beta_1\ln x)/E_1(1-x^2)^{\frac{1}{2}},$$

$$I_2L=1-2x^2+\beta_1^2x^2+\pi\alpha Z\beta_1x(1-x),$$

$$I_2R=-\frac{2x(1-x^2)^{\frac{1}{2}}}{E_1}\left(1+\frac{\pi\alpha Z\beta_1x}{2(1+x)}\right),$$

with $R^2+L^2=1$ (to first order in αZ) and $\mathbf{n}$, $\boldsymbol{\zeta}_1$, and $\boldsymbol{\zeta}_2$ are unit vectors defined in Sec. II, $x=\sin\frac{1}{2}\theta$.

(1) Conditions of Validity

a. Second Born approximation: $(\alpha Z/\beta_1)^2\ll 1$.
b. No screening: $\alpha Z^{1/3}\ll q_0$.
c. Point-charge nucleus: $R_A\ll 2\pi/p_1$.
d. Infinitely heavy nucleus: $2E_1\, m_0/M_0\ll 1$.
e. Nucleus with negligible spin effects: $(q_0/Z)^2(m_0/M_0)^2\ll 1$.

(2) References

This formula was obtained from second Born calculations as given for example by Gürsey (G 57), Banerjee (Ba 58), and Toptygin (To 59).

Formula (1A–402)

[The Johnson–Weber–Mullin formula: point nucleus with no screening.]

$$d\sigma(\boldsymbol{\zeta}_1, \boldsymbol{\zeta}_2, \mathbf{n})/d\Omega = \tfrac{1}{2}[d\sigma/d\Omega]_{106}[1+(\mathbf{n}\cdot\boldsymbol{\zeta}_1)(\mathbf{n}\cdot\boldsymbol{\zeta}_2)+S\mathbf{n}\cdot(\boldsymbol{\zeta}_1+\boldsymbol{\zeta}_2)+(L\cos\theta-R\sin\theta)(\mathbf{n}\times\boldsymbol{\zeta}_1)\cdot(\mathbf{n}\times\boldsymbol{\zeta}_2)+(R\cos\theta+L\sin\theta)\mathbf{n}\cdot(\boldsymbol{\zeta}_1\times\boldsymbol{\zeta}_2)],$$

where

$$[d\sigma/d\Omega]_{106} = (4Z^2r_0^2E_1^2/q_0^4)I_3 = \text{formula (1A–106)},$$

$$I_3 = 1-\beta_1^2x^2+\pi\alpha Z\beta_1x(1-x)+(\alpha Z)^2x\{L_2(1-x^2)-4L_2(1-x)+2x\ln^2x+\pi^2(1-x)/2+\pi^2x/6+\beta_1^2x[L_2(1-x^2)+(x^2\ln^2x)/(1-x^2)+\pi^2(1-x)/4(1+x)-\pi^2/6]\},$$

$$I_3S = \frac{2\alpha Zx^3}{E_1(1-x^2)^{\frac{1}{2}}}\left[\beta_1\ln x+\pi\alpha Z\left\{\ln x+\ln 4/x-\frac{1+x}{x^2}\ln(1+x)\right\}\right],$$

$$I_3L = 1-2x^2+\beta_1^2x^2+\pi\alpha Z\beta_1x(1-x)+(\alpha Z)^2x\{(1+2x)L_2(1-x^2)-4L_2(1-x)+2x\ln^2x+\pi^2/2(1-4x/3)+\beta_1^2x[-L_2(1-x^2)+(x^2\ln^2x)/(1-x^2)+\pi^2(1-x)/4(1+x)+\pi^2/6]\},$$

and R may be obtained from the relationship:

$$S^2+R^2+L^2=1.$$

Also, $L_2(x)=$ Euler's dilogarithm (Mi 49), Sec. X, $x=\sin\frac{1}{2}\theta$, and $\mathbf{n}$, $\boldsymbol{\zeta}_1$, and $\boldsymbol{\zeta}_2$ are unit vectors defined in Sec. II.

(1) Conditions of Validity

a. Higher order Born approximation: $(\alpha Z/\beta_1)^3 \ll 1$.
b. No screening: $\alpha Z^{1/3} \ll q_0$.
c. Point-charge nucleus: $R_A \ll 2\pi/p_1$.
d. Infinitely heavy nucleus: $2E_1(m_0/M_0) \ll 1$.
e. Nucleus with negligible spin effects: $(q_0/Z)^2(m_0/M_0)^2 \ll 1$.

(2) References

J 61, formulas (19), (25), and (26).

(3) Notes

a. A comparison of the values of S obtained from the above approximate formula and the Mott–exact formula (1A–403a) for different values of β_1, Z, and θ is shown in Fig. 2 of Ref. J 61.

b. Another formula for this cross section, which is less accurate than formula (1A–402), has been calculated with a lower order Born approximation by Johnson and Mullin [formula (23) in Ref J 60] and by Gürsey [formulas (5) and (11) in Ref. G 57].

c. See Note c in formula (1A–106).

Formula (1A–403)

[The Mott–exact "phase-shift" formula: (a) point nucleus with no screening, and (b) point or finite nucleus with arbitrary screening.]

$$d\sigma(\boldsymbol{\zeta}_1, \boldsymbol{\zeta}_2, \mathbf{n})/d\Omega = \tfrac{1}{2}[d\sigma/d\Omega]_{109}[1+(\mathbf{n}\cdot\boldsymbol{\zeta}_1)(\mathbf{n}\cdot\boldsymbol{\zeta}_2)+S\mathbf{n}\cdot(\boldsymbol{\zeta}_1+\boldsymbol{\zeta}_2)+(L\cos\theta-R\sin\theta)(\mathbf{n}\times\boldsymbol{\zeta}_1)\cdot(\mathbf{n}\times\boldsymbol{\zeta}_2)+(R\cos\theta+L\sin\theta)\mathbf{n}\cdot(\boldsymbol{\zeta}_1\times\boldsymbol{\zeta}_2)],$$

or

$$d\sigma(\boldsymbol{\zeta}_1, \boldsymbol{\zeta}_2, \mathbf{n})/d\Omega = \tfrac{1}{2}(|f|^2+|g|^2)+\tfrac{1}{2}(|f|^2-|g|^2)(\boldsymbol{\zeta}_1\cdot\boldsymbol{\zeta}_2)+|g|^2(\mathbf{n}\cdot\boldsymbol{\zeta}_1)(\mathbf{n}\cdot\boldsymbol{\zeta}_2)+\mathrm{Re}\,fg^*\mathbf{n}\cdot(\boldsymbol{\zeta}_1\times\boldsymbol{\zeta}_2)-\mathrm{Im}\,fg^*\mathbf{n}\cdot(\boldsymbol{\zeta}_1+\boldsymbol{\zeta}_2),$$

where

$$[d\sigma/d\Omega]_{109}=(r_0/\alpha p_1)^2(|F'|^2\csc^2\tfrac{1}{2}\theta+|G|^2\sec^2\tfrac{1}{2}\theta)=|f|^2+|g|^2=\text{formula (1A-109)},$$

$$f=(r_0/\alpha p_1)(G-F'),$$

$$g=(r_0/\alpha p_1)(F'\cot\tfrac{1}{2}\theta+G\tan\tfrac{1}{2}\theta),$$

$$F'=i\alpha ZF/p_1,$$

$$S=(-2i\csc\theta)(F'G^*-GF'^*)/(|F'|^2\csc^2\tfrac{1}{2}\theta+|G|^2\sec^2\tfrac{1}{2}\theta)=i(fg^*-gf^*)/(|f|^2+|g|^2),$$

$$R=2\csc\theta(F'G^*+GF'^*)/(|F'|^2\csc^2\tfrac{1}{2}\theta+|G|^2\sec^2\tfrac{1}{2}\theta)$$

$$=[\cos\theta(fg^*+f^*g)-\sin\theta(|f|^2-|g|^2)]/(|f|^2+|g|^2),$$

$$L=(|G|^2\sec^2\tfrac{1}{2}\theta-|F'|^2\csc^2\tfrac{1}{2}\theta)/(|F'|^2\csc^2\tfrac{1}{2}\theta+|G|^2\sec^2\tfrac{1}{2}\theta)$$

$$=[\sin\theta(fg^*+f^*g)+\cos\theta(|f|^2-|g|^2)]/(|f|^2+|g|^2).$$

Also, $S^2+R^2+L^2=1$, and $\mathbf{n}$, $\boldsymbol{\zeta}_1$, and $\boldsymbol{\zeta}_2$ are unit vectors defined in Sec. II.

(a) Point nucleus with no screening: For this case, the basic pair of functions F and G which are used in the above equations, are defined in formula (1A–109a).

For an unscreened, point nucleus, values of $[d\sigma/d\Omega]_{109}$, S, R, and L for various energies, atomic numbers, and angles are given in Tables III and VII, and Figs. 8–12.

(b) Point or finite nucleus with arbitrary screening: For this case, the basic pair of functions, f and g, which are used in the above equations, are defined in formula (1A–109b).

For a point nucleus with Hartree screening, values of $[d\sigma/d\Omega]_{109}$ are given in Table XII. Results for a finite nucleus are noted in formula (1A–109).

(1) Conditions of Validity

a. Infinitely heavy nucleus: $2E_1(m_0/M_0)\ll 1$.

b. Nucleus with negligible spin effects: $(q_0/Z)^2(m_0/M_0)^2\ll 1$.

c. For point-charge nucleus: $R_A\ll 2\pi/p_1$.

d. For no screening: $\alpha Z^{1/3}\ll q_0$.

(2) References

T 56, Eq. (3.8). Also: Me 55, M 49, S 56, G 57, B 58, and M 61

(3) Notes

Recent results pertaining to cases (a) and (b) are given in formula (1A–109).

Formula (1A–500)

[The Mott–Born formula: point nucleus with (a) exponential, (b) Thomas–Fermi, and (c) Hartree-type screening.]

(a) Exponential screening:

$$\sigma=\frac{\pi Z^2r_0^2}{\beta_1^2(\frac{1}{2}\Lambda)^2[1+(\Lambda/2p_1)^2]},$$

where $\Lambda=(\mu/0.885)(Z^{\frac{1}{3}}/137)$ in units of λ_0^{-1}, with Λ defined by the exponential potential $V(r)=-(Ze^2/r)\times\exp(-\Lambda r)$, $\mu\approx 0.72$ (B 60), ≈ 1.12 or 1.8 (N 59).

For light elements, more accurate estimates are given by this formula according to Ref. (M 41) if μ is placed equal to 0.66 and if $Z^{\frac{1}{3}}$ is replaced by following factors:

Atom	Li	C	N	O	F	Ne
Factor replacing $Z^{\frac{1}{3}}$	2.7	11	10.5	9.5	13.5	9.8

(b) or (c) Thomas–Fermi or Hartree-type screening:

$$\sigma=2\pi\int_\Omega\frac{f^2(q_0)}{(1-\beta_1^2)}\left[1-\left(\frac{q_0}{2E_1}\right)^2\right]\sin\theta\,d\theta=\frac{2\pi}{\beta_1^2}\int_0^{2p_1}f^2(q_0)\left[1-\left(\frac{q_0}{2E_1}\right)^2\right]q_0\,dq_0\approx\frac{2\pi}{\beta_1^2}\int_0^{2p_1}f^2(q_0)\,q_0\,dq_0,$$

where the term containing $(q_0/2E_1)^2$ makes a negligible contribution to σ. The scattering amplitude $f(q_0)$ is defined in formula (1A–102) and is related to the atomic form factor $F(q_0)$ by the following equation:

$$f^2(q_0)=(4Z^2r_0^2/q_0^4)[1-F(q_0)]^2.$$

Estimates of $F(q_0)$ and of the scattering amplitude $f(q_0)$, are given as a function of q_0 for various elements by Ibers (I 62) for both Thomas–Fermi and Hartree-type screening. Table IX gives a summary of values for the function, $f^2(q_0)$, for the atomic numbers 1, 7, 13, 47, and 80: in the region where $0\leq q_0\leq 0.0582$, $f(q_0)^2$ is evaluated with Hartree-type screening (I 62) and with Thomas–Fermi screening [Molière approximation, formula (1A–102b)] where $0.0582\leq q_0\leq 1.0$.

The total cross section σ given above by formula (1A–500b) is evaluated for different atomic numbers in Table X and Fig. 14. These results were obtained with the Hartree form factor given in Tables VI and IX for q_0 in the region $0\leq q_0\leq 0.0582$, and with the Molière form factor given in formula (1A–102b) for q_0 in the region $0.0582\leq q_0\leq 2p_1$.

(1) *Conditions of Validity*

a. Central-type screening potential with electron kinetic energy >1 keV.

b. Point-charge nucleus: $R_A\ll 2\pi/p_1$.

c. Infinitely heavy nucleus: $2E_1(m_0/M_0)\ll 1$.

d. Nucleus with negligible spin effects: $(q_0/Z)^2(m_0/M_0)^2\ll 1$.

e. Validity of different screening approximations is discussed in Sec. V.

(2) *References*

a. Exponential screening: Ma 52, formula (27).

b. Thomas–Fermi screening: M 55, formula (1.11); Ma 52, formula (26).

c. Hartree-type screening: M 55, formula (1.11).

(3) *Notes*

a. An exact screening formula for hydrogen and helium is given in Ref. M 49, formula (10), p. 185.

b. For Thomas–Fermi screening, formula (26) in Ref. Ma 52 gives the cross section directly in terms of the Thomas–Fermi potential, and the general results for any Z are shown in Fig. 23, p. 190 of Ref. M 49 as well as in Ref. B 30.

c. Most of the contribution to the total cross section σ comes from the region of small q_0 values where the Born calculations are reasonably valid and where the Mott to Rutherford cross-section ratio is approximately unity. Therefore corrections to the total cross section are expected to be small for large q_0 values where formulas (1A–500a)–(1A–500c) breaks down. Because screening effects are important for small q_0 values, the total cross section is very sensitive to the type of screening that is used.

d. In the extreme-relativistic limit, the total cross section becomes independent of the incident electron energy as shown by formulas (1A–500b) and (1A–500c).

e. For Hartree screening, Mohr (M 43) has evaluated σ for gold with the results that:

Electron kinetic energy: 0.392 MeV 1.06 MeV ∞

σ: $0.15\,\pi a_0^2$ $0.12\pi a_0^2$ $0.11\pi a_0^2$.

f. An approximate analytical formula for the total cross section in the first Born approximation with atomic screening is given by Tietz (T 59).

Formula (1A–501)

[The nonrelativistic Mott–exact formula: point nucleus with arbitrary screening for nonrelativistic electrons.]

(a) Spin-independent cross section:

$$\sigma=\frac{4\pi(137r_0)^2}{p_1^2}\sum_{l=0}^{\infty}(2l+1)\sin^2\eta_l,$$

where $l\hbar$ is the orbital angular momentum of the electron, and l has integer values from zero to infinity. For a given l, η_l is a constant known as the phase shift, which is related to the angular momentum of the scattered particle. The value of η_l depends on p_1 and on the scattering potential of the atom. In general, η_l is not explicitly defined by a single, closed analytical formula [see Eq. (19) in Chap. II of Ref. M 49] and it must be evaluated for given elements by numerical integration according to the procedures discussed in Chap. VII of Ref. M 49.

For $\beta_1\ll1$, only the zero-order phase ($l=0$) is important and $\sigma=[4\pi(137r_0)^2/p_1^2]\sin^2\eta_0$. As β_1 approaches unity, the number of phases that are not negligible in contributing to the total cross section increases.

(b) Spin-dependent cross section:

$$\sigma=\frac{2\pi(137r_0)^2}{p_1^2}\sum_{l}\sum_{j=l\pm\frac{1}{2}}(2j+1)\sin^2\eta_{lj},$$

where η_{lj} is the phase shift for an electron with energy E_1 and with a given spin orientation with respect to its orbital angular momentum $l\hbar$. This formula is given in general form by Wu and Ohmura (p. 155 and 136 of Ref. Wu 62) and was applied for a particular case in electron elastic scattering in the presence of a resonance by Simpson and Fano (S 63).

(1) *Conditions of Validity*

a. Infinitely heavy nucleus: $2E_1(m_0/M_0)\ll1$.

b. Nonrelativistic electrons: $\beta_1\ll1$.

(2) *References*

a. M 49, formula (18) on p. 24 for spin-independent cross section.

b. S 63, formula (1) and Wu 62 (pp. 155 and 136) for spin-dependent cross section.

(3) *Notes*

a. Formula (1A–501a) is the integrated form of formula (1A–110) and is only valid for nonrelativistic energies.

b. When $\eta_l\ll\frac{1}{2}\pi$, the value of $\sin\eta_l$ (and therefore of σ) does not show an oscillatory dependence on E_1. For this condition of small values of η_l, the first Born approximation is valid.

c. The contribution of all phases η_l with $l>S$, can be neglected if $V(r)\ll S(S+1)/2r^2$ for $p_1r\sim\{S(S+1)\}^{\frac{1}{2}}$. The convergence is best for small Z and T_1.

d. For a given T_1 (with $\beta_1\ll1$), the rate of convergence of the series for σ as well as the magnitude of the terms in the series depends critically on the atomic potential $V(r)$. Because the atomic potentials have widely different dependences on r (for example the atomic fields of the alkali elements extend to much greater distances than the noble gases), the cross sections σ for the different elements have a wide range of magnitudes.

e. For a given Z, the rate of convergence of the series for σ as well as the magnitude of the terms in the series depends critically on T_1 (with $\beta_1\ll1$). The dependence of the cross section on T_1 has a qualitative behavior which can show minima or maxima and which is characteristic of the class of potentials of the elements belonging to a given column in the periodic table. (See M 49 p. 206–210.)

f. Various estimates of this cross section have been made for specific cases of T_1 and Z. In these calculations the phase shifts have been evaluated with different screening approximations and in some cases with the inclusion of exchange and polarization effects. A summary of the results of these calculations is given in Chap. X of Ref. M 49 and Chap. III of M 52.

g. Because of screening effects, the total cross section σ has a finite value. Otherwise for a pure Coulomb field, $\sigma\to\infty$. With screening, $d\sigma/d\Omega$ flattens out to a constant value as $\theta\to0$, and, therefore, the integrated cross section σ is insensitive to whether or not the lower limit of the angular integration is zero or an arbitrarily small cutoff angle θ_c which corresponds to an impact parameter equal to the atomic radius R_{TF} so that $\theta_c\approx(p_1R_{TF})^{-1}$.

h. Some results in the electron-volt energy region of the total cross section for electron Coulomb scattering by various elements are given in Refs. Ma 56 (Fig. 7), N 61, Mo 62, and C 62.

TABLE VI.[a] Hartree-Fock atomic scattering amplitudes, $f(q_0)$, in Ångstrom (Å) units, for small values of q_0.

	q_0																
Z	0	0.0024	0.0049	0.0073	0.0097	0.012	0.015	0.017	0.019	0.024	0.029	0.034	0.039	0.044	0.049	0.053	0.058
1	0.529	0.508	0.453	0.382	0.311	0.249	0.199	0.160	0.131	0.089	0.064	0.048	0.037	0.029	0.024	0.020	0.017
2	0.445	0.431	0.403	0.368	0.328	0.288	0.250	0.216	0.188	0.142	0.109	0.086	0.068	0.055	0.046	0.038	0.032
3	3.31	2.78	1.88	1.17	0.75	0.530	0.400	0.31	0.26	0.19	0.14	0.11	0.09	0.08	0.06	0.05	0.05
4	3.09	2.82	2.23	1.63	1.16	0.830	0.610	0.47	0.37	0.25	0.19	0.15	0.12	0.10	0.08	0.07	0.06
5	2.82	2.62	2.24	1.78	1.37	1.04	0.80	0.62	0.50	0.33	0.24	0.18	0.14	0.12	0.10	0.08	0.07
6	2.45	2.26	2.09	1.74	1.43	1.15	0.92	0.74	0.60	0.41	0.30	0.22	0.18	0.14	0.12	0.10	0.08
7	2.20	2.10	1.91	1.68	1.44	1.20	1.00	0.83	0.69	0.48	0.35	0.27	0.21	0.17	0.14	0.11	0.10
8	2.01	1.95	1.80	1.62	1.42	1.22	1.04	0.88	0.75	0.54	0.40	0.31	0.24	0.19	0.16	0.13	0.11
9	1.84	1.77	1.69	1.53	1.38	1.20	1.05	0.91	0.78	0.59	0.44	0.35	0.27	0.22	0.18	0.15	0.13
10	1.66	1.59	1.53	1.43	1.30	1.17	1.04	0.92	0.80	0.62	0.48	0.38	0.30	0.24	0.20	0.17	0.14
11	4.89	4.21	2.97	2.11	1.59	1.29	1.09	0.95	0.83	0.64	0.51	0.40	0.33	0.27	0.22	0.18	0.16
12	5.01	4.60	3.59	2.63	1.95	1.50	1.21	1.01	0.87	0.67	0.53	0.43	0.35	0.29	0.24	0.20	0.17
13	6.1	5.36	4.24	3.13	2.30	1.73	1.36	1.11	0.93	0.70	0.55	0.45	0.36	0.30	0.25	0.22	0.19
14	6.0	5.26	4.40	3.41	2.59	1.97	1.54	1.23	1.02	0.74	0.58	0.47	0.38	0.32	0.27	0.23	0.20
15	5.4	5.07	4.38	3.55	2.79	2.17	1.70	1.36	1.12	0.80	0.61	0.49	0.40	0.33	0.28	0.24	0.21
16	4.7	4.40	4.00	3.46	2.87	2.32	1.86	1.50	1.22	0.86	0.64	0.51	0.42	0.35	0.30	0.25	0.22
17	4.6	4.31	4.00	3.53	2.99	2.47	2.01	1.63	1.34	0.93	0.69	0.54	0.44	0.37	0.31	0.26	0.23
18	4.71	4.40	4.07	3.56	3.03	2.52	2.07	1.71	1.42	1.00	0.74	0.58	0.46	0.38	0.32	0.27	0.24
19	9.0	7.0	5.43	4.10	3.15	2.60	2.14	1.90	1.49	1.07	0.79	0.61	0.49	0.40	0.34	0.29	0.25
20	10.46	8.71	6.40	4.54	3.40	2.69	2.20	1.84	1.55	1.12	0.84	0.65	0.52	0.42	0.35	0.30	0.26
21	9.7	8.35	6.30	4.63	3.50	2.75	2.29	1.92	1.62	1.18	0.89	0.69	0.54	0.44	0.37	0.32	0.27
22	8.9	7.95	6.20	4.63	3.55	2.84	2.34	1.97	1.67	1.23	0.93	0.72	0.57	0.47	0.39	0.33	0.29
23	8.4	7.60	6.06	4.60	3.57	2.88	2.39	2.02	1.72	1.28	0.97	0.76	0.60	0.49	0.41	0.35	0.30
24	8.0	7.26	5.86	4.55	3.56	2.89	2.42	2.06	1.76	1.32	1.01	0.80	0.63	0.51	0.43	0.36	0.31
25	7.7	7.00	5.72	4.48	3.55	2.91	2.44	2.08	1.79	1.36	1.04	0.83	0.66	0.54	0.45	0.38	0.32
26	7.4	6.70	5.55	4.41	3.54	2.91	2.45	2.11	1.82	1.39	1.08	0.86	0.69	0.56	0.47	0.39	0.34
27	7.1	6.41	5.41	4.34	3.51	2.91	2.46	2.12	1.84	1.42	1.11	0.89	0.71	0.58	0.49	0.41	0.35
28	6.8	6.22	5.27	4.27	3.48	2.90	2.47	2.13	1.86	1.46	1.14	0.92	0.74	0.61	0.50	0.43	0.36
29	6.5	6.00	5.11	4.19	3.44	2.88	2.46	2.12	1.87	1.47	1.16	0.95	0.77	0.63	0.52	0.45	0.38
30	6.2	5.84	4.98	4.11	3.39	2.86	2.45	2.11	1.88	1.48	1.19	0.96	0.78	0.65	0.54	0.46	0.39
31	7.5	6.70	5.62	4.51	3.64	3.00	2.53	2.18	1.91	1.50	1.20	0.98	0.81	0.67	0.56	0.47	0.41
32	7.8	6.89	5.93	4.81	3.87	3.16	2.63	2.24	1.94	1.51	1.22	0.99	0.83	0.69	0.58	0.49	0.42
33	7.8	6.99	6.05	5.01	4.07	3.32	2.74	2.31	1.99	1.54	1.23	1.01	0.85	0.71	0.59	0.50	0.43
34	7.7	6.99	6.15	5.18	4.24	3.47	2.86	2.40	2.05	1.57	1.23	1.02	0.86	0.72	0.61	0.52	0.44
35	7.3	6.80	6.15	5.25	4.37	3.60	2.97	2.49	2.12	1.60	1.27	1.04	0.88	0.73	0.62	0.53	0.45
36	7.1	6.70	6.13	5.31	4.47	3.71	3.08	2.58	2.19	1.64	1.29	1.05	0.90	0.75	0.64	0.55	0.47
47	8.8	8.24	7.47	6.51	5.58	4.75	4.05	3.46	2.97	2.22	1.70	1.35	1.09	0.90	0.76	0.66	0.57
74	14.0	...	11.80	...	7.43	...	5.16	...	3.85	2.99	2.39	1.96	1.63	1.38	1.18	1.02	0.89
80	13.3	12.3	10.8	9.18	7.70	6.48	5.50	4.72	4.09	3.16	2.51	2.05	1.70	1.44	1.23	1.07	0.93

[a] This table is condensed from Table 3.3.3A(1) which is given by Ibers in Ref. I 62 where Hartree–Fock designates various types of self-consistent field calculations. The atomic scattering amplitude $f(q_0)$ applies to the Born-approximation cross section in formula (1A-102) and is related to the conventional x-ray atomic form factor $F(q_0)$ by the equation $f(q_0)=(2Zr_0/q_0^2)\,[1-F(q_0)]$.

TABLE VII. The Doggett-Spencer results for the ratio of the Mott-exact [formula (1A-109a)] to the Rutherford [formula (1A-100)] cross sections.

	Electron kinetic energy (MeV)								
θ	10	4	2	1	0.7	0.4	0.2	0.1	0.05
					$Z=6$				
0°	1.000	1.000	1.000	1.000	1.000	1.000	1.000	1.000	1.000
15	0.999	0.999	1.000	1.000	1.001	1.002	1.003	1.004	1.004
30	0.961	0.962	0.963	0.967	0.970	0.977	0.987	0.996	1.001
45	0.888	0.890	0.894	0.903	0.911	0.929	0.954	0.976	0.990
60	0.788	0.790	0.797	0.814	0.828	0.860	0.906	0.946	0.974
75	0.666	0.669	0.680	0.705	0.728	0.776	0.846	0.909	0.953
90	0.532	0.537	0.551	0.586	0.617	0.683	0.781	0.868	0.930
105	0.397	0.403	0.421	0.466	0.505	0.590	0.714	0.826	0.905
120	0.269	0.277	0.298	0.352	0.400	0.501	0.651	0.786	0.882
135	0.1591	0.1680	0.1923	0.254	0.308	0.425	0.596	0.751	0.862
150	0.0742	0.0839	0.1106	0.1787	0.238	0.366	0.554	0.725	0.846
165	0.0206	0.0310	0.0591	0.1310	0.1938	0.328	0.527	0.708	0.836
180	0.0024	0.0129	0.0416	0.1148	0.1786	0.316	0.518	0.702	0.833
					$Z=13$				
0°	1.000	1.000	1.000	1.000	1.000	1.000	1.000	1.000	1.000
15	1.020	1.020	1.020	1.020	1.019	1.019	1.018	1.015	1.013
30	0.997	0.998	0.999	1.001	1.003	1.008	1.013	1.017	1.017
45	0.935	0.936	0.939	0.947	0.954	0.968	0.988	1.004	1.013
60	0.838	0.840	0.846	0.861	0.874	0.903	0.943	0.977	0.999
75	0.714	0.718	0.727	0.752	0.773	0.818	0.883	0.941	0.970
90	0.575	0.580	0.594	0.628	0.658	0.722	0.815	0.898	0.955
105	0.431	0.438	0.455	0.499	0.538	0.621	0.743	0.852	0.928
120	0.294	0.302	0.323	0.377	0.424	0.525	0.674	0.808	0.902
135	0.1742	0.1831	0.207	0.270	0.324	0.441	0.613	0.769	0.879
150	0.0813	0.0912	0.1179	0.1868	0.247	0.376	0.566	0.738	0.861
165	0.0226	0.0329	0.0614	0.1342	0.1980	0.334	0.536	0.719	0.850
180	0.0024	0.0131	0.0419	0.1163	0.1811	0.320	0.526	0.712	0.846
					$Z=29$				
0°	1.000	1.000	1.000	1.000	1.000	1.000	1.000	1.000	1.000
15	1.069	1.068	1.068	1.066	1.064	1.059	1.050	1.038	1.026
30	1.094	1.093	1.093	1.092	1.091	1.089	1.082	1.070	1.054
45	1.066	1.066	1.068	1.072	1.074	1.080	1.085	1.082	1.072
60	0.987	0.988	0.993	1.004	1.013	1.032	1.057	1.073	1.076
75	0.865	0.868	0.876	0.896	0.914	0.952	1.004	1.045	1.067
90	0.712	0.716	0.729	0.761	0.788	0.847	0.931	1.003	1.047
105	0.543	0.549	0.566	0.610	0.648	0.729	0.848	0.952	1.022
120	0.375	0.383	0.405	0.460	0.508	0.611	0.763	0.900	0.995
135	0.224	0.234	0.259	0.325	0.382	0.505	0.687	0.852	0.970
150	0.1052	0.1157	0.1446	0.218	0.282	0.420	0.626	0.813	0.960
165	0.0289	0.0402	0.0710	0.1497	0.218	0.366	0.587	0.789	0.937
180	0.0026	0.0141	0.0456	0.1261	0.1964	0.348	0.573	0.780	0.932
					$Z=50$				
0°	1.000	1.000	1.000	1.000	1.000	1.000	1.000	1.000	1.000
15	1.124	1.123	1.121	1.115	1.109	1.096	1.072	1.043	1.018
30	1.235	1.234	1.231	1.223	1.216	1.197	1.161	1.113	1.060
45	1.292	1.292	1.290	1.284	1.279	1.264	1.232	1.183	1.120
60	1.274	1.274	1.275	1.277	1.277	1.276	1.262	1.228	1.173
75	1.177	1.179	1.184	1.197	1.208	1.227	1.246	1.242	1.207
90	1.013	1.017	1.028	1.055	1.078	1.126	1.188	1.226	1.225
105	0.801	0.807	0.825	0.869	0.907	0.988	1.101	1.190	1.230
120	0.569	0.578	0.602	0.664	0.718	0.832	0.999	1.142	1.229
135	0.348	0.359	0.390	0.467	0.535	0.682	0.899	1.093	1.225
150	0.1651	0.1781	0.214	0.305	0.385	0.557	0.815	1.053	1.221
165	0.0452	0.0594	0.0983	0.1980	0.285	0.475	0.760	1.026	1.219
180	0.0033	0.0180	0.0581	0.1608	0.251	0.446	0.741	1.017	1.219
					$Z=82$				
0°	1.000	1.000	1.000	1.000	1.000	1.000	1.000	1.000	1.000
15	1.127	1.125	1.120	1.108	1.008	1.074	1.042	1.024	1.024
30	1.358	1.354	1.344	1.315	1.290	1.230	1.133	1.040	0.998
45	1.658	1.653	1.638	1.599	1.564	1.479	1.328	1.157	1.023
60	1.918	1.912	1.897	1.857	1.819	1.728	1.555	1.336	1.122
75	2.044	2.040	2.029	2.000	1.971	1.896	1.741	1.518	1.267
90	1.981	1.980	1.979	1.974	1.966	1.936	1.844	1.672	1.435
105	1.726	1.731	1.745	1.777	1.801	1.842	1.859	1.786	1.614
120	1.324	1.335	1.366	1.444	1.510	1.640	1.799	1.866	1.799
135	0.855	0.874	0.924	1.050	1.159	1.385	1.698	1.920	1.978
150	0.422	0.446	0.513	0.683	0.830	1.143	1.592	1.955	2.100
165	0.1158	0.1444	0.222	0.422	0.595	0.969	1.514	1.974	2.233
180	0.0068	0.0368	0.1187	0.328	0.511	0.908	1.486	1.978	2.267

TABLE VIII. Partial summary of experimental results on electron Coulomb scattering for $q_0<10$.

Reference	Z	Parameters $0.51T_1$ (MeV)	θ (deg)	Comparison with Theory[a]
(V 46), (B 47), (M 48)	4, 13, 29, 47, 78, 79	1.27–2.27	20–60	Yes (a)
(P 52), (K 52)	Up to $Z=78$	0.150–2.2	60–120	No (a)
(Ch 55)	13	0.4, 0.5	100–150	Yes (a)
(B 55)	13, 79	0.6, 1.0, 1.7	30–150	Yes (a)
(B 56)	92	0.4, 0.5	90, 105	Yes (a)
(P 56)	79	0.20	70–150	Yes (a)
(Da 56)	47, 78, 92	4.33	45, 60, 90	Yes (a)
(Ke 59)	36, 54, 80	0.15	60, 90, 120, 135	Yes (a)
(S 59)	13, 28, 47, 79	1.00, 1.75, 2.50	60, 90, 120, 150	No (a)
(Mo 63), (L 64)	29, 50, 79	8.05, 0.10, 0.20, 0.40	20–110	Yes (b)

[a] These results are compared with formula (1A-109). Cases with reasonable agreement or disagreement, respectively, are designated by Yes(a) or No(a) for formula (1A-109a), and Yes(b) or No(b) for formula (1A-109b).

TABLE IX. Atomic scattering function[a] $f^2(q_0)$.

q_0	$Z=1$	$Z=7$	$Z=13$	$Z=47$	$Z=80$
0	2.80×10^{-17}	4.84×10^{-16}	3.72×10^{-15}	7.74×10^{-15}	1.77×10^{-14}
0.00243	2.58×10^{-17}	4.41×10^{-16}	2.87×10^{-15}	6.79×10^{-15}	1.50×10^{-14}
0.00485	2.05×10^{-17}	3.65×10^{-16}	1.80×10^{-15}	5.58×10^{-15}	1.17×10^{-14}
0.00728	1.46×10^{-17}	2.82×10^{-16}	9.80×10^{-16}	4.24×10^{-15}	8.43×10^{-15}
0.00970	9.70×10^{-18}	2.07×10^{-16}	5.29×10^{-16}	3.11×10^{-15}	5.93×10^{-15}
0.0121	6.20×10^{-18}	1.44×10^{-16}	2.99×10^{-16}	2.26×10^{-15}	4.20×10^{-15}
0.0146	4.00×10^{-18}	1.00×10^{-16}	1.85×10^{-16}	1.64×10^{-15}	3.03×10^{-15}
0.0170	2.60×10^{-18}	6.89×10^{-17}	1.23×10^{-16}	1.20×10^{-15}	2.23×10^{-15}
0.0194	1.70×10^{-18}	4.76×10^{-17}	8.65×10^{-17}	8.82×10^{-16}	1.67×10^{-15}
0.0243	7.90×10^{-19}	2.30×10^{-17}	4.90×10^{-17}	4.93×10^{-16}	9.99×10^{-16}
0.0291	4.10×10^{-19}	1.23×10^{-17}	3.03×10^{-17}	2.89×10^{-16}	6.30×10^{-16}
0.0340	2.30×10^{-19}	7.29×10^{-18}	2.03×10^{-17}	1.82×10^{-16}	4.20×10^{-16}
0.0388	1.40×10^{-19}	4.41×10^{-18}	1.30×10^{-17}	1.19×10^{-16}	2.89×10^{-16}
0.0437	8.40×10^{-20}	2.89×10^{-18}	9.00×10^{-18}	8.10×10^{-17}	2.07×10^{-16}
0.0485	5.80×10^{-20}	1.96×10^{-18}	6.30×10^{-1}	5.78×10^{-17}	1.51×10^{-16}
0.0534	4.00×10^{-20}	1.21×10^{-18}	4.84×10^{-18}	4.36×10^{-17}	1.15×10^{-16}
0.0582	2.90×10^{-20}	1.00×10^{-18}	3.61×10^{-18}	3.25×10^{-17}	8.65×10^{-17}
0.07	6.70×10^{-21}	5.20×10^{-19}	1.68×10^{-18}	1.84×10^{-17}	4.80×10^{-17}
0.08	4.39×10^{-21}	3.16×10^{-19}	1.03×10^{-18}	1.15×10^{-17}	3.06×10^{-17}
0.09	2.98×10^{-21}	2.02×10^{-19}	6.64×10^{-19}	7.89×10^{-18}	2.03×10^{-17}
0.10	2.08×10^{-21}	1.35×10^{-19}	4.48×10^{-19}	5.17×10^{-18}	1.40×10^{-17}
0.12	1.10×10^{-21}	6.74×10^{-20}	2.24×10^{-19}	2.65×10^{-18}	7.24×10^{-18}
0.14	6.28×10^{-22}	3.73×10^{-20}	1.24×10^{-19}	1.49×10^{-18}	4.12×10^{-18}
0.16	3.84×10^{-22}	2.22×10^{-20}	7.47×10^{-20}	9.01×10^{-19}	2.50×10^{-18}
0.18	2.48×10^{-22}	1.40×10^{-20}	4.72×10^{-20}	5.77×10^{-19}	1.61×10^{-18}
0.20	1.67×10^{-22}	9.29×10^{-21}	3.14×10^{-20}	3.87×10^{-19}	1.08×10^{-18}
0.22	1.17×10^{-22}	6.41×10^{-21}	2.18×10^{-20}	2.69×10^{-19}	7.54×10^{-19}
0.24	8.37×10^{-23}	4.53×10^{-21}	1.54×10^{-20}	1.92×10^{-19}	5.40×10^{-19}
0.25	7.16×10^{-23}	3.87×10^{-21}	1.31×10^{-20}	1.64×10^{-19}	4.64×10^{-19}

[a] This scattering function is defined as $f^2(q_0)=(4Z^2r_0^2/q_0^4)\,[1-F(q_0)]^2$. Hartree-type (I 62) and Thomas-Fermi [Molière approximation, formula (1A-102b)] form factors are used in the regions where $0\leqq q_0\leqq 0.0582$ and $0.07\leqq q_0\leqq 1.0$, respectively.

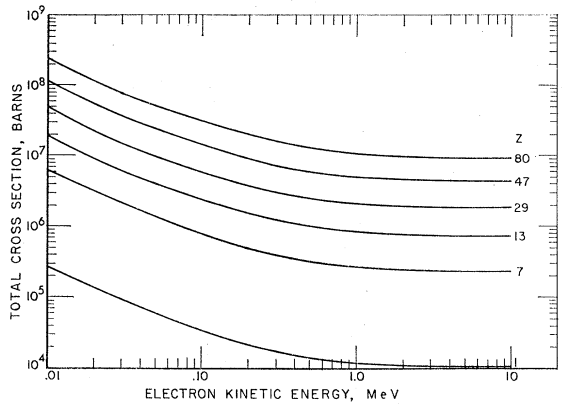

FIG. 14. Dependence of the total cross section σ on the electron kinetic energy for different atomic numbers. This cross section was computed from formula (1A–500c) with the Hartree form factor (given in Tables VI and IX) for q_0 in the region $0 \leq 0.0582$ and the Molière form factor [given in formula (1A–102b)] for q_0 in the region $0.0582 \leq q_0 \leq 2p_1$.

TABLE X. Dependence of total Coulomb scattering cross section σ on Z.

Z	$\beta_1^2\sigma$ [For $\beta_1>0.2$] (barns)
1	1.02×10^4
2	1.49×10^4
3	10.4×10^4
4	16.5×10^4
5	20.1×10^4
6	21.8×10^4
7	23.4×10^4
8	24.8×10^4
9	25.6×10^4
10	26.0×10^4
11	43.9×10^4
12	56.5×10^4
13	73.2×10^4
14	83.5×10^4
15	91.0×10^4
16	92.0×10^4
17	100.0×10^4
18	106.0×10^4
19	142.0×10^4
20	173.0×10^4
21	177.0×10^4
22	179.0×10^4
23	181.0×10^4
24	181.0×10^4
25	182.0×10^4
26	183.0×10^4
27	184.0×10^4
28	185.0×10^4
29	185.0×10^4
30	185.0×10^4
31	208.0×10^4
32	224.0×10^4
33	238.0×10^4
34	251.0×10^4
35	261.0×10^4
36	271.0×10^4
47	435.0×10^4
80	924.0×10^4

VIII. DISCUSSION OF CROSS-SECTION FORMULAS

The cross-section formulas in Sec. VII are classified in Table IV according to the type of calculation, the principal authors, and the form of the cross section. The cross-section symbols are defined in Sec. II. No single formula in Table IV is universally applicable to all conditions in electron scattering. In fact, formulas must be selected according to the type of approximation and the region of validity imposed by experimental conditions. The accuracy of a formula depends on which approximations are satisfied: for example, in the region of small q_0, the cross sections predicted by a first Born

TABLE XI. Selection of formulas for different q_0 values.

Range of q_0 values[a]	Cross-section formula	Comments
$0 \leq q_0 \leq 0.06$	(1A–111) (1A–102c)	Accuracy is uncertain and depends on choice of screening potential.
$0.06 \leq q_0 \leq 1.0$	(1A–109b) with Hartree-type screening, or	For high $Z(\geq 50)$, and for $T_1 \geq 0.2$.
	(1A–109a) multiplied by the factor $[1-F(q_0)]^2$, where $F(q_0)$ is the Hartree atomic form factor given in Tables VI and IX.	For low $Z(\leq 50)$, and for $T_1 \geq 0.2$.
$1.0 \leq q_0 \leq 10.0$	(1A–109a)	Atom behaves like point charge.
$10.0 \leq q_0 \leq 2p_1$	(1A–104)	For proton or neutron.
	(1A–109b)	Nuclear form factor must be specified.
	(1A–108) (1A–103)	Accuracy is uncertain and depends on choice of nuclear form factor and on Z.

[a] For muons with q_0 in units of $m_\mu c$, these limits must be multiplied by the factor m_0/m_μ.

calculation with Hartree-type screening may be more accurate than that predicted by a higher order Born calculation with simple exponential screening. When formulas are used outside their regions of validity, the accuracy cannot be specified unless comparisons can be made with experimental data.

The most important single criterion that can be used as the basis for the selection of these formulas is the magnitude of the momentum transfer q_0. The relative importance of the charge and the magnetic structures of the atom and the nucleus and the validity of the Born approximation depend to a large extent on the region of q_0 values that occur in the scattering process for a given case. Atomic screening effects are important for small q_0 values where the impact parameter is larger than the K shell radius ($q_0 < Z/137$) and nuclear effects are important for large q_0 values where the impact parameter is smaller than the nuclear radius ($q_0 \gtrsim 100A^{-\frac{1}{3}}$).

In addition, a quantitative criterion for the validity

TABLE XII. Ratio[a] of the screened to the unscreened cross section evaluated by Lin.

θ (deg)	400 keV		200 keV		100 keV		50 keV	
	$Z=79$	$Z=29$	$Z=79$	$Z=29$	$Z=79$	$Z=29$	$Z=79$	$Z=29$
10	0.771	0.987	0.636	0.939	0.469	0.869	0.307	0.732
30	0.935	1.03	0.892	1.00	0.794	0.986	0.631	0.966
			(1.07)	(0.980)	(1.16)	(0.991)		
60	0.995	0.981	0.987	1.00	0.957	1.01	0.870	1.02
			(0.794)	(0.948)	(0.927)	(0.964)		
90	0.997	0.984	1.01	0.999	1.02	1.02	1.00	1.04
			(0.592)	(0.925)	(0.692)	(0.942)		
120	1.01	0.996	1.03	1.01	1.07	1.04	1.11	1.05
			(0.481)	(0.916)	(0.544)	(0.929)		
150	1.02	1.03	1.05	1.01	1.11	1.01	1.19	1.05
			(0.420)	(0.913)	(0.454)	(0.925)		

[a] These ratios are evaluated by Lin (L 64) for the electron kinetic energies, electron scattering angles θ, and the target atomic numbers designated above. The unscreened cross section is evaluated from the Mott phase-shift formula (1A–109a) and the screened cross section is evaluated with Hartree-type screening (see Refs. By 56, Mo 63, and L 64) from the Mott phase-shift formula (1A–109b). For the ratios in the parentheses, the screened cross section is evaluated from the Dalitz formula (1A–107) where the exponential screening factor $\Lambda=R_{TF}^{-1}$.

of the Born approximation formulas is that

$$(Zq_0/137E_1)\ll 1.$$

On the basis of these conditions, the selection of formulas is made according to the region of momentum transfer q_0 as shown by the tentative suggestions given in Table XI.

The accuracy of these formulas can only be determined from comparisons with experimental data, as given for example in Table VIII and in Ref. H 56 for large q_0 values. The most accurate cross sections are obtained from the phase-shift calculations in formulas (1A–109), (1A–110), and (1A–111). However, these formulas cannot be readily evaluated for all cases. With the inclusion of accurate potentials for the atom and the nucleus, the phase-shift calculations become exceedingly involved in particular regions of q_0. In such cases, it is necessary to use formulas (1A–105), (1A–106), (1A–107), and (1A–108) which in some cases may give close approximations to the exact phase-shift formulas. A partial summary of cross sections predicted by the Mott phase-shift formula (1A–109b) with Hartree-type screening and by the Dalitz formula (1A–107) with simple exponential screening is shown in Table XII, which is condensed from the results obtained by Lin (L 64). A detailed summary of the cross-section behavior predicted by the exact phase-shift formula (1A–109a) for a point nucleus without screening corrections is given by the curves in Figs. 15–22. These data give the exact cross sections for various atomic numbers, energies, and angles, in terms of the simple Mott–Born formula (1A–102). Figures 19–22 show a comparison of the corrections necessary for the first Born formula (1A–102) and the second Born formula (1A–105). The data in these curves can be used to estimate correction factors for the bremsstrahlung Born cross sections as indicated in Eq. (4.10) and to help determine accurate potentials for the atom and the nucleus.

The polarization sensitivity of the cross section can be estimated from the Mott–exact formulas (1A–403), (1A–302), and (1A–203), and from the higher order Born formulas shown in Table IV. The most accurate estimates for an unscreened point nucleus are given by the Mott phase-shift formulas.

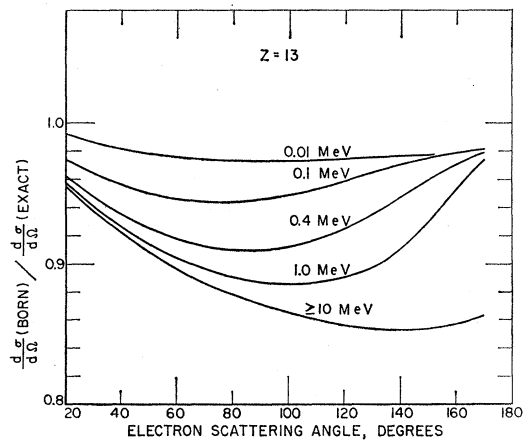

FIG. 15. Dependence of the cross-section ratio for aluminum on the electron scattering angle for different electron kinetic energies. The ratio is given by the Mott–Born formula (1A–101) for $d\sigma/d\Omega$ (BORN) and by the Mott–exact formula (1A–109a) for $d\sigma/d\Omega$ (EXACT) for a point nucleus without screening. Above 10 MeV the curves for this ratio are approximately the same.

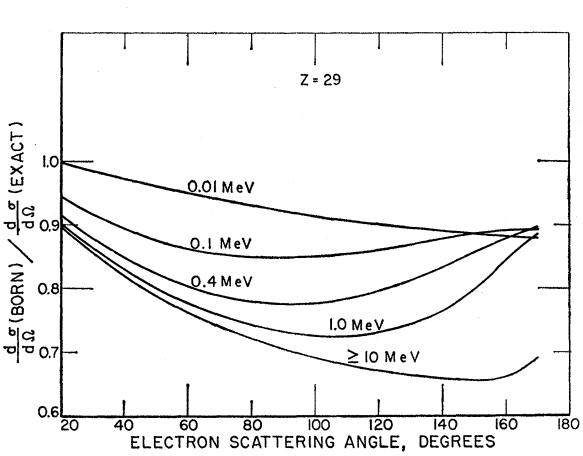

FIG. 16. Same caption as Fig. 15 except that aluminum is replaced by copper.

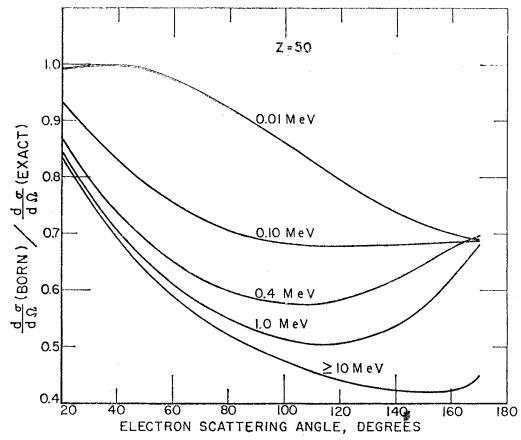

FIG. 17. Same caption as Fig. 15 except that aluminum is replaced by tin.

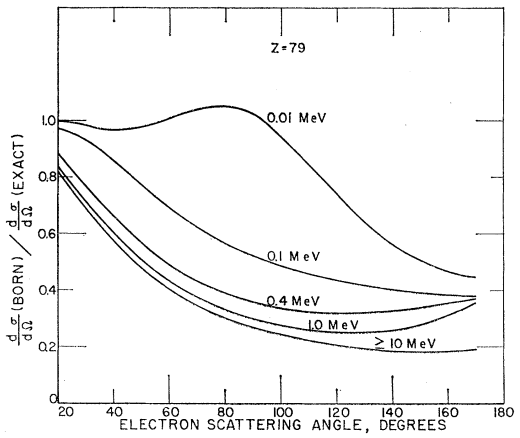

FIG. 18. Same caption as Fig. 15 except that aluminum is replaced by gold.

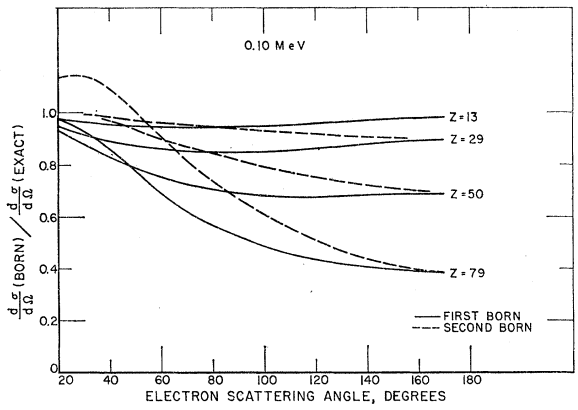

FIG. 19. Dependence of the cross-section ratio at an electron kinetic energy of 0.10 MeV on the electron scattering angle for different atomic numbers. The ratio is given by the Mott–Born formula (1A–101) (solid lines) for $d\sigma/d\Omega$ (BORN) and by the Mott–exact formula (1A–109a) for $d\sigma/d\Omega$ (EXACT) for a point nucleus without screening. For the dashed lines, $d\sigma/d\Omega$ (BORN) is given by the McKinley–Feshbach formula (1A–105).

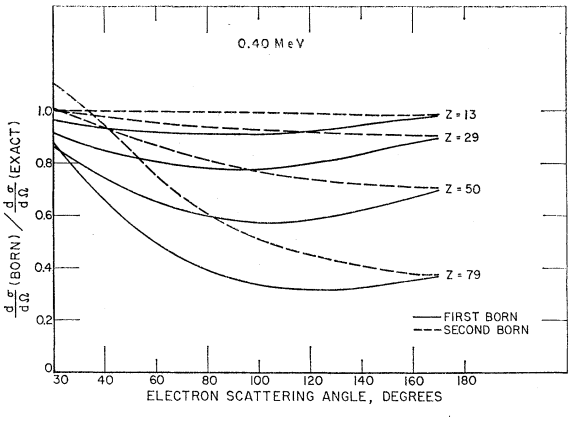

FIG. 20. Same caption as Fig. 19, except that the energy 0.10 MeV is replaced by 0.40 MeV.

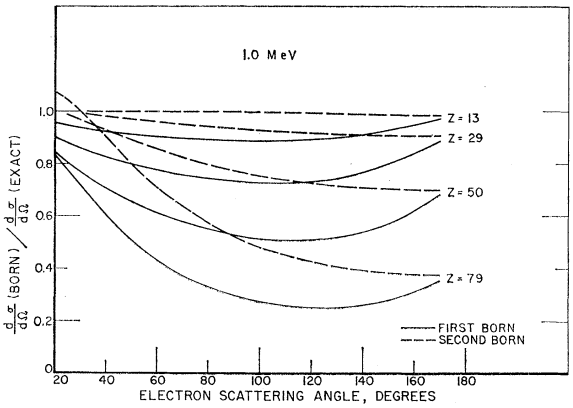

FIG. 21. Same caption as Fig. 19, except that the energy 0.10 MeV is replaced by 1.0 MeV.

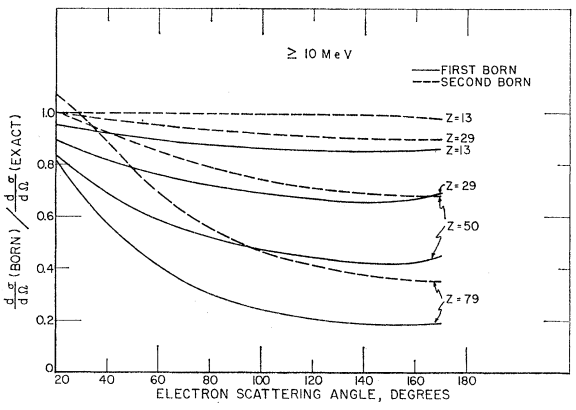

FIG. 22. Same caption as Fig. 19, except that the energy 0.10 MeV is replaced by $\geq$ 10 MeV, where the curves for this ratio are approximately the same for energies greater than 10 MeV.

TABLE XIII. Values for Euler's dilogarithm $L_2(x)$.

x	0.00	0.01	0.02	0.03	0.04	0.05	0.06	0.07	0.08	0.09
0.0	0.000	0.010	0.020	0.030	0.040	0.051	0.061	0.071	0.082	0.092
0.1	0.103	0.113	0.124	0.134	0.145	0.156	0.167	0.178	0.189	0.200
0.2	0.211	0.222	0.233	0.245	0.256	0.268	0.279	0.291	0.303	0.314
0.3	0.326	0.338	0.350	0.362	0.374	0.387	0.400	0.411	0.424	0.437
0.4	0.449	0.462	0.475	0.488	0.501	0.514	0.528	0.541	0.555	0.568
0.5	0.582	0.596	0.610	0.624	0.639	0.653	0.678	0.682	0.697	0.712
0.6	0.728	0.743	0.758	0.774	0.790	0.806	0.822	0.839	0.855	0.872
0.7	0.889	0.907	0.924	0.942	0.960	0.978	0.997	1.016	1.035	1.055
0.8	1.075	1.095	1.116	1.137	1.159	1.181	1.203	1.226	1.250	1.275
0.9	1.300	1.326	1.353	1.381	1.410	1.441	1.473	1.508	1.546	1.589

The total cross section is estimated from the screened Mott–Born formula (1A–500). The accuracy of the formula is uncertain and depends appreciably on the choice of the atomic form factor. In the nonrelativistic region, it is necessary to use the more complicated nonrelativistic phase-shift formula (1A–501).

ACKNOWLEDGMENTS

We wish to thank Leonard Kaplan for his numerical computations of the data shown in many of the figures in this review and for his constructive comments. In addition, we wish to thank Dr. J. Coyne for providing the FORTRAN code for formula (1A–109a) and for evaluating the data given in Table III and in Figs. 11 and 12. We are also grateful to Dr. H. Mendlowitz and Dr. L. C. Maximon for helpful discussions.

X. MATHEMATICAL APPENDIX

Euler's dilogarithm appears in many of the formulas in this survey, which are given in analytical form. Euler's dilogarithm is designated by the function $L_2(x)$, which is defined as

$$L_2(x) = -\int_0^x \frac{\ln(1-\eta)}{\eta}\, d\eta.$$

This function (sometimes called the Spence function) has been evaluated by Mitchell (Mi 49) for nine-place tables of $L_2(x)$, $-1 \leq x \leq 1$. A condensed version of Mitchell's results for $0 \leq x \leq 1$ is given in Table XIII. $L_2(x)$ for other values of x may be obtained from Table XIII using the transformation formulas:

$$x \geq 1: \quad L_2(x) = \tfrac{1}{3}\pi^2 - \tfrac{1}{2}\ln^2 x - L_2(1/x),$$

$$-1 \leq x \leq 1: \quad L_2(-x) = \tfrac{1}{2}L_2(x^2) - L_2(x),$$

$$x < 0: \quad L_2(x) = -\tfrac{1}{6}\pi^2 + L_2[1/(1-x)] - \tfrac{1}{2}\ln(1-x)\ln[x^2/(1-x)].$$

BIBLIOGRAPHY

B 30 E. C. Bullard and H. S. W. Massey, Proc. Cambridge Phil. Soc. **26,** 556 (1930).
B 31 V. Bush and S. H. Caldwell, Phys. Rev. **38,** 1898 (1931).
B 39 J. H. Bartlett, Jr., and R. E. Watson, Phys. Rev. **56,** 612 (1939); Proc. Am. Acad. Arts and Sci. **74,** 53 (1940).
B 41 J. H. Bartlett, Jr., and T. A. Welton, Phys. Rev. **59,** 281 (1941).
B 47 W. W. Buechner, R. J. Van de Graaff, A. Sperduto, E. A. Burrill, and H. Feshbach, Phys. Rev. **72,** 678 (1947).
B 50 J. Blaton, Kgl. Danske Videnskab. Selskab, Mat. Fys. Medd. **24,** No. 20 (1950).
B 53 H. A. Bethe, Phys. Rev. **89,** 1256 (1953).
B 54 H. A. Bethe and L. C. Maximon, Phys. Rev. **93,** 768 (1954).
B 55 R. T. Bayard and J. L. Yntema, Phys. Rev. **97,** 372 (1955).
B 56 B. Brown, E. Matsukawa, and E. A. Stewardson, Proc. Phys. Soc. (London) **69A,** 496 (1956).
By 56 W. J. Byatt, Phys. Rev. **104,** 1298 (1956).
B 57 H. A. Bethe and E. E. Salpeter, in *Encyclopedia of Physics*, edited by S. Flügge (Springer-Verlag, Berlin, 1957), Volume XXXV, Atoms I, pp. 411 and 171.
B 58 M. Bernardini, P. Brovetto, and S. Ferroni, Nucl. Phys. **8,** 294 (1958).
Ba 58 Haridas Banerjee, Acta Phys. Austriaca **12,** 70 (1958).
B 60 I. Berkes and I. Demeter, Nucl. Phys. **15,** 421 (1960).
B 61 A. M. Baldin, V. I. Gol'Danskii, and I. L. Rozenthal, *Kinematics of Nuclear Reactions* (Pergamon Press Ltd., London, 1961).
Bu 61 F. Bumiller, M. Crosseaux, E. Dally, and R. Hofstadter, Phys. Rev. **124,** 1623 (1961).
B 62 R. E. Burge and G. H. Smith, Proc. Phys. Soc. (London) **79,** 673 (1962).
Bu 62 P. G. Burke and Kenneth Smith, Rev. Mod. Phys. **34,** 458 (1962).
B 63 R. A. Bonham and T. G. Strand, J. Chem. Phys. **39,** 2200 (1963); also, T. G. Strand and R. A. Bonham, *ibid.* **40,** 1686 (1964).
B 64 C. P. Bhalla, Natl. Bur. Std. (U.S.) Monograph **81** (1964).
C 55 R. M. Curr, Proc. Phys. Soc. (London) **68A,** 156 (1955).
Ch 55 K. R. Chapman, E. Matsukawa, P. H. Rose, and E. A. Stewardson, Proc. Phys. Soc. (London) **68A,** 928 (1955).
C 62 J. W. Cooper and J. B. Martin, Phys. Rev. **126,** 1482 (1962).
D 51 R. H. Dalitz, Proc. Roy. Soc. (London) **A206,** 509 (1951).
D 54 H. Davies, H. A. Bethe, and L. C. Maximon, Phys. Rev. **93,** 788 (1954).
D 56 J. A. Doggett and L. V. Spencer, Phys. Rev. **103,** 1597 (1956).
Da 56 K. K. Damodaran and R. M. Curr, Proc. Phys. Soc. (London) **69A,** 196 (1956).
D 62 S. D. Drell and R. H. Pratt, Phys. Rev. **125,** 1394 (1962).
E 50 L. R. B. Elton, Proc. Phys. Soc. (London) **63A,** 1115 (1950).
E 52 L. R. B. Elton and H. H. Robertson, Proc. Phys. Soc. (London) **65A,** 145 (1952).
E 60 F. J. Ernst, R. G. Sachs, and K. C. Wali, Phys. Rev. **119,** 1105 (1960).
F 30 V. Fock, Z. Physik **61,** 126 (1930).
F 54 E. Freese and K. Hain, Z. Naturforsch. **9a,** 456 (1954).
F 57 U. Fano, Rev. Mod. Phys. **29,** 74 (1957); also, J. Opt. Soc. Am. **39,** 859 (1949); Phys. Rev. **93,** 121 (1954).
F 58 J. Franklin and B. Margolis, Phys. Rev. **109,** 525 (1958).
F 61 G. Felsner and M. E. Rose, Nuovo Cimento **20,** 509 (1961).
F 63 H. Frauenfelder and A. Rossi, in *Methods of Experimental Physics*, edited by Luke C. L. Yuan and C. S. Wu (Academic Press Inc., New York, 1963), Vol. 5 Nuclear Physics Part B.
G 57 F. Gürsey, Phys. Rev. **107,** 1734 (1957).

G 61 V. G. Gorshkov, Zh. Eksperim. i Teor. Fiz. **41,** 977 (1961) [English transl.: Soviet Phys.—JETP **14,** 694 (1962)].
Gi 61 H. B. Gilbody, R. F. Stebbings, and W. Fite, Phys. Rev. **121,** 794 (1961).
G 62 V. G. Gorshkov, Zh. Eksperim. i Teor. Fiz. **43,** 1714 (1962); [English transl.: Soviet Phys.—JETP **16,** 1211 (1963)].
G 63 J. Goldemberg and Y. Torizuka, Phys. Rev. **129,** 312 (1963).
G 64 E. S. Ginsberg and R. H. Pratt, Phys. Rev. **134,** B773 (1964).
H 28 D. R. Hartree, Proc. Cambridge Phil. Soc. **24,** 89, 111 (1928).
H 56 R. Hofstadter, Rev. Mod. Phys. **28,** 214 (1956).
H 57 R. Hofstadter, Ann. Rev. Nucl. Sci. **7,** 231 (1957).
H 60 R. Herman and R. Hofstadter, *High-Energy Electron Scattering Tables* (Stanford University Press, Stanford, California, 1960).
H 63 L. N. Hand, D. G. Miller, and R. Wilson, Rev. Mod. Phys. **35,** 335 (1963).
I 62 J. A. Ibers, *International Tables for X-Ray Crystallography,* (The Kynoch Press, Birmingham, England, 1962), Vol. III, p. 201.
J 40 J. M. Jauch, Helv. Phys. Acta **13,** 451 (1940).
J 54 J. M. Jauch and F. Rohrlich, Helv. Phys. Acta **27,** 613 (1954).
J 55 J. M. Jauch and F. Rohrlich, *The Theory of Photons and Electrons* (Addison-Wesley Press, Inc., Reading, Massachusetts, 1955).
J 60 W. R. Johnson and C. J. Mullin, Phys. Rev. **119,** 1270 (1960).
J 61 W. R. Johnson, T. A. Weber, and C. J. Mullin, Phys. Rev. **121,** 933 (1961).
K 52 E. Kinzinger and W. Bothe, Z. Naturforsch. **7A,** 390 (1952); **8A,** 312 (1953).
K 56 D. G. Keiffer and G. Parzen, Phys. Rev. **101,** 1244 (1956).
K 59 H. W. Koch and J. W. Motz, Rev. Mod. Phys. **31,** 920 (1959).
Ke 59 J. Kessler, Z. Physik **155,** 350 (1959).
K 60 B. K. Kerimov and V. M. Arutyunyan, Zh. Eksperim. i Teor. Fiz. **38,** 1798 (1960) [English transl.: Soviet Phys.—JETP **11,** 1294 (1960)].
Kr 60 A. A. Kresnin and B. I. Tishchenko, Ukr. Fiz. Zh. (USSR) **5,** 437 (1960).
K 61 H. Kolbenstvedt and H. Olsen, Nuovo Cimento **22,** 610 (1961).
K 62 A. S. Krass, Phys. Rev. **125,** 2172 (1962).
K 64 J. Karle and R. A. Bonham, J. Chem. Phys. **40,** 1396 (1964).
L 37 R. Langer, Phys. Rev. **51,** 669 (1937).
L 54 F. Lenz, Z. Naturforsch. **9a,** 185 (1954).
L 56 R. R. Lewis, Jr., Phys. Rev. **102,** 537 (1956).
L 63 Shin-R Lin, N. Sherman, and J. K. Percus, Nucl. Phys. **45,** 492 (1963).
L 64 Shin-R Lin, Phys. Rev. **133,** A965 (1964).
M 41 L. Marton and L. I. Schiff, J. Appl. Phys. **12,** 759 (1941).
Ma 41 H. S. W. Massey and C. B. O. Mohr, Proc. Roy. Soc. (London) **A177,** 341 (1941).
M 43 C. B. O. Mohr, Proc. Roy. Soc. (London) **A182,** 189 (1943).
M 47 G. Molière, Z. Naturforsch. **2a,** 133 (1947).
M 48 W. A. McKinley, Jr., and H. Feshbach, Phys. Rev. **74,** 1759 (1948).
M 49 N. F. Mott and H. S. W. Massey, *The Theory of Atomic Collisions* (Oxford University Press, London, 1949), 2nd ed.
Mi 49 K. Mitchell, Phil. Mag. **40,** 351 (1949).
M 52 H. S. W. Massey and E. H. S. Burhop, *Electronic and Ionic Impact Phenomena* (Oxford University Press, London, 1952).
Ma 52 H. S. W. Massey, *Advances in Electronics* (Academic Press Inc., New York, 1952), Vol. IV, p. 1.
M 53 H. Mitter and P. Urban, Acta Phys. Austriaca **7,** 311 (1953).
M 54 C. B. O. Mohr and L. J. Tassie, Proc. Phys. Soc. (London) **A67,** 711 (1954).
M 55 M. J. Moravcsik, Phys. Rev. **100,** 1009 (1955).
Me 55 H. Mendlowitz and K. M. Case, Phys. Rev. **97,** 33 (1955); H. Mendlowitz, Am. J. Phys. **26,** 17 (1958).
M 56 P. T. McCormick, D. G. Keiffer, and G. Parzen, Phys. Rev. **103,** 29 (1956).
Ma 56 H. S. W. Massey, in *Encyclopedia of Physics,* edited by S. Flügge (Springer-Verlag, Berlin, 1956), Vol. 36, p. 232.
M 61 W. H. McMaster, Rev. Mod. Phys. **33,** 8 (1961).
M 62 K. T. Mahanthappa, Phys. Rev. **126,** 329 (1962).
Mo 62 B. L. Moiseiwitsch, *Atomic and Molecular Processes* (Academic Press Inc., New York, 1962), p. 280.
M 63 N. Meister and D. R. Yennie, Phys. Rev. **130,** 1210 (1963).
Mi 63 L. Mikaelyan, A. Borovoi, and E. Denisov, Nucl. Phys. **47,** 328 (1963).
Mo 63 J. W. Motz, R. C. Placious, and C. E. Dick, Phys. Rev. **132,** 2558 (1963).
M 64 L. C. Maximon and D. B. Isabelle, Phys. Rev. **133,** B1344, (1964).
N 55 A. T. Nelms and I. Oppenheim, J. Res. Natl. Bur. Std. **55,** 53 (1955).
N 59 B. P. Nigam, M. K. Sundareson, and Ta-You-Wu, Phys. Rev. **115,** 491 (1959).
Ne 59 D. F. Nelson and R. W. Pidd, Phys. Rev. **114,** 728 (1959).
N 60 Bengt Nagel, Trans. Roy. Inst. Tech. Stockholm **157,** 3 (1960).
N 61 R. Neynaber, L. Marino, E. Rothe, and S. Trujillo, Phys. Rev. **123,** 148 (1961); **124,** 135 (1961).
O 57 H. Olsen, L. C. Maximon, and H. Wergeland, Phys. Rev. **106,** 27 (1957).
O 59 H. Olsen and L. C. Maximon, Phys. Rev. **114,** 887 (1959).
O 63 H. Olsen, Phys. Rev. **131,** 406 (1963).
O 64 H. Olsen and K. Mork (to be published).
P 50 G. Parzen, Phys. Rev. **80,** 355 (1950).
P 52 W. Paul and H. Reich, Z. Physik **131,** 326 (1952).
P 56 W. G. Pettus, H. G. Blosser, and F. L. Hereford, Phys. Rev. **101,** 17 (1956).
P 58 W. G. Pettus, Phys. Rev. **109,** 1458 (1958).
R 11 E. Rutherford, Phil. Mag. **21,** 669 (1911).
R 34 G. Racah, Nuovo Cimento **11,** 461 (1934).
R 50 M. N. Rosenbluth, Phys. Rev. **79,** 615 (1950).
R 58 G. H. Rawitscher, Phys. Rev. **112,** 1274 (1958).
R 60 L. Rosenberg, L. Spruch, and T. F. O'Malley, Phys. Rev. **119,** 164 (1960).
R 63 B. Rosen, J. Math. Phys. **4,** 392 (1963).
S 49 J. Schwinger, Phys. Rev. **75,** 898 (1949).
S 52 L. I. Schiff, Phys. Rev. **87,** 750 (1952).
S 55 H. Suura, Phys. Rev. **99,** 1020 (1955).
Sc 55 L. I. Schiff, Phys. Rev. **98,** 756 (1955).
S 56 N. Sherman, Phys. Rev. **103,** 1601 (1956).
S 59 V. Spiegel, Jr., T. F. Ruane, D. J. Anthony, B. Waldman, and W. C. Miller, Ann. Phys. (N.Y.) **6,** 70 (1959).
Sc 59 J. H. Scofield, Phys. Rev. **113,** 1599 (1959).
S 62 R. G. Sachs, Phys. Rev. **126,** 2256 (1962).
S 63 J. A. Simpson and U. Fano, Phys. Rev. Letters **11,** 158 (1963).
Sc 63 William T. Scott, Rev. Mod. Phys. **35,** 231 (1963).
T 56 H. A. Tolhoek, Rev. Mod. Phys. **28,** 277 (1956).
T 57 L. J. Tassie, Phys. Rev. **107,** 1452 (1957).
T 59 T. Tietz, Acta Phys. Acad. Hung. **10,** 19 (1959).
To 59 I. N. Toptygin, Zh. Eksperim. i Teor. Fiz. **36,** 488 (1959) [English transl.: Soviet Phys.—JETP **9,** 340 (1959)].
T 60 Yung-Su Tsai, Phys. Rev. **120,** 269 (1960).
T 61 Yung-Su Tsai, Phys. Rev. **122,** 1898 (1961).
Te 61 A. Temkin and J. C. Lamkin, Phys. Rev. **121,** 788 (1961).
V 46 R. J. Van de Graaff, W. W. Buechner, and H. Feshbach, Phys. Rev. **69,** 452 (1946).
W 27 E. T. Whittaker and G. N. Watson, *A Course of Modern Analysis* (Cambridge University Press, London, 1927), 4th Ed.
W 62 J. D. Walecka and R. H. Pratt, High Energy Physics Laboratory Report No. 272, Stanford University, Stanford, California (unpublished).
Wu 62 Ta-You Wu and Takashi Ohmura, *Quantum Theory of Scattering* (Prentice-Hall, Inc., Englewood Cliffs, New Jersey, 1962).
Y 54 D. R. Yennie, D. G. Ravenhall, and R. N. Wilson, Phys. Rev. **95,** 500 (1954).
Y 57 D. R. Yennie, M. M. Levy, and D. G. Ravenhall, Rev. Mod. Phys. **29,** 144 (1957).
Y 61 D. R. Yennie, S. C. Frautschi, and H. Suura, Ann. Phys. (N.Y.) **13,** 379 (1961).